Summer 5-2015

CHARACTERIZING THE EFFECTS OF BOTH SYNTHETIC AND NATURAL INHIBITORS ON THE FUNCTION OF HOLOCARBOXYLASE SYNTHETASE AND LIPID METABOLISM

Elizabeth Cordonier
University of Nebraska-Lincoln, elizabeth.cordonier@huskers.unl.edu

CHARACTERIZING THE EFFECTS OF BOTH SYNTHETIC AND NATURAL INHIBITORS ON THE FUNCTION OF HOLOCARBOXYLASE SYNTHETASE AND LIPID METABOLISM

by

Elizabeth Cordonier

A DISSERTATION

Presented to the Faculty of

The Graduate College at the University of Nebraska

In Partial Fulfillment of Requirements

For the Degree of Doctor of Philosophy

Major: Interdepartmental Nutrition Program

Under the Supervision of Professor Janos Zempleni

Lincoln, Nebraska

May, 2015

CHARACTERIZING THE EFFECTS OF BOTH SYNTHETIC AND NATURAL INHIBITORS ON THE FUNCTION OF HOLOCARBOXYLASE SYNTHETASE AND LIPID METABOLISM

Elizabeth Cordonier, Ph.D.

University of Nebraska, 2015

Advisor: Janos Zempleni

The central theme of this dissertation explores enzyme inhibition, through the use of both synthetic and natural occurring inhibitors of three biotin-associated enzymes; the mammalian biotin ligase, holocarboxylase synthetase(HLCS), and acetyl-CoA carboxylases 1 and 2 (ACC1 and 2), whose activity is dependent on biotinylation by HLCS, and are involved in fatty acid synthesis and regulation of beta-oxidation, respectively. No null HLCS individual has ever been reported and individuals with inherited mutations in the HLCS gene, which render it incapable of biotinylating carboxylases, exhibit varying degrees of symptoms associated with multiple carboxylase deficiency. Little is known with regard to the reaction mechanism and structure of HLCS. The first chapter of this dissertation focuses on the characterization of a novel class of HLCS inhibitors, the biotin-5'-AMP analogs, β-ketophosphonate and β-hydroxyphosphonate, that could be of potential use as an analytical tool in studies of HLCS-biotinylation between the well-known carboxylase targets and novel targets in other proteins. Adapting an existing *in vitro* protocol in our laboratory, the inhibitors were demonstrated to be competitive inhibitors of HLCS. We extend these studies of

HLCS in the next chapter by identifying resveratrol compounds as natural inhibitors of HLCS *in vitro* which protect *Drosophila melanogaster brummer* mutants from fat mass accumulation. The third chapter focuses on the effects of dual inhibition of ACC1 and ACC2 on adipocyte differentiation of 3T3-L1 cells. We report on the effects of Soraphen A, a natural occurring polyketide derived from *Sorangium cellulosum*, which targets the biotin carboxylase domain of the eukaryotic ACCs. We demonstrate that Soraphen A prevents adipogenic gene expression and lipid accumulation in 3T3-L1 cells suggesting dual inhibitors of ACC1 and ACC2 may be an effective strategy to prevent fat accumulation. In conclusion, we have demonstrated the inhibition of HLCS with both synthetic and natural compounds, and that ACC1 and ACC2 inhibition alters lipid metabolism in adipocytes.

ACKNOWLEDGEMENTS

I would like to express my sincere appreciation to Dr. Zempleni for providing me this opportunity to extend my education. I am grateful for his guidance, expertise, encouragement, and above all patience throughout my Ph.D. studies. I would like to extend my gratitude to my committee members Dr. Patrick Dussault, Dr. Donald Becker, Dr. Gautam Sarath, and past committee member, Dr. Vicki Schlegel.

I would like to thank my collaborators and lab mates, past and present, and undergraduate students who have given their time and patience to provide their guidance and expertise in the lab. I wish to thank Dr. Samudra Wijeratne, Dr. Mahendra Singh, Dr. Yong Li, Dr. Wantanee Sittiwong, Sarah Jarecke, Frannie Hollinger, Shingo Esaki, Riem Adjam, Dave Giraud, Dr. Jing Xue, Dr. Dandan Liu, Dr. Daniel Camara Teixeira, Scott Baier, Tovah Wolf, Kat Howard, Wei Key Eng, Thao Trinh, and Rio Kusuma.

I would like to extend my thanks to Lori Rausch, Lori Beals, Donna Hahn, Jolene Walker, Connie Wieser, and Ann Grasmick for their help and patience in the day to day work that keeps this department and program going.

Finally, I express my deepest gratitude to the most important people in my life, my parents, other extended family, and friends, who have provided the utmost love, support, encouragement, and patience throughout this time.

TABLE OF CONTENTS

LIST OF FIGURES

INTRODUCTION

CHAPTER I

CHAPTER II

CHAPTER III

LIST OF TABLES

CHAPTER II

CHAPTER III

APPENDIX

(CHAPTER I)

(CHAPTER II)

The first part of this introduction will focus on the biological significance of holocarboxylase synthetase (HLCS), current understanding of its catalytic mechanism and a discussion of inhibitors developed against its bacterial homolog BirA. The second part of this section will introduce the acetyl-CoA carboxylase (ACC) enzymes, Soraphen A, a dual ACC1/ACC2 inhibitor, and ACC inhibition as a potential inhibitor of adipocyte differentiation.

I.HLCS

Background and Significance

The *HLCS* gene is located on chromosome 21q22.13 and contains 18 exons. The enzyme holocarboxylase synthetase (HLCS) is generated by a 6019 bp gene which consists of 726 amino acids and M_r 80,629. Holocarboxylase synthetase (HLCS) catalyzes the attachment of biotin to five carboxylase proteins. The five biotin-dependent carboxylases are propionyl-CoA carboxylase (PCC), methylcrotonoyl-CoA carboxylase (MCC), pyruvate carboxylase (PC), and acetyl-CoA carboxylase 1 and 2 (ACC1 and 2)[1]. ACC1 is located in the cytosol, ACC2 is anchored in the outer mitochondrial membrane and the remaining three enzymes reside within the mitochondria [2]. These enzymes are involved in odd-chain fatty acid metabolism, leucine catabolism, gluconeogenesis and fatty acid synthesis, and regulation of fatty acid oxidation, respectively[1]. Additionally, HLCS-dependent methylation of the nuclear co-repressor N-CoR and the histone methyltransferase EHMT1 is partially responsible for the formation of a multiprotein gene repression complex[3, 4].

Consistent with its importance in intermediary metabolism, HLCS is essential for survival as no living HLCS null individual has been reported. Additionally, mutations and single nucleotide polymorphisms in the HLCS gene result in decreased HLCS activity resulting in abnormal gene regulation and metabolic abnormalities due to the inability of HLCS to biotinylate carboxylase proteins essential to intermediary metabolism[5, 6]. These mutations are inherited in an autosomal recessive pattern and the disorder manifests in infancy, with numerous complications including skin rash, hair loss, difficulties in breathing or eating, and lack of energy. Treatment with pharmacological doses of biotin is necessary for the entirety of an affected person's life [7].

Much of what is known about HLCS structure and function comes from studies of its bacterial homolog BirA, the biotin protein ligase(BPL) of *Escherichia coli*, which has 21% sequence similarity to HLCS [8]. BirA catalyzes the attachment of biotin to the acetyl-coA carboxylase subunit, biotin carboxyl carrier protein (BCCP). In addition to its function as a biotin ligase, BirA also serves as a repressor of transcription initiation [9]. In both situations, biotinyl-5'-AMP, serves as the reaction intermediate[9, 10]. Functional complementation studies in *E.coli* demonstrate that HLCS clones are capable of biotinylating BCCP, in *E. coli birA104* cells, mutants defective in biotin ligase [11]. These studies indicate that BirA and HLCS share a similar catalytic mechanism.

Catalytic mechanism of HLCS

HLCS-dependent biotinylation occurs via a condensation reaction involving two steps. In the first step, biotin is activated by ATP hydrolysis generating the mixed anhydride, biotin-

5’-adenosine monophosphate (Bio-5’-AMP)(1). Bio-5’-AMP serves as an acylating agent, covalently linking an amide bond between the valeric acid side chain of the tetrahydrothiophene ring in biotin and the epsilon amino group of a target lysine in the carboxylase protein (2)[12]. This lysine residue is found within a biotin acceptor sequence (AMKM) whose residues allow the biotinylated residues to swing the carboxyl group to the receiving substrate from the site of activation.

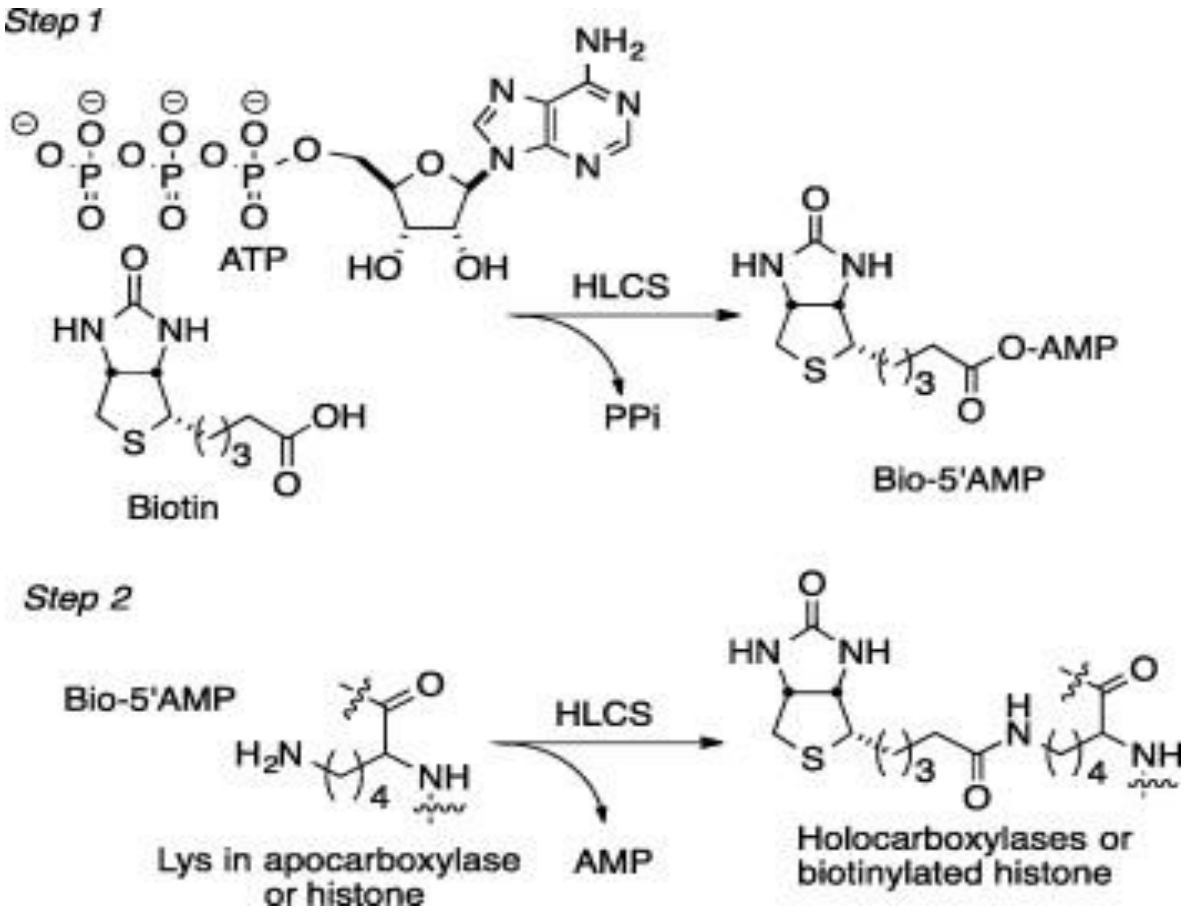

Fig 1. Catalytic mechanism of HLCS

(Reprinted with permission from Bioorganic and Medicinal Chemistry Letters, 2014, 24, 5568-5571)

HLCS structure-current understanding

Limited structural knowledge of HLCS is available due to the inability to generate a high-resolution structure of HLCS[13]. Three structural domains are predicted in the HLCS protein, one in the N-terminus(amino acids 166-290) and two in the C-terminus (amino acids 460-669 and 670-726) and 349 residues of the C-terminal region has been shown to be minimally functional [14]. This C-terminal portion is highly conserved across all species and is required for the cross-species biotinylation of BCCP and p67, the last 67 amino acids within propionyl-CoA carboxylase [14, 15]. The N-terminal region is not conserved among biotin protein ligases and the N-terminus of HLCS has not been implicated in transcriptional regulation unlike its bacterial counterpart which contains a DNA-binding motif within its N-terminus [11, 13]. The N-terminal region has been implicated in catalysis even though it's not necessary for HLCS activity. HLCS with C- and N-terminal deletions evaluated for their ability to catalyze biotinylation of human and bacterial substrates after expression in *E.coli* revealed that the region between Leu166 and Arg290 is necessary for catalysis while smaller deletions (the first 58, 80 or 165 amino acids of the N-terminus) were able to restore growth in E.coli and biotinylate both p67 and BCCP87, the last 87 residues of BCCP [14]. The authors speculate that when this region encompassing Leu166 and Arg290 is removed it blocks the active site, whereas removing the whole domain restores activity.

Individuals with mutations in either the C- or N-terminus of the HLCS gene have been reported [6] and this information has provided some additional insight into the catalytic mechanism of HLCS. These mutations are divided into two groups. The K_m mutants are

those in which HLCS has a decreased affinity for biotin and pharmacological doses of biotin are successful in treating patients with these mutations. The activity of the HLCS enzyme is compromised in V_{max} mutants, but successful treatment of MCD with biotin supplementation varies. The majority of amino acid substitutions that cluster around the biotin and ATP sites in the C-terminal catalytic portion are those that result in an increased K_m. The most notable of these substitutions occurs in Arg508, a highly conserved residue in all BPLs, Gly518 which lies in the biotin binding pocket, and Asp571 which positions Lys579 in the AMP binding pocket [16]. Substitutions at Arg183, Leu216 and Leu237, all map to the N-terminus and are grouped as V_{max} mutants because the patients who have these mutations show variable responses to biotin treatment. Five of seven patients with the Leu216➔Arg mutation died between 3 days and 3 years despite three of the patients being administered biotin after presenting with severe acidosis[17]. Despite being on either 40mg or 80mg/day of biotin treatment, individuals with the Leu237➔Pro mutation show delays in development and lower IQ even though other symptoms were resolved [18].

Inhibitors of BirA

A couple of non-hydrolyzable analogs of biotinyl-5'-AMP have been developed as inhibitors against the bacterial biotin protein ligases to study their reaction mechanism. These non-hydrolyzable analogs, an ester and a sulfamoyl derivative, were used to study allosteric regulation of *BirA* [9]. The ester derivative biotinol-AMP, inhibits biotin transfer to the acceptor protein through tight binding to the Escherichia coli biotin repressor (K_D=1.5 ± 0.2 nM) [19]. Inhibitors against *Staphylococcus aureus* and *Mycobacterium tuberculosis* have been developed as a potential novel class of antibiotics [10, 20]. Soares

de costa et al. reported on the selective inhibition of *S. aureus* BPL over HLCS by linking biotin to an adenosine with a 1,2,3 triazole. The biotin 1,2,3 triazole demonstrated potent inhibition (K_i=90nM) of BPL from S. aureus with >1100 fold selectivity over the human homologue. Additionally, it showed anti-microbial activity against *S. aureus* while showing no toxicity in HepG2 cells[10]. A bisusbtrate inhibitor of mycobacterial protein ligase (*Mt*BPL) was characterized and described previously[20]. Its design was similar to that of the sulfamide derivative but the 5'-oxygen atom was replaced with a nitrogen atom. The inhibitor binds approximately 1700-fold more tightly to *Mt*BPL than biotin and has an IC_{50}=135 ± 9 nM. It was effective at inhibiting growth of multi-drug resistant and extensively drug-resistant at 0.16-0.625 μM concentrations and was ineffective against other microbial species and non-cytotoxic to mammalian cells [20].

Naturally occurring inhibitors of HLCS

To date, there have not been any naturally occurring compounds in food products that have been found to inhibit HLCS activity. We received a library of extracts that we screened for HLCS activity *in vitro*. It was initially observed that grape leaf extracts potently inhibited HLCS activity *in vitro*. Resveratrol has been shown to delay or prevent heart disease, cancer, diabetes, pathological inflammation, and even obesity [21].

Objectives

The objective of these studies was to identify and characterize synthetic and naturally occurring compounds that inhibit HLCS, providing a tool to study HLCS biotinylation events in distinct cellular structures.

II. ACC1 and ACC2

Background and significance

Acetyl-CoA is the starting compound of fatty acid synthesis [22] and is formed in the mitochondria from the decarboxylation of pyruvate. It is subsequently transported as citrate via the citrate pyruvate shuttle to the cytosol where it is reconverted to acetyl-CoA by ATP citrate lyase. The rate-limiting step of fatty acid synthesis, carboxylation of acetyl-CoA to malonyl-CoA is catalyzed by acetyl-CoA carboxylase (ACC). The mammalian ACC enzymes consist of a single polypeptide chain encoding a biotin carboxylase(BC), biotin carboxyl carrier protein(BCCP), and a carboxyltransferase (CT) domain [23]. The bacterial and yeast ACCs exist as dimeric enzymes and other eukaryotic ACCs are believed to exist as either dimers or oligomers [24]. In addition to malonyl-CoA serving as the carbon donor in fatty acid biosynthesis [25], it is a potent inhibitor of the carnitine palmitoyl-CoA shuttle system. The rate limiting step of β-oxidation, transfer of an acyl group of a long-chain fatty acyl CoA from coenzyme A to L-carnitine to form an acyl carnitine is catalyzed by carnitine palmitoyltransferase I (CPT1) [26, 27] (**Figure 2**). There are two ACC genes, ACC1 or ACCα, and ACC2 or ACCβ and the catalytic mechanism is the same in the two enzymes.

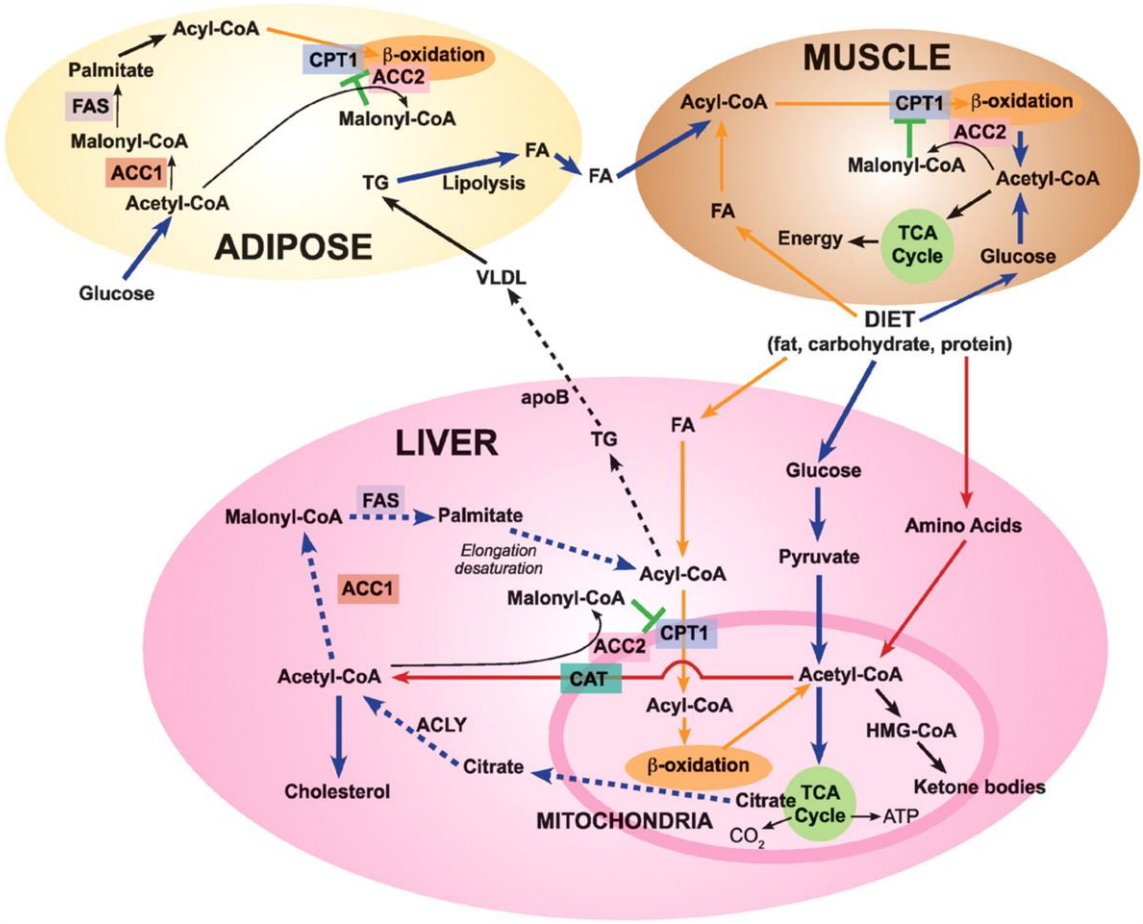

Salih J. Wakil, and Lutfi A. Abu-Elheiga J. Lipid Res. 2009

Figure 2. ACC1 and ACC2 in liver, adipose tissue, and skeletal muscle. In liver, FA are converted to acyl-CoA; glucose undergoes glycolysis and generates pyruvate, which is oxidized in the mitochondria through pyruvate dehydrogenase to acetyl-coenzyme A (acetyl-CoA). Acetyl-CoA is also produced through amino acid metabolism. Acetyl-CoA is oxidized through the citric acid cycle to yield energy, H2O, and CO2 or it is converted to citrate, which exits to the cytosol and generates acetyl-CoA through ATP citrate lyase (ACLY) or carnitine/acetyl-CoA (CAT), which exits from the mitochondria to the cytosol. In the cytosol acetyl-CoA is carboxylated to malonyl-CoA by ACC1 and utilized through fatty acid synthase (FAS) reactions to generate palmitate, which is utilized in the synthesis of triglycerides (TG)

and VLDL. Also, acetyl-CoA is carboxylated by ACC2 at the mitochondrial membrane to form malonyl-CoA, which inhibits the CPT1 and reduces acyl-CoA transfer to mitochondria for β-oxidation. Basically comparable reactions, with appropriate modifications, occur in adipose and muscle tissues.

(Reprinted with permission from the Journal of Lipid Research, 2009, S138-S143)

The catalytic mechanism is dependent on the prosthetic group biotin bound to the BCCP and proceeds in two steps. In the first step, the N1 atom in the ureido group of biotin is carboxylated by biotin carboxylase. Bicarbonate serves as the carboxyl group donor and the reaction is driven by ATP hydrolysis. In the second step, the activated carboxyl group is transferred from the N1 atom of biotin to the methyl group of acetyl-CoA to produce malonyl-CoA, by the carboxyltransferase domain [23, 28]. Biotin can translocate between the active sites of the BC and CT domain due to its position at the end of a 'swinging arm', which is made up of 8 methylene groups and 10 rotatable single bonds that forms between the backbone of the BCCP and the bicyclic ring of biotin (**Figure 3**)[28].

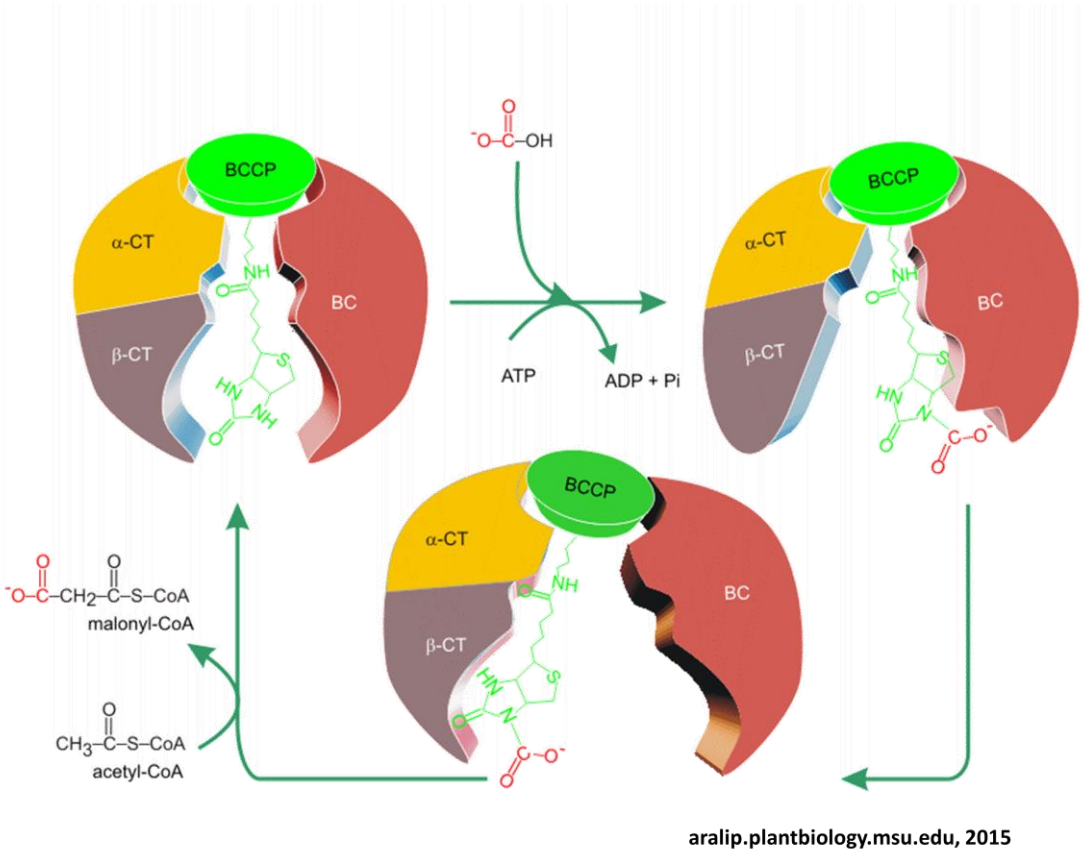

Figure 3. Catalytic mechanism of acetyl-CoA carboxylase enzymes

A single gene encoding the multifunctional polypeptide (265 kDa) of ACC1 maps to chromosome 17q12. ACC1 is found in the cytoplasm and is primarily expressed in lipogenic tissues such as adipose tissue, mammary gland tissue and the liver Malonyl-CoA produced from ACC1 feeds into fatty acid synthesis [29].

ACC2 was first discovered in rat heart and is localized to chromosome 12q23 [30]. Human liver ACC2 cDNA nucleotide sequence has an open reading frame of 7,449 nucleotides, encoding 2,483 amino acids to give a calculated molecular weight of ~280kDa [31].

There are 114 additional amino acids at the N-terminus of ACC2 with hydrophobic residues making up the first several amino acids, suggesting that ACC2 is a membrane-associated enzyme [31]**.** Affinity-purified anti-ACC2 antibodies and immunocytochemical methods demonstrated that anti-ACC2 is associated with the mitochondrial membrane [2]**.** Expression of ACC2 is primarily in the heart and skeletal muscle [29].

Regulation of ACC

ACCs are regulated at both the transcriptional and post-translational levels. At the transcriptional level, multiple promoters exist for the mammalian ACCs and the use of various promoters results in modulation of the N-terminal sequence of the encoded proteins due to alternative splicing at the 5'end. An alternative trancript of ACC1 that results from the PIII promoter lacks the phosphorylation site of AMPK[32]. A transcript lacking the N-terminal sequence which targets ACC2 to the mitochondrial membrane is a product of alternative splicing [29]. Transcription factors such as sterol regulatory element binding proteins (SREBP1a and SREBP1c) and carbohydrate response element binding protein (ChREBP) activate ACC gene expression upon feeding of a high carbohydrate diet either in dependently or independently of insulin action, respectively [33]. PGC-1β, a peroxisome proliferator-activated receptor γ coactivator-1 regulates SREBP-1c expression and has crucial roles in lipogenesis[34].

At the post-translational level, citrate, long chain acyl-CoAs, and AMPK play roles in regulating ACC activity. Citrate promotes polymerization of ACCs and its subsequent activation. Long chain acyl-CoAs, such as palmitoyl-CoA have an opposing effect; they

bind tightly to ACC (K_i= 5.5nM) preventing its polymerization[35]. Both ACCs can be phosphorylated by AMPK under physiological conditions, inhibiting their activity through reductions in V_{max} [36]. AMPK phosphorylates serine residues located next to the BC domain, Ser79 in ACC1 and Ser218 in ACC2, and this inhibition may be enough to block activity of the enzymes[36].

Effects of ACC animal models on diet-induced obesity and diabetes

Interest in ACCs as therapeutic targets was generated with the publication of several studies reporting on the effects of knocking out ACC2 *in vivo* [37, 38]. Mutant Acc2-/- mice fed a high-fat/high carbohydrate diet or high-fat diet for 4 months, had lower body weight than their wild type cohorts. The Acc2-/- mice were protected from diabetes as evidenced by insulin and glucose levels being maintained within a normal range and significantly lower than WT mice. Palmitate oxidation in soleus muscle was decreased upon stimulation with insulin while fatty acid oxidation was unchanged in soleus muscle of ACC2-/- mice. Additionally, the amount of triglyceride in the liver of ACC2-/- mice fed a standared diet was lower than those of WT mice. However, fatty acid synthase activity and malonyl-CoA levels were the same in liver extracts of the mutant and wild type mice [37].

Another study found that Acc2-/- mice had increased total energy expenditure, and respiratory quotient (RQ) profiles that suggested an increase in fat and carbohydrate oxidation. Hyperinsulinemic-euglycemic clamp experiments revealed that plasma insulin concentrations were 26% lower in the Acc2-/- mice indicating increased insulin clearance while glucose uptake in the skeletal muscle and white adipose tissue were increased by

66% and 100% in these mice, suggesting increased insulin sensitivity. Decreased triglycerides and long-chain acyl-CoAs in the liver and skeletal muscle of Acc2-/- mice were observed in the high-fat-fed Acc2-/- mice as compared to high-fat-fed WT mice [38].

However, other studies of ACC2-/- knockout models contradict the results obtained by Abu-Elheiga. Mice with global knockout of ACC2 had similar body weights and food intake, as compared to wild-type controls [39, 40]. These ACC2-/- deficient had decreased malonyl CoA levels in cardiac and skeletal muscle and increased fatty acid oxidation(~57%) in isolated soleus muscle. Accumulation of triglyceride in the liver and muscle and overall energy expenditure was the same in both WT and ACC2-/- mice while glycogen stores were elevated in muscle and there was increased use of glucose for lipid synthesis. Additionally, there was no difference in adiposity or body weight between WT and ACC2-/- deficient mice challenged with a HFD [39].

A null ACC1 mutation is embryonically lethal in mice [41]. Liver-specific knockouts of ACC1 (LACC1-/-) generated by Kusunoki's and Wakil's groups have also produced controversial results [42, 43]. There were no differences in fatty acid synthesis of malonyl-CoA levels in Kusonoki's LACC1-/- mice liver samples compared to WT mice while liver samples from Wakil's LACC1-/- produced the opposite effects [42, 43]. There exists the possibility that either ACC enzyme can compensate for the other indicating the necessity of inhibiting both ACC enzymes may be required to alter energy balance. A number of dual ACC1/ACC2 inhibitors have been developed, and reviewed by Bourbeau and Bartberger [44].

Soraphen A, a nonselective potent inhibitor of ACCs

Soraphen A(SA), a macrocylic polyketide derived from the soil-dwelling myxobacterium *Sorangium cellulosum* that displays antifungal activity. Biochemical studies in yeast demonstrated that SA inhibited the glycerol biosynthesis pathway necessary for growing cells, but not resting cells. Subsequent genetic studies showed that ACC1 was tightly linked to SA resistance and that ACC activity was inhibited by SA treatment [45, 46]. Structural studies demonstrate that the compound acts by binding to the BC domain of the ACC enzymes preventing its dimerization or oligomerization of eukaryotic ACCs [23]. SA inhibits ACCs at concentrations as low as 1nM [23].

In addition to working as a fungicide, SA has also been shown to work against mammalian ACCs. In LNCaP and PC-3M prostate cancer cells, and liver HepG2 cells, SA stimulates fatty acid oxidation and inhibits fatty acid synthesis [47, 48]. The inability to synthesize phospholipids, the major end product of fatty acids in cancer cells was accompanied by a decrease in proliferation and in viability, reaching 50% and 70% viability in LNCaP and PC-3M cells, respectively [47]. Induction of apoptosis is responsible for the death of LNCaP cells while autophagy contributed to PC-3M cell death. The phospholipid content was unaltered in premalignant BPH-1 cells and cell viability was unaffected in nonmalignant fibroblasts and BPH-1 cells. Supplementation with palmitate suppresses the cytotoxicity of SA treatment in LNCaP and PC-3M cells [47]. Additional studies in HepG2 and LNCaP cells showed that SA also blocks fatty acid elongation of products derived from exogenous saturated and unsaturated fatty acids, and de novo lipogenesis leading to an accumulation of unsaturated fatty acids derived from polyunsaturated and

saturated precursors. This inhibitory effect of SA could not be abrogated by overexpression with the fatty acid elongases, Elovl5 and Elovl6 [48].

To date, one animal study has observed the effects of SA on high fat diet-induced insulin resistance in mice. Male C57Bl/6 mice fed a high fat diet supplemented with SA had reduced weight gain, adipose tissue, fasting plasma insulin levels, and beta-hydroxybutyrate as compared to mice fed high fat diets without SA supplementation and levels comparable to those of the control. Glucose infusion rate during hyperinsulinemic euglycemic clamp experiments was higher in mice fed diets supplemented with SA as compared to those fed a high fat diet. Lipogenic gene expression was unchanged between treatment groups in the liver, adipose tissue, and skeletal muscle; the only difference was an increase in fatty acid synthase (FAS) in the liver of the high fat fed mice, including those supplemented with SA [49]. Malonyl-CoA is converted to fatty acids by FAS.

Adipocyte differentiation and fat mass expansion

The hypothesis that ACC inhibition prevents adipocyte differentiation has yet to be tested. Lodhi et al. reported on the effects of a knockdown of FAS in adult adipose tissue and PexRap, a protein required for adipogenesis and alkyl ether lipid transcriptional activity. Fat specific knockout of FAS in mice lessened diet-induced obesity and increased brown fat-like cells in these mice. Knockout of PexRap resulted in a similar decrease in diet induced obesity in PexRap knockout mice [50]. Because ACCs are upstream of FAS in the fatty acid biosymthesis pathways, it's possible that dual inhibition of ACC1 and ACC2 may prevent adipocyte differentiation (**Figure 4**).

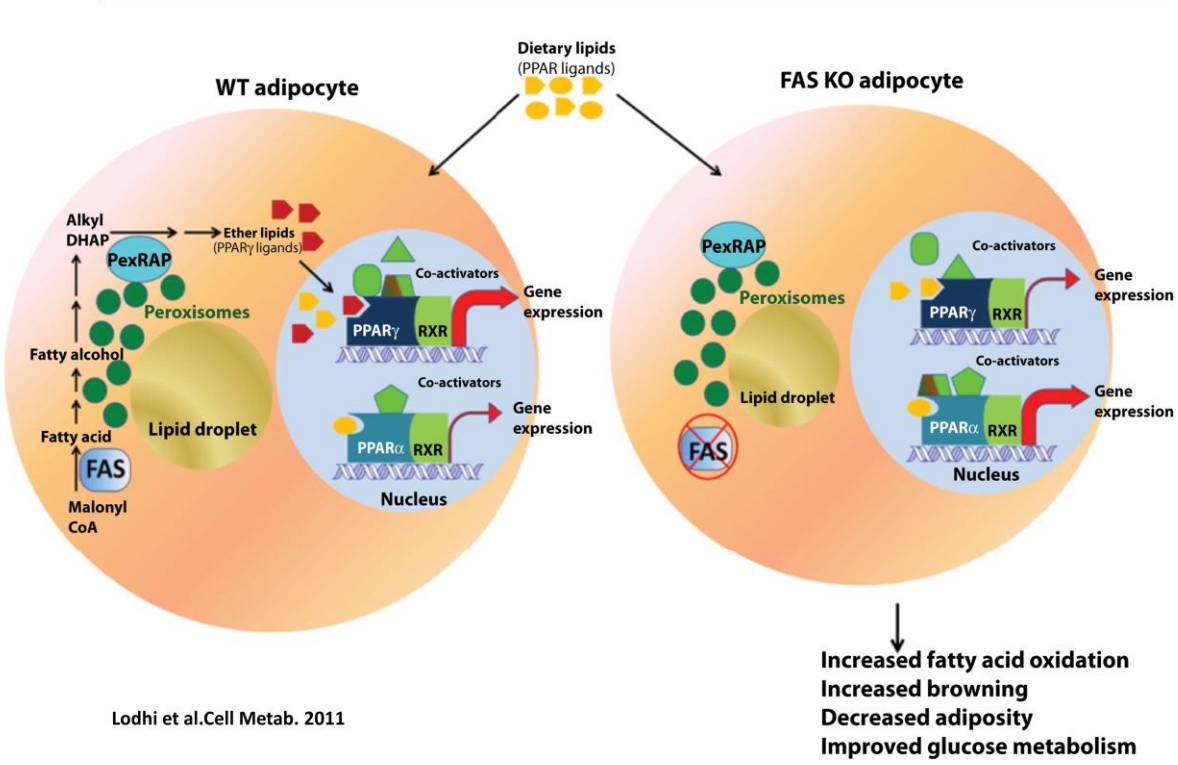

Figure 4. Disruption of FAS blocks adipogenesis and promotes thermogenesis. FAS synthesizes lipids that serve as substrate for PexRap which generates alkyl ether lipids which are potential endogenous PPARγ ligands. ACCs produce malonyl-CoA that is converted into fatty acids by FAS.

(Reprinted with permission from Cell Metabolism, 2012, 16, 189-201)

Adipocytes are specialized eukaryotic cell types that contain organelles called lipid droplets, which store energy as fat. The number of adipocytes is set in childhood and adolescence with approximately 10% of adipocytes turning over in adult human adipose tissue every year. [51]. When energy intake exceeds energy expenditure, fat mass expands primarily through hypertrophy of existing adipocytes and through hyperplasia (occurs only

in children and adolescents) [51]. The stromal vascular fraction of adipose tissue contains pluripotent mesnchymal stem cells, which are capable of differentiating into adipocytes, osteoblasts, myocytes, and chondrocytes [52]. These cells differentiate into adipocytes when host animals undergo lipodystrophy or high fat feeding, states that are conducive to fat mass expansion [52].

Adipogenesis or adipocyte differentiation is a highly regulated process that is divided into two phases, determination and terminal differentiation. The determination phase is defined by the conversion of the stem cell into a pre-adipocyte; these cells are unable to differentiate into another cell type but remain indistinguishable from their stem cell precursors. When the pre-adipocyte starts taking on features of a mature adipocyte, this is the terminal differentiation phase [53]. One of the hallmark features of a mature adipocyte is the accumulation of triglyceride, which is stored in lipid droplets. De novo lipogenesis is associated with triglyceride accumulation as measured by incorporation of ^{14}C-acetate in 3T3-L1 cells. Most of ^{14}C-acetate incorporation is directed into triglyceride synthesis (~80%) with 9 and 6% incorporated into free fatty acids and phospholipids, respectively [54].

The other hallmark of adipocyte differentation is the expression and activation of peroxisome proliferator-activated receptor gamma(PPARγ) which is crucial for adipogenesis and maintenance of differentiated adipocytes. In its absence, no other factor is capable of promoting adipogenesis [53]. De-differentiation of adipocytes with loss of lipid accumulation and decreased expression of adipocyte markers occurs when dominant negative PPARγ is introduced into mature 3T3-L1 adipocytes [55]. Two isoforms,

PPARγ1 and PPARγ2 are both induced during adipogenesis but PPARγ2 promotes adipogenesis more efficiently [56]. The DNA binding domain of PPARγ binds to a consensus sequence, a direct repeat of AGGTCA separated by a single nucleotide, known as a PPAR response element (PPRE) in its target genes, with retinoid-X-receptor α (RXRα) to induce transcription of target genes [57]. Activation of PPARγ is dependent on cAMP production during early adipogenesis but ligand activation of PPARγ is not required for PPARγ-dependent gene expression in mature adipocytes [58]. Even though PPARγ activation is dependent on cAMP production, an endogenous ligand of PPARγ has remained elusive [53].

PPARγ induces the expression of genes involved in lipogenesis, lipolysis, and insulin sensitivity during adipocyte differentiation. These genes include fatty acid binding protein (FABP4, also known as adipocyte protein, aP2), glucose transporter GLUT4, perilipin, lipoprotein lipase (LPL), and the secreted factors, leptin and adiponectin [52]. FABP4 is an intracellular binding protein transporting fatty acids into the nucleus and to and from lipid droplets. It has been found that FABP4 may underlie transcriptional activation of PPARγ through continuous nucleocytoplasmic shuttling [59]. Glucose transport into adiopcytes is facilitated by GLUT4 [60]. Perilipin, a protein associated with the surface of lipid droplets protects against the action of lipases and regulates lipid storage [61]. Adiponectin and leptin are hormones released from adipocytes that regulate glucose metabolism, and food intake, respectively [62]. Although important, these are just some of the features of adipogenesis. There are several elements that contribute to adipogenesis, including other transcription factors and cofactors, and signaling cascades.

Hypothesis

We hypothesize that dual inhibition of ACC antagonizes expression of PPARγ and transcriptional activation of its downstream targets resulting in inhibition of adipocyte differentiation.

This hypothesis was tested in the preadipocyte line, 3T3-L1 with the dual ACC1 and ACC2 inhibitor, Soraphen A and had the following objectives:

1. To determine the extent to which ACC inhibition by SA alters adipogenic gene expression and lipid accumulation in 3T3-L1 cells.

2. To determine the extent to which fatty acid oxidation plays a role in differentiating adipocytes.

References

1. Suzuki Y, Aoki Y, Ishida Y, et al. Isolation and characterization of mutations in the human holocarboxylase synthetase cDNA. Nat Genet 1994;8:122-128
2. Abu-Elheiga L, Brinkley WR, Zhong L, et al. The subcellular localization of acetyl-CoA carboxylase 2. Proc Natl Acad Sci USA 2000;97:1444-1449
3. Liu D, Zempleni J. Holocarboxylase synthetase interacts physically with nuclear receptor co-repressor, histone deacetylase 1 and a novel splicing variant of histone deacetylase 1 to repress repeats. Biochem J 2014;461:477-486
4. Xue J, Wijeratne S, Zempleni J. Holocarboxylase synthetase synergizes with methyl CpG binding protein 2 and DNA methyltransferase 1 in the transcriptional repression of long-terminal repeats. Epigenetics 2013;8:504-511
5. Esaki S, Malkaram SA, Zempleni J. Effects of single nucleotide polymorphisms in the human *holocarboxylase synthetase* gene on enzyme catalysis. Eur J Hum Genet 2012;20:428-433
6. Suzuki Y, Yang X, Aoki Y, Kure S, Matsubara Y. Mutations in the holocarboxylase synthetase gene *HLCS*. Human Mutat 2005;26:285-290
7. Nyhan WL. Multiple carboxylase deficiency. Int J Biochem 1988;20:363-370
8. Hassan YI, Moriyama H, Olsen LJ, Bi X, Zempleni J. N- and C-terminal domains in human holocarboxylase synthetase participate in substrate recognition. Mol Genet Metab 2009;96:183-188
9. Brown PH, Cronan JE, Grotli M, Beckett D. The biotin repressor: modulation of allostery by corepressor analogs. J Mol Biol 2004;337:857-869

10. Soares da Costa TP, Tieu W, Yap MY, et al. Selective inhibition of biotin protein ligase from Staphylococcus aureus. J Biol Chem 2012;287:17823-17832

11. Leon-Del-Rio A, Leclerc D, Akerman B, Wakamatsu N, Gravel RA. Isolation of a cDNA encoding human holocarboxylase synthetase by functional complementation of a biotin auxotroph of Escherichia coli. Proc Natl Acad Sci USA 1995;92:4626-4630

12. Lane MD, Young DL, Lynen F. The Enzymatic Synthesis of Holotranscarboxylase from Apotranscarboxylase and (+)-Biotin. I. Purification of the Apoenzyme and Synthetase; Characteristics of the Reaction. Journal of Biological Chemistry 1964;239:2858-2864

13. Pendini NR, Bailey LM, Booker GW, et al. Microbial biotin protein ligases aid in understanding holocarboxylase synthetase deficiency. Biochim Biophys Acta 2008;1784:973-982

14. Campeau E, Gravel RA. Expression in *Escherichia coli* of N- and C-terminally deleted human holocarboxylase synthetase. Influence of the N-terminus on biotinylation and identification of a minimum functional protein. Journal of Biological Chemistry 2001;276:12310-12316

15. Leon-Del-Rio A, Gravel RA. Sequence requirements for the biotinylation of carboxyl-terminal fragments of human propionyl-CoA carboxylase alpha subunit expressed in Escherichia coli. Journal of Biological Chemistry 1994;269:22964-22968

16. Dupuis L, Campeau E, Leclerc D, Gravel RA. Mechanism of biotin responsiveness in biotin-responsive multiple carboxylase deficiency. Mol Genet Metabol 1999;66:80-90

17. Wilson CJ, Myer M, Darlow BA, et al. Severe holocarboxylase synthetase deficiency with incomplete biotin responsiveness resulting in antenatal insult in samoan neonates. Journal of Pediatrics 2005;147:115-118

18. Aoki Y, Suzuki Y, Sakamoto O, et al. Molecular analysis of holocarboxylase synthetase deficiency: a missense mutation and a single base deletion are predominant in Japanese patients. Biochim Biophys Acta 1995;1272:168-174

19. Naganathan S, Beckett D. Nucleation of an allosteric response via ligand-induced loop folding. J Mol Biol 2007;373:96-111

20. Duckworth BP, Geders TW, Tiwari D, et al. Bisubstrate adenylation inhibitors of biotin protein ligase from Mycobacterium tuberculosis. Chemistry & biology 2011;18:1432-1441

21. Baur JA, Sinclair DA. Therapeutic potential of resveratrol: the in vivo evidence. Nature reviews Drug discovery 2006;5:493-506

22. Wilson AC, Murtadha M, Wakil SJ. Fatty acid synthesis in aorta. Isolation of fatty acid synthetase from chicken aorta. Atherosclerosis 1977;26:103-115

23. Shen Y, Volrath SL, Weatherly SC, Elich TD, Tong L. A mechanism for the potent inhibition of eukaryotic acetyl-coenzyme A carboxylase by soraphen A, a macrocyclic polyketide natural product. Mol Cell 2004;16:881-891

24. Weatherly SC, Volrath SL, Elich TD. Expression and characterization of recombinant fungal acetyl-CoA carboxylase and isolation of a soraphen-binding domain. Biochem J 2004;380:105-110

25. Wakil SJ, Stoops JK, Joshi VC. Fatty acid synthesis and its regulation. Annu Rev Biochem 1983;52:537-579

26. McGarry JD, Leatherman GF, Foster DW. Carnitine palmitoyltransferase I. The site of inhibition of hepatic fatty acid oxidation by malonyl-CoA. J Biol Chem 1978;253:4128-4136

27. McGarry JD, Takabayashi Y, Foster DW. The role of malonyl-coa in the coordination of fatty acid synthesis and oxidation in isolated rat hepatocytes. J Biol Chem 1978;253:8294-8300

28. Knowles JR. The mechanism of biotin-dependent enzymes. Ann Rev Biochem 1989;58:195-221

29. Tong L. Acetyl-coenzyme A carboxylase: crucial metabolic enzyme and attractive target for drug discovery. Cell Mol Life Sci 2005;62:1784-1803

30. Thampy KG. Formation of malonyl coenzyme A in rat heart. Identification and purification of an isozyme of A carboxylase from rat heart. J Biol Chem 1989;264:17631-17634

31. Abu-Elheiga L, Almarza-Ortega DB, Baldini A, Wakil SJ. Human acetyl-CoA carboxylase 2. Molecular cloning, characterization, chromosomal mapping, and evidence for two isoforms. Journal of Biological Chemistry 1997;272:10669-10677

32. Mao J, Chirala SS, Wakil SJ. Human acetyl-CoA carboxylase 1 gene: presence of three promoters and heterogeneity at the 5'-untranslated mRNA region. Proc Natl Acad Sci U S A 2003;100:7515-7520

33. Eberle D, Hegarty B, Bossard P, Ferre P, Foufelle F. SREBP transcription factors: master regulators of lipid homeostasis. Biochimie 2004;86:839-848

34. Lin J, Yang R, Tarr PT, et al. Hyperlipidemic effects of dietary saturated fats mediated through PGC-1beta coactivation of SREBP. Cell 2005;120:261-273

35. Ogiwara H, Tanabe T, Nikawa J, Numa S. Inhibition of rat-liver acetyl-coenzyme-A carboxylase by palmitoyl-coenzyme A. Formation of equimolar enzyme-inhibitor complex. Eur J Biochem 1978;89:33-41

36. Park SH, Gammon SR, Knippers JD, et al. Phosphorylation-activity relationships of AMPK and acetyl-CoA carboxylase in muscle. J Appl Physiol 2002;92:2475-2482

37. Abu-Elheiga L, Oh W, Kordari P, Wakil SJ. Acetyl-CoA carboxylase 2 mutant mice are protected against obesity and diabetes induced by high-fat/high-carbohydrate diets. Proc Natl Acad Sci USA 2003;100:10207-10212

38. Choi CS, Savage DB, Abu-Elheiga L, et al. Continuous fat oxidation in acetyl-CoA carboxylase 2 knockout mice increases total energy expenditure, reduces fat mass, and improves insulin sensitivity. Proc Natl Acad Sci USA 2007;104:16480-16485

39. Hoehn KL, Turner N, Swarbrick MM, et al. Acute or chronic upregulation of mitochondrial fatty acid oxidation has no net effect on whole-body energy expenditure or adiposity. Cell metabolism 2010;11:70-76

40. Olson DP, Pulinilkunnil T, Cline GW, Shulman GI, Lowell BB. Gene knockout of Acc2 has little effect on body weight, fat mass, or food intake. Proc Natl Acad Sci USA 2010;107:7598-7603

41. Abu-Elheiga L, Matzuk MM, Kordari P, et al. Mutant mice lacking acetyl-CoA carboxylase 1 are embryonically lethal. Proc Natl Acad Sci USA 2005;102:12011-12016

42. Harada N, Oda Z, Hara Y, et al. Hepatic de novo lipogenesis is present in liver-specific ACC1-deficient mice. Mol Cell Biol 2007;27:1881-1888

43. Mao J, DeMayo FJ, Li H, et al. Liver-specific deletion of acetyl-CoA carboxylase 1 reduces hepatic triglyceride accumulation without affecting glucose homeostasis. Proc Natl Acad Sci U S A 2006;103:8552-8557

44. Bourbeau MP, Bartberger MD. Recent advances in the development of acetyl-CoA carboxylase (ACC) inhibitors for the treatment of metabolic disease. J Med Chem 2015;58:525-536

45. Gerth K, Bedorf N, Irschik H, Hofle G, Reichenbach H. The soraphens: a family of novel antifungal compounds from Sorangium cellulosum (Myxobacteria). I. Soraphen A1 alpha: fermentation, isolation, biological properties. J Antibiot (Tokyo) 1994;47:23-31

46. Vahlensieck HF, Pridzun L, Reichenbach H, Hinnen A. Identification of the yeast ACC1 gene product (acetyl-CoA carboxylase) as the target of the polyketide fungicide soraphen A. Curr Genet 1994;25:95-100

47. Beckers A, Organe S, Timmermans L, et al. Chemical inhibition of acetyl-CoA carboxylase induces growth arrest and cytotoxicity selectively in cancer cells. Cancer Res 2007;67:8180-8187

48. Jump DB, Torres-Gonzalez M, Olson LK. Soraphen A, an inhibitor of acetyl CoA carboxylase activity, interferes with fatty acid elongation. Biochem Pharmacol 2011;81:649-660

49. Schreurs M, van Dijk TH, Gerding A, et al. Soraphen, an inhibitor of the acetyl-CoA carboxylase system, improves peripheral insulin sensitivity in mice fed a high-fat diet. Diabetes Obes Metab 2009;11:987-991

50. Lodhi IJ, Yin L, Jensen-Urstad AP, et al. Inhibiting adipose tissue lipogenesis reprograms thermogenesis and PPARgamma activation to decrease diet-induced obesity. Cell Metab 2012;16:189-201

51. Spalding KL, Arner E, Westermark PO, et al. Dynamics of fat cell turnover in humans. Nature 2008;453:783-787

52. Lowe CE, O'Rahilly S, Rochford JJ. Adipogenesis at a glance. J Cell Sci 2011;124:2681-2686

53. Rosen ED, MacDougald OA. Adipocyte differentiation from the inside out. Nat Rev Mol Cell Biol 2006;7:885-896

54. Mackall JC, Student AK, Polakis SE, Lane MD. Induction of lipogenesis during differentiation in a "preadipocyte" cell line. J Biol Chem 1976;251:6462-6464

55. Tamori Y, Masugi J, Nishino N, Kasuga M. Role of peroxisome proliferator-activated receptor-gamma in maintenance of the characteristics of mature 3T3-L1 adipocytes. Diabetes 2002;51:2045-2055

56. Mueller E, Drori S, Aiyer A, et al. Genetic analysis of adipogenesis through peroxisome proliferator-activated receptor gamma isoforms. J Biol Chem 2002;277:41925-41930

57. Varga T, Czimmerer Z, Nagy L. PPARs are a unique set of fatty acid regulated transcription factors controlling both lipid metabolism and inflammation. Biochim Biophys Acta 2011;1812:1007-1022

58. Tzameli I, Fang H, Ollero M, et al. Regulated production of a peroxisome proliferator-activated receptor-gamma ligand during an early phase of adipocyte differentiation in 3T3-L1 adipocytes. J Biol Chem 2004;279:36093-36102

59. Ayers SD, Nedrow KL, Gillilan RE, Noy N. Continuous nucleocytoplasmic shuttling underlies transcriptional activation of PPARgamma by FABP4. Biochemistry 2007;46:6744-6752

60. James DE, Brown R, Navarro J, Pilch PF. Insulin-regulatable tissues express a unique insulin-sensitive glucose transport protein. Nature 1988;333:183-185

61. Brasaemle DL, Subramanian V, Garcia A, Marcinkiewicz A, Rothenberg A. Perilipin A and the control of triacylglycerol metabolism. Mol Cell Biochem 2009;326:15-21

62. Rondinone CM. Adipocyte-derived hormones, cytokines, and mediators. Endocrine 2006;29:81-90

CHAPTER I β-KETO AND β-HYDROXYPHOSPHONATE ANALOGS OF BIOTIN-5'-AMP ARE INHIBITORS OF HOLOCARBOXYLASE SYNTHETASE

Wantanee Sittiwong a,†,‡, Elizabeth L. Cordonier b,†, Janos Zempleni b,*, Patrick H. Dussault a,*

[a]Department of Chemistry, University of Nebraska-Lincoln, Lincoln, NE 68588-0304, USA

[b]Department of Nutrition and Health Sciences, University of Nebraska-Lincoln, Lincoln, NE 68583-0806, USA

* Corresponding authors. Fax: +1 402 472 1587 (J.Z.), +1 402 472 9402 (P.H.D.).
E-mail addresses: jzempleni2@unl.edu (J. Zempleni), pdussault1@unl.edu (P.H. Dussault).

† These authors contributed equally to the research.

‡Current address: Department of Chemistry, Thammasat University, Pathumthani 12120, Thailand.

Abstract

Holocarboxylase synthetase (HLCS) catalyzes the covalent attachment of biotin to cytoplasmic and mitochondrial carboxylases, nuclear histones, and over a hundred human proteins. Nonhydrolyzable ketophosphonate (β-ketoP) and hydroxyphosphonate (β-hydroxyP) analogs of biotin-5′-AMP inhibit holocarboxylase synthetase (HLCS) with IC_{50} values of 39.7 μM and 203.7 μM. By comparison, an IC_{50} value of 7 μM was observed with the previously reported biotinol-5′-AMP. The K_i values, 2.0 μM and 10.4 μM, respectively, are consistent with the IC_{50} results, and close to the K_i obtained for biotinol-5′-AMP (7 μM). The β-ketoP and β-hydroxyP molecules are competitive inhibitors of HLCS while biotinol-5′-AMP inhibited HLCS by a mixed mechanism.

Introduction

Holocarboxylase synthetase (HLCS) is the sole enzyme in the human proteome capable of catalyzing the covalent attachment of biotin to lysine residues.[1] HLCS localizes in the cytoplasm, mitochondria, and cell nuclei.[1,2] HLCS catalyzes biotinylation of five carboxylases in mitochondria and cytoplasm, which play key roles in gluconeogenesis, fatty acid metabolism, and leucine metabolism.[3] In addition, a recent mass spectrometry screen identified 108 novel biotinylated proteins; heat shock proteins and enzymes from glycolysis are overrepresented among these proteins.[4] HLCS orchestrates the assembly of a multiprotein gene repression complex in human chromatin, partially mediated through HLCS-dependent methylation of the histone methyltransferase EHMT1 and the nuclear receptor co-repressor N-CoR.[5] Consistent with the importance of HLCS in intermediary metabolism and cell function, no living HLCS null person has ever been reported, and persons with HLCS mutations require lifelong treatment with pharmacological doses of biotin.[6]

HLCS-dependent biotinylation involves basically two steps (Fig. 1). In the first, activation of biotin by ATP generates the mixed anhydride biotin-5′-adenosine monophosphate (Bio-5′-AMP) (1). In the second step, the phosphate anhydride serves as an acylating agent for a target lysine in carboxylases (2), histones (3), and other proteins,[3,4,7] covalently linking biotin to the substrate via an amide bond.

The objective of this study was to develop a new class of synthetic HLCS inhibitors which could potentially be targeted to distinct cellular structures. Such an inhibitor would be a useful analytical tool in studies of HLCS-dependent biotinylation events in the cytoplasm,

mitochondria, and nucleus. We based these studies on analogs of biotin-5′-AMP, namely biotin β-ketophosphonate-5′-AMP (β-ketoP) and biotin β-hydroxyphosphonate-5′-AMP (β-hydroxyP), that substitute a hydrolytically stable phosphonate for the acyl phosphate found in biotin-5′-AMP (Figure 2a). The use of phosphonates as unreactive isosteres of phosphates is well established.[8] For example, nonhydrolyzable aminoacyl analogs of aspartyl adenylate exhibit potent inhibitory activity against *E. coli* aspartyl-tRNA synthetase.[9] There is precedence for the efficacy of structurally analogous compounds sulfamides, sulfonamides, and 1,2,3-triazoles in the inhibition of a microbial biotin protein ligase, the HLCS ortholog BirA (Fig. 2b).[10-13] We also investigated biotinol-5′-AMP, a known phosphate analog of biotin-5′-AMP which replaces the carbonyl oxygen with a methylene (CH_2). [10,14]

Materials and Methods

Inhibitor synthesis (This work was done by W. Sittiwong; I have included it as part of the manuscript).

The central element of the synthesis is the formation of a protected version of a biotin ketophosphonate (4a) via condensation of a biotin derived ketophosphonic acid (3) with a protected adenosine (Scheme 1). The synthesis begins with biotin methyl ester (1), prepared via the acid-catalyzed esterification of biotin.15 Reaction with the carbanion derived from methyl phosphonate was anticipated to offer a convenient route to a precursor of the desired phosphonates. However, reaction of ester 1 with the lithiated methylphosphonate, generated using lithium bis(trimethylsilyl)amide (LiHMDS) or n-butyl lithium (n-BuLi), 100 resulted in poor yields. Fortunately, reaction of the ester with a large

excess of the lithiated phosphonate, followed by quenching with deionized water to minimize demethylation of the phosphonate diester product, produced a 69% yield of dimethyl b-ketophosphonate 2.[16] Selective monodemethylation with lithium bromide provides a good yield of mono ester 3. The pyridinium salt of 3 underwent coupling with 20,30 isopropylidineadenosine (i-PrA) in the presence of O-(benzotriazol-1-yl)-N,N,N0 ,N0-tetramethyluronium hexafluorophosphate (HBTU) to provide a mixed phosphonate diester (4a) in 79% yield for two steps.[17,18] 110 No coupling was observed if N,N0-dicyclohexylcarbodiimide (DCC) was substituted for HBTU. The acidic methylene of the ketone phosphonate was observed (NMR) to readily undergo H/D exchange upon dissolution in d4-MeOH.

Reduction of the ketone with NaBH4 resulted in formation of the corresponding alcohol (4b) as a mixture of diastereomers at the newly formed stereocenter. Stirring the ketone diester (4a) or the alcohol diester (4b) in pyridine/water resulted in selective demethylation to afford monoesters 5a or 5b, respectively. Removal of the acetonide protecting group from the sugar followed by neutralization with ammonium bicarbonate provided the target 120 biotin b-ketophosphonate (b-ketoP) 6a in 58% yield for two steps. The same procedure, when applied to alcohol 5b, furnished biotin-b-hydroxyphosphonate (b-hydroxyP) 6b in 99% yield.

Results

Inhibition of HLCS: Biotin β-ketophosphonate-5′-AMP (β -ketoP, **6a**) inhibited HLCS in a dose-dependent manner. The polypeptide p67 is a substrate for biotinylation by HLCS.

When recombinant p67 was incubated with recombinant HLCS and 20 μM biotin in the presence of 50 to 500 μM β-ketoBP, HLCS inhibition was maximal at the highest inhibitor concentration tested. For example, the inhibition at 500 μM β-ketoBP was 81.3±11.1% ($P<0.01$; n=4) compared with vehicle control (Fig. 3A). Data are presented as mean ± SD of 4 replicates. Incubation of p67 in the absence of HLCS produced no detectable signal (lane 6 in Fig. 3B). Under the conditions used here, IC_{50} and K_i for β-ketoBP equaled 39.7±1.9 μM and 2.0 ±0.1 μM, respectively. When tested under identical conditions, β-hydroxyP inhibited HLCS activity by 67.7 ±10.0% ($P=0.0001$; n=4) at concentrations of 500 μM inhibitor. The IC_{50} and K_i values calculated under these conditions were 203.7 ±3.7 μM and 10.4±0.2 μM, respectively. β-KetoP is a competitive inhibitor of HLCS, based on competition studies with biotin. In these studies, the concentration of the inhibitor was held constant at 250 μM while that of biotin was varied from 0-320 μM; a second curve was generated in the absence of inhibitor (Fig. 3C). The apparent V_{max} was similar for incubations with and without inhibitor [31.5±1.6 vs. 22.3±1.51 pmol biotinylated p67/(nmol HLCS *x* s); n=4] whereas the apparent K_m for biotin was increased by the addition of inhibitor (77.9±10.3 vs. 1.6±1.8 μM biotin; n=4). β-HydroxyP (**6b**) also acts as a competitive inhibitor as evidenced by similar apparent V_{max} values with and without inhibitor [20.6±1.8 vs. 22.6±1.4 pmol biotinylated p67/nmol HLCS *x* s); n=4] whereas reactions incubated with inhibitor increased the apparent K_m for biotin (82.5±20.4 vs. 1.9±1.8 μM biotin; n=4). As a negative control we conducted incubations with a biotin ketophosphonic acid (compound **3** in Scheme 1). This substrate incorporates an electrophilic carbonyl carbon beta to a charged phosphonate but lacks the adenosyl

fragment hypothesized as essential for mediating HLCS inhibition. Consistent with this theory, the ketophosphonic acid compound did not inhibit HLCS (data not shown).

The results were compared against assays conducted with biotinol-AMP, a known phosphate analog of biotin-5′-AMP which has previously been employed for inhibition of BirA (biotin protein ligase).[10,11] Biotinol-AMP reduces HLCS activity by 98.01±0.1% at concentrations of 500μM and has an IC_{50} value and K_i of 8.8±3.6 μM and 754 ± 303 nM, respectively. When reactions incubated with biotinol-AMP were challenged with increasing amounts of up to 320μM biotin, the apparent V_{max} decreased compared to reactions without inhibitor (22.6 ± 1.4 vs. 5.9 ± 1.4 pmol biotinylated p67/(nmol HLCS *x* s); n=4) and K_m increased (1.9 ± 1.8 vs. 146 ± 79; n=4) indicating the biotinol-AMP most likely acts as a mixed inhibitor.

Discussion

There remains limited knowledge regarding the structure of HLCS and the mechanism of catalysis.[11,13b,20] Similarly, little is known about the basis for selectivity between the classic carboxylase targets of HLCS and novel targets in chromatin and other proteins. The objective of this study was to develop a synthetic HLCS inhibitor capable of penetrating cell membranes and which could potentially be targeted to distinct cellular structures. Such an inhibitor would be a useful analytical tool in studies of carboxylase biotinylation in cytoplasm and mitochondria, studies of chromatin protein biotinylation and HLCS-dependent formation of multiprotein gene repression complexes in nuclei, and studies of newly discovered species of biotinylated proteins throughout the cell.

Consistent with the importance of HLCS in intermediary metabolism and epigenetics, no living HLCS null individual has ever been reported, suggesting embryonic lethality. HLCS knockdown in Drosophila melanogaster (30% residual activity) produces phenotypes such as decreased life span and reduced heat resistance.[21] Mutations and single nucleotide polymorphisms have been identified and characterized in the human HLCS gene; these mutations cause a substantial decrease in HLCS activity, aberrant gene regulation and metabolic abnormalities.[6,22] Unless diagnosed and treated at an early stage, homozygous severe HLCS deficiency is characteristically fatal.[23] Three independent cancer and patent databases correlate HLCS loss or mutation with an increase in detected tumors.[24]

Several classes of biotin-50-AMP analogs have been applied to study the function of biotin protein ligases (BPLs), exemplified by HLCS as well as BirA, an enzyme catalyzing biotinylation of acyl carrier protein in prokaryotes.[10,13,14] BirA from E. coli has 21% sequence similarity to HLCS.[25] Biotinol-50-AMP, a phosphate ester lacking the acyl carbonyl of biotin-50-AMP, binds tightly to the Escherichia coli biotin repressor (KD = 1.5 ± 0.2 nM)11,20 and inhibits biotin transfer to the acceptor protein.[10,14] Biotinol-50-AMP also binds tightly to Staphylococcus aureus BPL (Ki = 0.03 ± 0.01 lM). The activity of this analog would appear to suggest the key role of the phosphate moiety and the relative lack of importance of hydrogen-bonding interactions to the acyl carbonyl of biotin-50-AMP. However, other work has demonstrated that a sulfamoylcontaining bisubstrate analog, replacing the acyl phosphate with an acyl sulfonamide, strongly binds Mycobacteria tuberculosis BPL (MtBPL); a co-crystal revealing multiple hydrogen-bonding interactions between the protein and the acyl sulfonamide.[12] More recently, a biotin-50-AMP analog

replacing the acyl phosphate witha 1,2,3-triazole was found to bind tightly to BPL and exhibit >1100-fold selectivity for the S. aureus BPL over the human homologue.13 This suggests the possibility of designing potent inhibitors of bacterial BPL. However, no similar approach has been used to studythe function of HLCS or human BPL.

A model of the HLCS/biotin-50-AMP complex as well as the crystal structure of biotin-50-AMP with BPL from Pyrococcus horikoshii OT3 (pdb:1wqw) suggests the importance of hydrogen bonding involving the carbonyl and phosphonate oxygen (Fig. S1).[13b,22b] The b-ketophosphonate and b-hydroxyphosphonate analogs introducedhere maintain the natural charge state of biotin-AMP and place a basic oxygen atom beta to the phosphonate group. However, in contrast to the BirA inhibitors described above, the ketophosphonate (b-ketoP, 6) incorporates an electrophilic carbon at the location of the original acyl group in biotin-50-AMP. Although the reduced activity of the new inhibitors compared with biotinol-AMP suggests that preservation of an electrophilic center (C=O) or hydrogen bonding group (CHOH) beta to phosphonate is of limited importance in inhibitor design, we note that the1,2,3-triazole analogs completely lacking a carbonyl group show no inhibition toward human BPL. It is also possible that conformational differences between the acyl phosphate of biotin-50-AMP and the phosphonate of 6a and 6b might also contribute to the reduced binding observed.

In conclusion, we have described a new class of inhibitors of holocarboxylase synthetase HLCS based upon replacement of the ester of biotin-50-AMP with a ketone or a secondary alcohol. The analogs produce significant levels of inhibition with isolated enzyme. Efficacy of the new inhibitors in vivo has not been tested and further investigations are warranted.

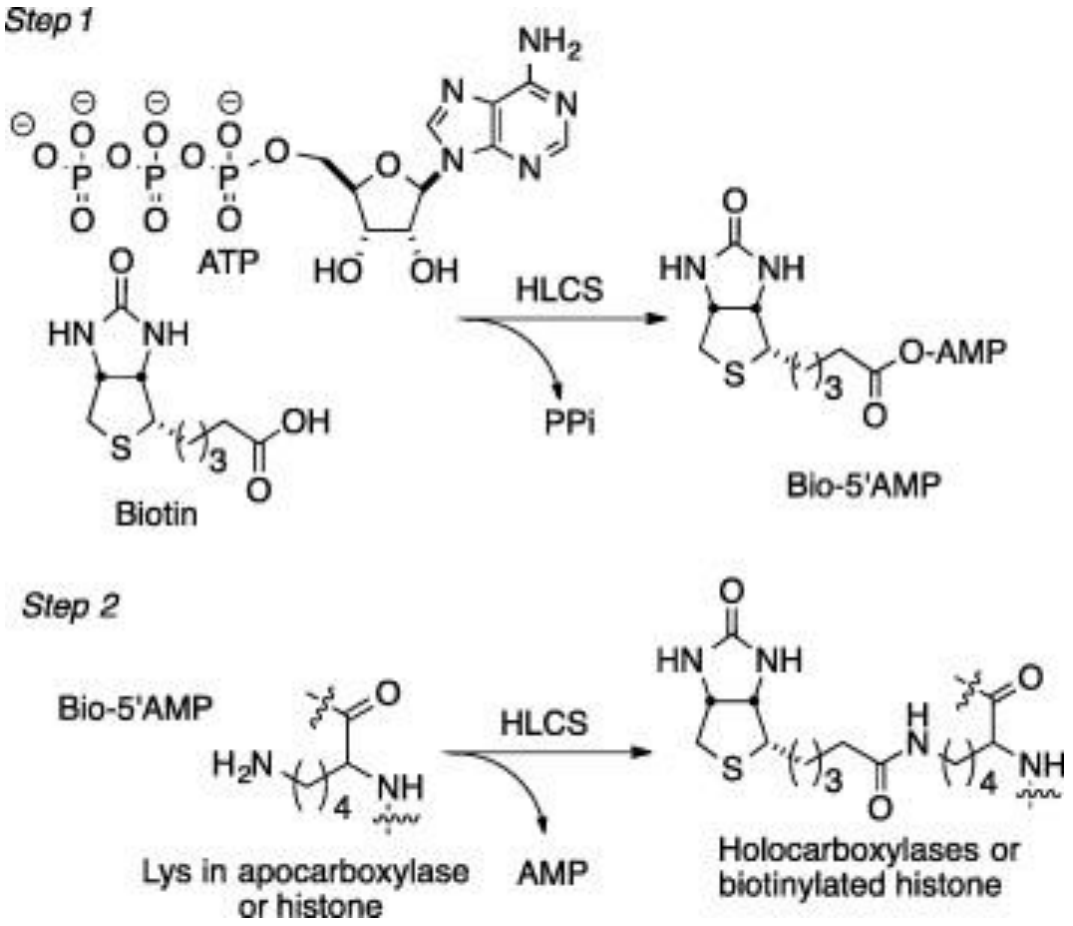

Fig 1. HLCS catalysis

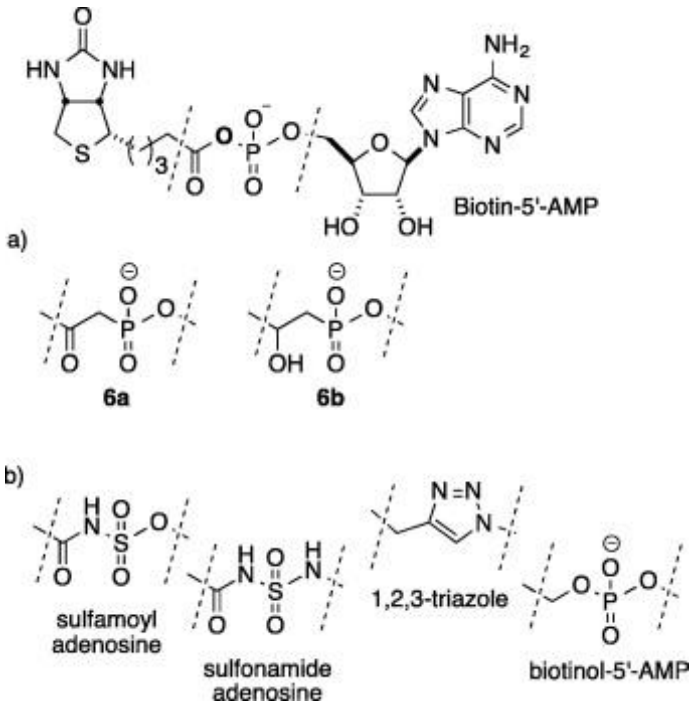

Figure 2. (a) Chemical structure of biotin-5′-AMP and ketophosphonate (6a) and hydroxyphosphonate (6b) analogs; (b) reported sulfamoyl, sulfonamide, triazole, and phosphate inhibitors.

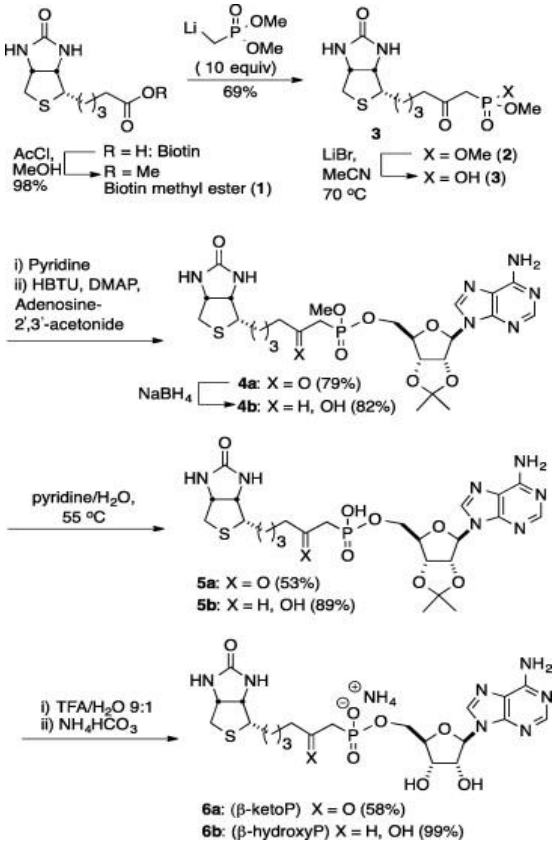

Scheme 1. Synthesis of ketophosphonate (β-ketoP) and hydroxyphosphonate (β-hydroxyP) analogs of biotin-5′-AMP

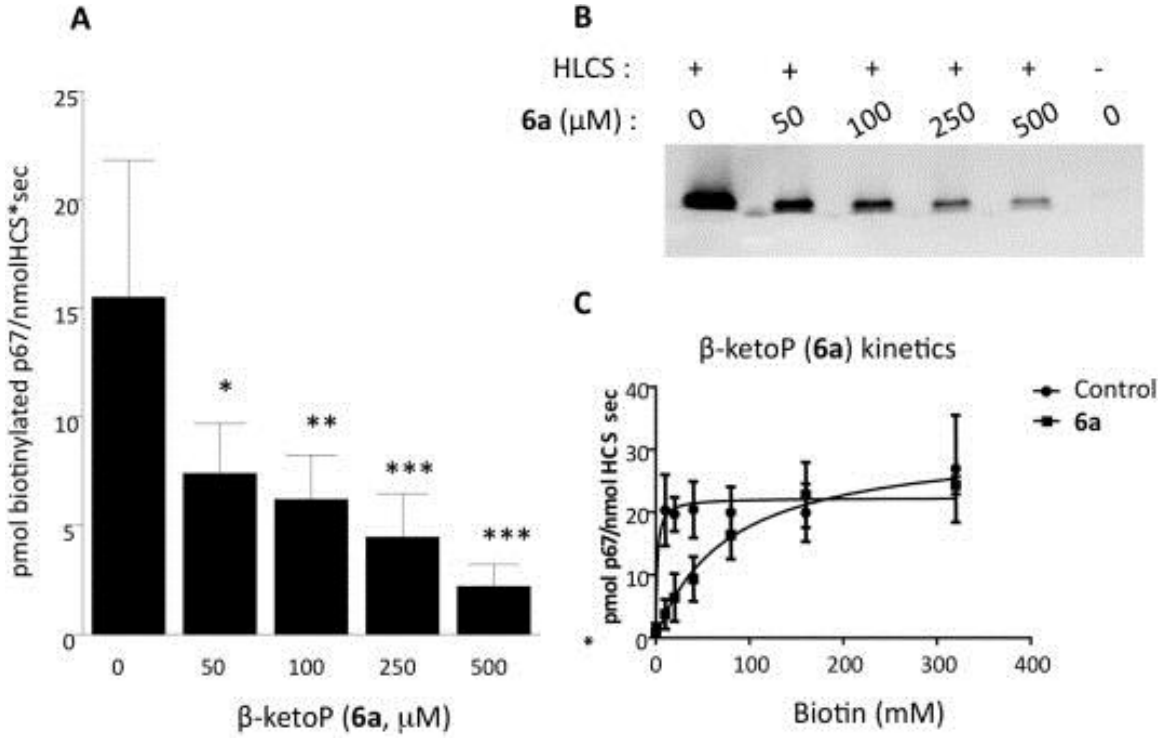

Figure 3. Inhibition of HLCS by biotin β-ketophosphonate-5′-AMP. (A) HLCS activity was quantified using infrared absorbance in the presence of 20 μM biotin and various concentrations of biotin β-ketophosphonate-5′-AMP (One way-ANOVA; $^{*}P<0.05$; N = 4; Dunnett's multiple t-test $^{*}p<0.05$, $^{**}p<0.01$, $^{***}p<0.001$). (B) Representative gel, depicting biotinylation of p67 in the presence of various concentrations of biotin β-ketophosphonate-5′-AMP. Lane 6 shows p67 incubated in the absence of HLCS. (C) Competitive inhibition of HLCS by biotin β-ketophosphonate-5′-AMP.

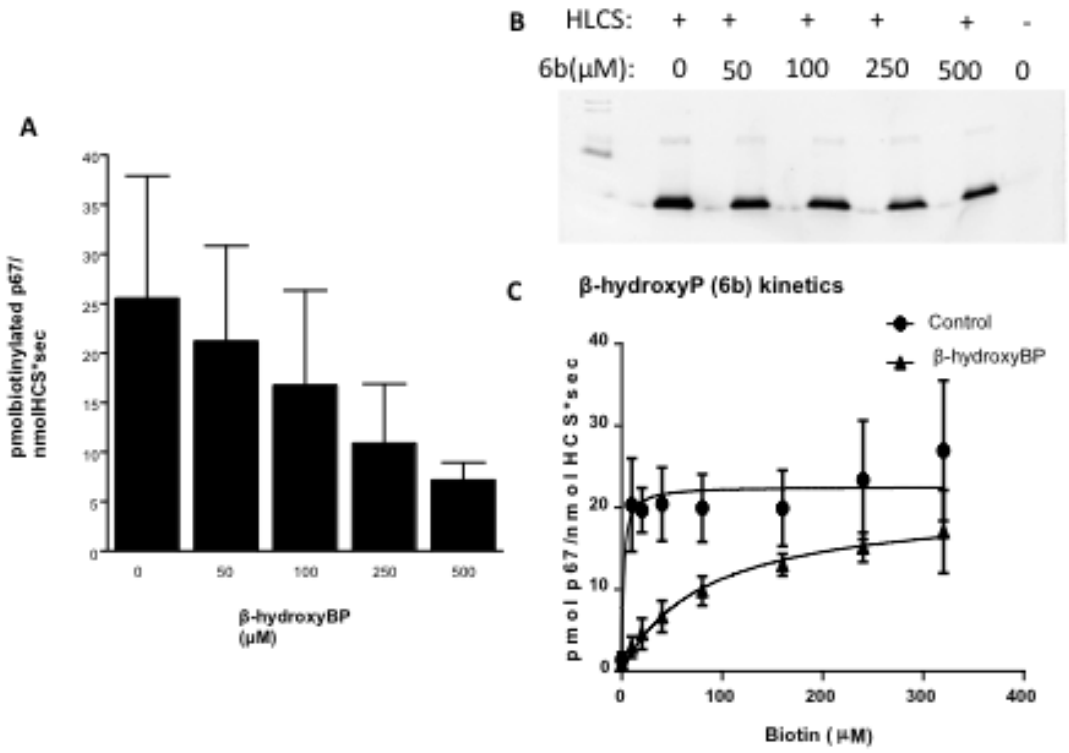

Figure 4. Inhibition of HLCS by biotin β-hydroxyphosphonate-5′-AMP. (A) HLCS activity was quantified using infrared absorbance in the presence of 20 μM biotin and various concentrations of biotin β-hydroxyphosphonate-5′-AMP (One way-ANOVA; $^{*}P<0.05$; N = 4; Dunnett's multiple t-test $^{*}p<0.05$, $^{**}p<0.01$, $^{***}p<0.001$). (B) Representative gel, depicting biotinylation of p67 in the presence of various concentrations of biotin β-hydroxyphosphonate-5′-AMP. Lane 6 shows p67 incubated in the absence of HLCS. (C) Competitive inhibition of HLCS by biotin β-hyroxyphosphonate-5′-AMP.

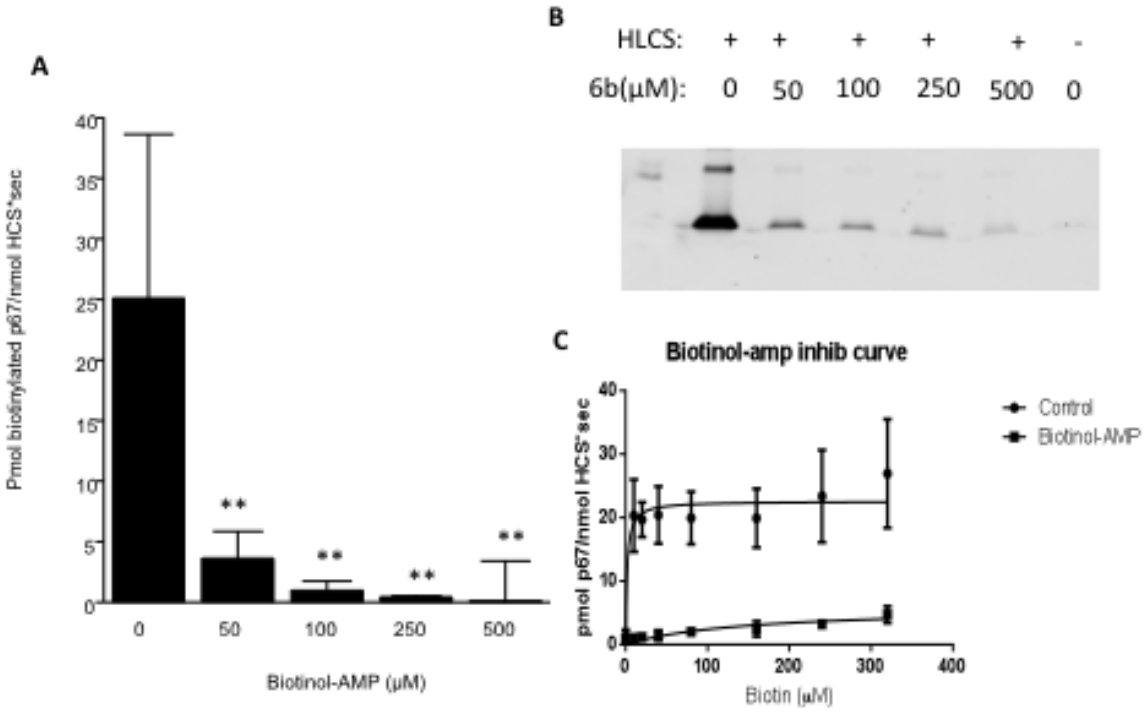

Figure 5. Inhibition of HLCS by biotinol-5′-AMP. (A) HLCS activity was quantified using infrared absorbance in the presence of 20 μM biotin and various concentrations of biotinol-5′-AMP (One way-ANOVA; $^{*}P<0.05$; N = 4; Dunnett's multiple t-test $^{*}p<0.05$, $^{**}p<0.01$, $^{***}p<0.001$). (B) Representative gel, depicting biotinylation of p67 in the presence of various concentrations of biotinol-5′-AMP. Lane 6 shows p67 incubated in the absence of HLCS. (C) Competitive inhibition of HLCS by biotin β-hyroxyphosphonate-5′-AMP.

References

1. (a) Chiba, Y.; Suzuki, Y.; Aoki, Y.; Ishida, Y.; Narisawa, K. Arch. Biochem. Biophys. 1994, 313, 8; (b) Suzuki, Y.; Aoki, Y.; Ishida, Y.; Chiba, Y.; Iwamatsu, A.; Kishino, T.; Niikawa, N.; Matsubara, Y.; Narisawa, K. Nat. Genet. 1994, 8, 122.

2. (a) Bailey, L. M.; Wallace, J. C.; Polyak, S. W. Arch. Biochem. Biophys. 2010, 496, 45; (b) Bao, B.; Wijeratne, S. S.; Rodriguez-Melendez, R.; Zempleni, J. Biochem. Biophys. Res. Commun. 2011, 412, 115.

3. Biotin; Zempleni, J., Wijeratne, S. S. K., Kuroishi, T., Eds.Present Knowledge in Nutrition; Erdman, J. W., Jr., Macdonald, I., Zeisel, S. H., Eds.; International Life Sciences Institute: Washington, D.C., 2012; 10, p 587.

4. Li, Y.; Malkaram, S. A.; Zhou, J.; Zempleni, J. J. Nutr. Biochem. 2014, 25, 475.

5. (a) Li, Y.; Hassan, Y. I.; Moriyama, H.; Zempleni, J. J. Nutr. Biochem. 2013, 24, 1446; (b) Xue, J.; Wijeratne, S.; Zempleni, J. Epigenetics 2013, 8(5), 504; (c) Liu, D.; Zempleni, J. Biochem. J. 2014, 461, 477.

6. Suzuki, Y.; Yang, X.; Aoki, Y.; Kure, S.; Matsubara, Y. Hum. Mutat. 2005, 26, 285.

7. Lane, M. D.; Young, D. L.; Lynen, F. J. Biol. Chem. 1964, 239, 2858.

8. (a) Thatcher, R. J.; Campbell, A. S. J. Org. Chem. 1993, 58, 2272; (b) Engel, R. Chem. Rev. 1977, 77, 349.

9. Bernier, S.; Akochy, P. M.; Lapointe, J.; Chênevert, R. Bioorg. Med. Chem. 2005, 13, 69.

10. Brown, P. H.; Cronan, J. E.; Grøtli, M.; Beckett, D. J. Mol. Biol. 2004, 337, 857.

11. Brown, P. H.; Beckett, D. Biochemistry 2005, 44, 3112.

12. Duckworth, B. P.; Geders, T. W.; Tiwari, D.; Boshoff, H. I.; Sibbald, P. A.; Barry, C.E.; Schnappinger, D.; Finzel, B. C.; Aldrich, C. C. Chem. Biol. 2011, 18, 1432.

13. (a) Soares da Costa, T.; Tieu, W.; Yap, M.; Pendini, N.; Polyak, S.; Pedersen, D.; Morona, R.; Turnidge, J.; Wallace, J.; Wilce, M.; Booker, G.; Abell, A. J. Biol. Chem. 2012, 287, 17823; (b) Paparella, A. S.; Soares da Costa, T.; Yap, M. Y.; Tieu, W.; Wilce, M. C. J.; Booker, G. W.; Abell, A. D.; Polyak, S. W. Curr. Top. Med. Chem. 2014, 14, 4.

14. Wood, Z. A.; Weaver, L. H.; Brown, P. H.; Beckett, D.; Matthews, B. W. J. Mol. Biol. 2006, 357, 509.

15. Slavoff, S. A.; Chen, I.; Choi, Y. A.; Ting, A. Y. J. Am. Chem. Soc. 2008, 130, 1160.

16. Maloney, K. M.; Chung, J. Y. L. J. Org. Chem. 2009, 74, 7574.

17. Balg, C.; Blais, S. P.; Bernier, S.; Huot, J. L.; Couture, M.; Lapointe, J.; Chênevert,R. Biorg. Med. Chem. 2007, 15, 295.

18. Campagne, J.-M.; Coste, J.; Jouin, P. J. Org. Chem. 1995, 60, 5214.

19. Kobza, K.; Sarath, G.; Zempleni, J. BMB Rep. 2008, 41, 310.

20. Naganathan, S.; Beckett, D. J. Mol. Biol. 2007, 373, 96. http://dx.doi.org/10.1016/j.jmb.2007.07.020.

21. Camporeale, G.; Giordano, E.; Rendina, R.; Zempleni, J.; Eissenberg, J. C. J. Nutr. 2006, 136, 2735.

22. (a) National Center for Biotechnology Information, Online Mendelian Inheritance in Man. 2008; http://www.ncbi.nlm.nih.gov/omim (accessed: 10/

29/2014).; (b) Esaki, S.; Malkaram, S. A.; Zempleni, J. Eur. J. Hum. Genet. 2012, 20, 428.

23. Thuy, L. P.; Belmont, J.; Nyhan, W. L. Prenat. Diagn. 1999, 19, 108.

24. UniProt UniProtKB. www.uniprot.org/uniprot/P50747 (accessed: 10/29/2014).; Massague, J.; Bos, P. Metastasis promoting genes and proteins. www.faqs.org/patents/app/20100029748 (accessed: 10/29/2014).; Institute for Biomedical Technologies. Genes-to-system breast cancer database. www.itb.cnr.it/breastcancer/php/showMostCorrelated.php?id=6664 (accessed: 10/29/2014).

25. Hassan, Y. I.; Moriyama, H.; Olsen, L. J.; Bi, X.; Zempleni, J. Mol. Genet. Metab. 2009, 96, 183.

Supplementary methods

Expression and purification of HLCS

ArcticExpress (DE3) Competent Cells (Agilent Technologies; Santa Clara, CA) transformed with HCS-pET41a(+) [Bao, Pestinger et al. 2011] were cultured in LB Broth Medium with 50 μg/ml of kanamycin and 20 μg/ml of gentamycin , and incubated overnight at 37°C. Bacteria were allowed to grow until an OD600 of 0.5- 1.0 was reached. Addition of isopropyl-beta-D-thiogalactopyranosid (IPTG) at a final concentration of 1mM induced protein expression and cells were incubated for an additional 24 hours at 12°C. Cells were centrifuged at 4°C (3,000 g for 30 minutes) and precipitated cells were resuspended in PBS with protease inhibitor cocktail (Sigma-Aldrich; St. Louis, MO). Samples were sonicated on ice (Branson 250 Digital Sonifier, Danbury, CT) three times for 10-second burst alternating between 10-second resting periods on ice. The lysate were centrifuged at 10,000 g for 10 minutes at 4°C. HCS fusion protein were purified by GSTrapTM FF Columns (GE Healthcare; Piscataway, NJ) on ÄKTA™protein purification system (GE Healthcare). HLCS in column fraction was identified by gel electrophoresis followed by coomassie blue staining.

Expression and purification of p67

The polypeptide p67 is frequently used to confirm biological activity of HCS. It is the C-terminal 67 amino acid biotin carboxyl carrier (BCC) domain of the propionyl- CoA

carboxylase (PCC) α subunit (Leu637-Glu703). RosettaTM 2(DE3) Competent Cells (EMD Chemicals; Gibbstown, NJ) transformed with p67- pET30 [Kobza, Sarath et al. 2008] were cultured in LB Broth containing 15 µl of kanamacyn, and incubated overnight at 37°C. Cells were grown until an OD600 of 0.5 - 0.6 was reached. p67 expression was induced by addition of 1mM IPTG and incubated for 16 hours at 37°C. After incubation, samples were centrifugated at 3,000 g for 30 minutes and purified using His Trap FF Columns (GE Healthcare) on an ÄKTA™ protein purification system (GE Healthcare). Because BirA ligase in Escherichia coli is known to biotinylate some of the recombinant p67, the biotinylated fraction of p67 was removed using avidin columns.

HLCS activity

This assay is based on the HLCS dependent biotinylation of the p67 polypeptide. Briefly, recombinant biotin-free p67 and human HLCS and were prepared as described.[1] The polypeptide p67 comprises the 67 C-terminal amino acids in PCC, including the biotin-binding site K694; p67 is a well-established substrate for biotinylation by HLCS. Briefly, 30 nM HLCS was incubated with 2 µM p67 in 75 mM Tris-acetate (pH 7.5), 45 mM $MgCl_2$, 7.5 mM ATP, 0.3 mM DTT, and 20 µM biotin in the presence of 0.05 to 0.5 mM biotin β-ketoP, β-hydroxyP, or bio-5'-AMP (50 µl final volume) at 37ºC for 2 h; controls were incubated in the absence of inhibitor. Reactions were stopped by the addition of 50 µl of Tricine loading dye (Invitrogen) and heating at 95ºC for 10 min. Proteins were run on 16% Tricine gels and transferred to polyvinylidene blots. Biotinylated p67 was probed

using anti-biotin and anti-goat conjugated secondary antibody, and was quantified using an Odyssey infrared imaging system.

Competitive inhibition assays

These experiments use a similar approach to HLCS activity assays with some modifications. Briefly, 30 nM HLCS was incubated with 6 µM p67 and cofactors as described previously. Reactions were incubated either in the presence or absence of 250 µM inhibitor and challenged with increasing amounts of biotin ranging from 0-360 µM. Reactions were stopped by addition of 50 µl Tricine loading dye (Invitrogen) and heating at 95ºC for 10 min, and proteins were analyzed by Western blot analysis as described previously. Data presented in the paper reflects mean±SD of 4 replicates.

IC_{50} and K_i Calculation

The Michaelis-Menten constant (K_m) and IC_{50} values were calculated using nonlinear regression analysis in Graph Pad Prism 6.0 software. The K_m was estimated by plotting substrate concentration vs. velocity obtained from enzyme activity and competition assays, and fitting the curve to the Michaelis-Menten equation. The half-maximal inhibitory concentration (IC_{50}) was calculated by plotting the logarithm of the concentration of substrate vs. binding and the curve generated was fit to the competition binding equation, One-site-Fit-logIC_{50}. K_i was calculated from IC_{50} using an online-based tool.[2]

Statistics

One-way ANOVA was used to determine whether differences among treatment groups were significantly different. Dunnett's multiple comparisons t-test was used to determine

if differences between the control and individual treatment groups were statistically significant. Statistical analysis was performed in Graph Pad Prism 6.0.

References

1. Camporeale, G.; Giordano, E.; Rendina, R.; Zempleni, J.; Eissenberg, J. C., J. Nutr. 2006, 136, 2735.

2. Cer R.Z.; Mudunuri, U.; Stephens, R.; Lebeda, F. J., Nucleic Acids Res. 2009, 37 (suppl 2): W441.

CHAPTER II. RESVERATROL COMPOUNDS INHIBIT HUMAN HOLOCARBOXYLASE SYNTHETASE AND CAUSE A LEAN PHENOTYPE IN *DROSOPHILA MELANOGASTER*

Elizabeth L. Cordonier[a]*, Riem Adjam[a]*, Daniel Camara Teixeira[a], Simone Onur[b], Richard Zbasnik[c], Paul E. Read[d], Frank Döring[b], Vicki L. Schlegel[c], Janos Zempleni[a,**]

(Last names are underlined)

[a]*Department of Nutrition and Health Sciences, University of Nebraska-Lincoln, 316 Ruth Leverton Hall, Lincoln, NE 68583-0806, USA*

[b]*Abteilung Molekulare Prävention, Institut für Humanernährung und Lebensmittelkunde, Universität Kiel, Heinrich-Hecht-Platz 10, 24118 Kiel, Germany*

[c]*Department of Food Science and Technology, University of Nebraska-Lincoln, 326 Filley Hall, Lincoln, NE 68583-0806, USA*

[d]*Department of Agronomy, University of Nebraska-Lincoln, 377 Plant Science Hall, Lincoln, NE 68583-0724, USA*

*These authors contributed equally to the paper.

**Corresponding author. Phone: (402) 472 3270; fax: (402) 472 1587; email: jzempleni2@unl.edu. Address: Department of Nutrition and Health Sciences, University of Nebraska-Lincoln, 316C Ruth Leverton Hall, Lincoln, NE 68583-0806, USA.

ABSTRACT

Holocarboxylase synthetase (HLCS) is the sole protein-biotin ligase in the human proteome. HLCS has key regulatory functions in intermediary metabolism, including fatty acid metabolism, and in gene repression through epigenetic mechanisms. The objective of this study was to identify foodborne inhibitors of HLCS that alter HLCS-dependent pathways in metabolism and gene regulation. When libraries of extracts from natural products and chemically pure compounds were screened for HLCS inhibitor activity, resveratrol compounds in grape materials caused an HLCS inhibition of >98% *in vitro*. The potency of these compounds was piceatannol > resveratrol > piceid. Grape-borne compounds other than resveratrol metabolites also contributed toward HLCS inhibition, e.g., p-coumaric acid and cyanidin chloride. HLCS inhibitors had meaningful effects on body fat mass. When *Drosophila melanogaster brummer* mutants, which are genetically predisposed to storing excess amounts of lipids, were fed diets enriched with grape leaf extracts and piceid, body fat mass decreased by more than 30% in males and females. However, Drosophila responded to inhibitor treatment with an increase in the expression of HLCS, which elicited an increase in the abundance of biotinylated carboxylases *in vivo*. We conclude that mechanisms other than inhibition of HLCS cause body fat loss in flies. We propose that the primary candidate is the inhibition of the insulin receptor/Akt signaling pathway.

Keywords: Grapes, fat mass, Drosophila, holocarboxylase synthetase, inhibitor, resveratrol compounds.

1. Introduction

Holocarboxylase synthetase (HLCS) has essential functions in intermediary metabolism and gene regulation. The roles of HLCS in intermediary metabolism are mediated by five carboxylases, which attain biological activity through HLCS-dependent binding of the coenzyme biotin to distinct lysine residues in acetyl-CoA carboxylases (ACC) 1 and 2, pyruvate carboxylase (PC), propionyl-CoA carboxylase (PCC), and 3-methylcrotonyl-CoA carboxylase (MCC) [1]. All five carboxylases catalyze the covalent binding of bicarbonate to organic acids. ACC1 and ACC2 convert acetyl-CoA to malonyl-CoA in key steps in cytoplasmic fatty acid synthesis and the regulation of mitochondrial fatty acid uptake, respectively. PC converts pyruvate to oxaloacetate in gluconeogenesis in the cytoplasm. PCC converts propionyl-CoA to methylmalonyl-CoA in the metabolism of odd-chain fatty acids in cytoplasm. MCC converts 3-methylcrotonyl-CoA to 3-methylglutaconyl-CoA in leucine metabolism in cytoplasm. Recently, 108 new biotinylated protein were discovered by mass spectrometry analysis [2]. The biological function of their biotinylation is unknown, despite some evidence that biotinylation plays a role in the functionality of heat shock proteins [2,3].

Theoretically, inhibition of HLCS-dependent biotinylation of ACC1 and ACC2 might lead to a decrease in body fat. For example, preventing the biotinylation of ACC2 in the outer mitochondrial membrane would lead to decreased production of malonyl-CoA in the mitochondrial microdomain. Malonyl-CoA is a strong inhibitor of carnitine palmitoyltransferase 1, thereby decreasing the uptake and β-oxidation of fatty acids in

mitochondria [4]. Consistent with this observation, de-repression of carnitine palmitoyltransferase 1 by loss of ACC2 causes an increase in the β-oxidation of fatty acids. For example, energy expenditure and resistance to diabetes increase in ACC2 knockout mice compared with wild-type mice [5]. While these findings are controversial [6-8], a targeted inhibition of HLCS-dependent biotinylation of ACC2 in the outer mitochondrial microenvironment might prove to be a productive approach to improving metabolic health. Here, we tested the effects of a novel class of HLCS inhibitors, resveratrol metabolites, on carboxylase biotinylation and body fat mass in *Drosophila melanogaster*. Specifically, we sought to determine whether loss of carboxylase biotinylation is a more likely mechanism for decreasing body fat than the recently reported inhibition of insulin receptor-dependent insulin/Akt signaling pathway [9].

2. Materials and methods

2.1. HLCS activity

Two types of assays were employed to quantify HLCS activity. The basic principle is the same for both assays: Recombinant, full-length human HLCS (rHLCS) is prepared and purified as described [10]. rHLCS is incubated with biotin, cofactors, and the recombinant polypeptide p67, which comprises the 67 C-terminal amino acids in PCC, including the biotin-binding site K694 [11]. HLCS-dependent binding of biotin to p67 is assessed using streptavidin as probe. In the high-throughput variation of the assay, p67 is adsorbed to the plastic surface in 96-well plates for subsequent biotinylation by HLCS and quantification

using IRDye®-800CW-streptavidin and an Odyssey infrared imaging system (LI-COR, Lincoln, NE, USA). In the low-throughput variation of the assay, samples are incubated in a test tube, resolved by gel electrophoresis, and p67-bound biotin in transblots is probed with IRDye®-800CW-streptavidin and the Odyssey infrared imaging system. HLCS- or p67-free samples are used as negative controls in both assays. The gel-based assay has the advantage of convenient variation of assay parameters at the expense of comparably low throughput.

2.2. HLCS inhibitors

The PECKISH library of natural compounds was used for screening for HLCS inhibitors [12]. Briefly, the library contains aqueous extracts from >880 raw materials, including but not limited to fruits, spices, and leaf extracts disbursed in 96-well plates; plates and raw extracts were stored at -80°C. A subset of 72 extracts was used to screen for HLCS inhibitor activity. Grape leaves (*Vitis vinifera*, variety *Gruner Veltliner*) were obtained from Waldviertel's Natureck (Plank am Kamp, Austria) and James Arthur Vineyards (varieties *St. Croix* and *Edelweiss*, Lincoln, NE). Extracts were prepared stirring 1 g of dried leafs into 10 mL of boiling distilled water and soaking the leaves for10 min. Red (Langers, Inc) and white grape juices (Best Choice, Inc.) and red and white table grapes were obtained at local food stores. Pomace are the solid remains from pressing grapes for juice. Fresh pomace was obtained from James Arthur Vineyards (variety *Edelweiss*) and extracted as described for grape leaves. Chemically pure gallic acid, quercetin, ferulic acid,

chlorogenic acid, ascorbic acid, phytic acid, caffeic acid, fumaric acid, 3-hydroxybenzoic acid, 4-hydroxybenzoic acid, catechin, cyanidin chloride, coenzyme Q10, hydroxyphenylethanol, ellagic acid, p-coumaric acid, citric acid, resveratrol, piceatannol and piceid were purchased from Sigma-Aldrich (St.Louis, MO, USA), Cayman Chemical (Ann Arbor, MI, USA) and Selleckchem (Houston, TX, USA) and used to prepare a second compound library with a focus on grape metabolites and for subsequent in-depth testing of individual compounds. For some compounds, the concentrations needed to cause a 50% inhibition of HLCS ($IC_{50\%}$) were estimated by testing serial dilutions of inhibitors and calculating $IC_{50\%}$ through non-linear regression with the Graphpad Prism software (GraphPad Software, Inc., La Jolla,CA, USA).

2.3. Identification of phenolics

Separation and identification of major phenolics was accomplished with a Waters Millipore HPLC system (W.R. Grace and Co., Albany, OR) using a Waters 600s Controller with a Vydac reverse phase C18 column (Millford, MA, USA) as described previously [13] with some modifications. Separation was achieved with a gradient mobile phase of (A) 50 mM $(NH_4)H_2PO_4$ at pH 2.6, (B) acetonitrile and 50 mM $(NH_4)H_2PO_4$ pH 2.6 at 80:20 (*v*:*v*) and (C) 200 mM H_3PO_4, pH 1.5 with 100% A for 4 minutes, 92% A and 8% B for 6 minutes, 14% B and 86% C for 12.5 minutes, 16.5% B and 83.5% C for 5 minutes, 25% B and 75% C for 22.5 minutes, 80% B and 20% C for 5 minutes, and 100% A for 5 minutes all at a flow rate of 1 ml per minute. Detection was performed using a Waters 2996 Photodiode

array detector scanning at 280 nm, 320 nm and 380 nm. Extracts of the grape leaves were passed through a 0.45 μm filter and were kept at 4°C before injection at 10 μl with a Waters 717Plus Autosampler. Sample areas were compared to a standard curve prepared from select phenols ranging from 50 μM to 6.25 μM.

2.4. Body fat percentage in Drosophila melanogaster brummer mutants

The *brummer* (*bmm*) gene encodes the lipid storage droplet-associated triacylglycerol lipase Brummer in *Drosophila melanogaster*, a homolog of mammalian adipose triglyceride lipase [14]. Loss of Brummer impairs the mobilizations from fat bodies in flies, i.e., *brummer* mutants are characterized by a large body fat mass [14]. Brummer mutants 15828 and 15959 were obtained from the Vienna Stock collection (Vienna, Austria) and reared on instant fly food (Formula 4-24 Plain, Carolina, Inc.; Burlington, NC, USA). The flies can live a maximum of 90 days with an average lifespan of 45 days. Seven days after eclosure, male and female virgins were separated and fed diets containing 0.05% or 1% (by weight) grape leaf extracts (*Gruner Veltliner*) or piceid (0.012 or 0.12 μmol/L) for 21 days. Soraphen A is an inhibitor of ACC1 and ACC2 [15] and was used as a positive control (5 μmol/L, 21 days). Flies were frozen (-80°C) and homogenized in a 5% Tween 20 solution. Triacylglycerols in the heat-inactivated (5 min at 70°C) extracts were incubated with Infinity Triglycerides solution (Thermo Scentific) at 37°C for 35 min and quantified colorimetrically (540 nm) using triolein as standard [16]. Biotinylated carboxylases were

isolated from fly homogenates as described previously [17] and analyzed by streptavidin blot analysis.

2.5. Statistics

Bartlett's test was used to confirm that variances were homogenous. One-way ANOVA and Fisher's Protected Least Significant Difference was used to determine whether differences among treatment groups were significantly different. The unpaired t-test was used for pairwise comparisons. Statview 4.5 was used for all calculations [18]. $P < 0.05$ was considered statistically different. Data are reported as means ± SD.

3. Results

3.1. HLCS inhibitors

When the PECKISH library was screened for HLCS inhibitor activity using the 96-well plate assay, 21 extracts inhibited HLCS to an activity of <2% compared with inhibitor-free controls (see **Fig. 1** for a representative image), including grape leaf extracts. The pool of candidate inhibitors was narrowed down as follows. First, extracts that caused a shift in the assay pH were disregarded. Representative examples include extracts from oranges and maté leaves (*Ilex paraguariensis*). Second, compounds that do not play a quantitatively meaningful role in diets were disregarded. Representative examples include *Cassia fistula* and *Syzygium cumini*. Grape leaf extract passed these screening steps and was further

investigated, partially because of the links of grape compounds such as resveratrol and its metabolites to cancer prevention, adipocyte differentiation, inhibition of inflammatory processes, and low body fat mass [9,19-24].

The effects of grape leaf extract on HLCS activity were confirmed in independent experiments. First, raw material from the PECKISH library was re-extracted and analyzed using the gel-based assay. When aqueous extracts from 1 mg of grape leafs (in 10 µL) were incubated with HLCS (50 µL final volume), biotinylation of p67 was considerably lower compared with inhibitor-free sample (**Fig. 2A**); an HLCS-free sample was used as negative control and produced no signal. Effects of mate leaf extract, oranges extracts, and a synthetic HLCS inhibitor are shown for completeness. Second, new raw material was obtained from Waldviertel's Natureck Inc., extracted, and analyzed for inhibitor activity. The results were essentially the same as for previous assays (not shown). Third, leaf extracts were prepared from local varieties of grapes (*St. Croix* and *Edelweiss*). These extracts also were potent inhibitors of HLCS although their activities were less than that of extracts from *Gruner Veltliner* (**Fig. 2B**). Fourth, grape juices and extracts from crushed table grapes were tested for inhibitor activity. Juices and white grapes inhibited HLCS to a meaningful extent (**Fig. 2C,D**); crushed red grapes also were effective inhibitors of HLCS but, at the highest concentrations tested, these effects might have been caused by shifts in the assay pH (not shown). Fifth, HLCS inhibitor activity was also detected in pomace (**Fig. 2E**).

Resveratrol and its metabolites piceatannol and piceid account for the inhibition of HLCS by grape materials, but other compounds in grapes also contribute toward HLCS

inhibition. When 19 compounds in grapes were assessed regarding their HLCS inhibitor activity by using the gel-based assay, 8 compounds inhibited HLCS by more than 90%, including the three resveratrol derivatives that were tested (**Table 1**). Piceatannol had a stronger effect on HLCS than resveratrol, which had a stronger effect than piceid, judged by dose-response studies comparing the three compounds (**Fig. 3**). $IC_{50\%}$ values were 0.28±2.12 µmol/L units for piceatannol, 3.70±0.0085 µmol/L units for resveratrol, and 21.30±0.014 µmol/L units for piceid. Note that grape compounds other than resveratrol and its metabolites also inhibited HLCS. For example, *p*-coumaric acid and cyanidin chloride had an effect similar to that of resveratrol (**Table 1**).The concentrations of resveratrol and other polyphenols varied between grape varieties (**Table 2**).

3.2. Body fat in Drosophila melanogaster brummer mutants

Grape leaf extracts and chemically pure piceid caused a significant loss of body fat in *brummer* mutants flies. When flies were fed diets containing an aqueous extract equaling 0.05 and 1% dried grape leaves for 21 days, the body fat mass was about 50% lower in males and females compared with controls (**Fig. 4A-D**). The same pattern was observed for *brummer* mutants 15828 (panels A and B) and 15959 (panels C and D). Likewise, when flies were fed diets containing 0.012 or 0.12 µmol/L piceid for 21 days, the body fat mass was about 30% lower in males and females compared with controls (**Fig. 5A, B**). Soraphen A, an inhibitor of ACC1 and ACC2, was used as positive control and caused a more than 60% decrease in body fat (**Fig. 5C, D**).

3.3. Biotinylation of carboxylases in Drosophila melongaster brummer mutants

Grape leaf extracts increased the amount of biotinylated carboxylases in *brummer* mutant flies. When flies were fed diets containing 1% dried grape leaves there was an increase in biotinylated ACC, MCC, PCC, and PC in males and an increase in biointylated PC in females. The absence of detectable ACC1, ACC2, MCC, and PCC was previously reported in female flies [17]. This was accompanied by an increase in HLCS protein (**Fig. 6**).

4. Discussion

This is the first report to identify naturally occurring inhibitors of HLCS. Our discoveries are relevant for human nutrition for two reasons. First, red and white grapes contain about 5 mg/L and 0.6 mg/L, respectively, of total resveratrol, piceid, and piceatannol [25-27]. The comparably low HLCS inhibitor activity of piceid compared with piceatannol and resveratrol is partially offset by its high levels in grape-borne materials [25]. Second, table grapes and grape juice are consumed in fairly large quantities in the United States and other countries. For example, the annual per person consumption of grapes (white and red) was 8.6 pounds in 2008 in the U.S., in addition to 5.7 pounds consumed in the form of grape juice [28]. Inhibitor activity was detected in all grape-based materials that were tested. Importantly, our studies provide unambiguous evidence that resveratrol and its metabolites inhibit HLCS not only *in vitro* but also cause body fat loss in Drosophila feeding studies.

While resveratrol metabolites inhibited HLCS efficiently *in vitro*, these effects were not seen in Drosophila feeding experiments *in vivo*. In fact, we found that there was an increase in biotinylated carboxylases in male and female flies fed diets containing 20% grape leaf extracts. This is due to an increase in HLCS expression. Interestingly, a similar pattern was observed when HEK-293 cells were treated with either piceatannol or grape leaf extract, or the synthetic HLCS inhibitor, β-ketophosphonate-5'-AMP (Online **Supplementary Figs 1 and 2**). Likewise, treatment of NIH/3T3 cells with the synthetic HLCS inhibitors β-hydroxyphosphonate-5'-AMP and biotin-5'-AMP [29] resulted in an increase in biotinylated carboxylases **(Online Supplementary Fig. 3)**. We propose that HLCS is essential for cell survival and that cells and organisms respond to any perturbation of HLCS activity with an increase in HLCS expression. This proposal is based on the following rationale. The importance of HLCS is apparent in that no HLCS null individual has ever been reported, suggesting embryonic lethality, and mutations in the human *HLCS* gene cause a substantial decrease in HLCS activity and metabolic abnormalities [30,31]. Additionally, HLCS knockdowon (~30% residual activity) in *Drosophila melanogaster* results in a reduced life span and heat tolerance [32] and aberrant gene regulation in human cell lines [33,34].

When considering that resveratrol metabolites do not appear to inhibit HLCS activity *in vivo*, the decrease in body fat mass in Drosophila observed in this study likely is due to the mechanism proposed by Kwon et al. [9]. They propose that piceatannol inhibits differentiation of 3T3-L1 cells by delaying mitotic clonal expansion and in parallel preventing phosphorylation of the insulin receptor/Akt signaling pathway, leading to its

inhibition. The substantial decrease in body fat mass in Drosophila fed a diet supplemented with grape leaf extract and piceid illustrates the potential benefits of these compounds for human health, considering the current epidemic of obesity and obesity-related diseases [35-37].

A few key observations in this study are worthwhile pointing out. First, no apparent difference was noted when comparing materials from red and white grapes. Second, the variety of grapes might be important regarding HLCS inhibitor activity, e.g., leaf extracts from *Gruner Veltliner* were more effective than extracts from *Edelweiss*. Third, bioactive compounds other than resveratrol and its metabolites, also contribute toward HLCS inhibitor activity in grape materials, e.g., *p*-coumaric acid and cyanidin chloride. Therefore, synergisms need to be considered in future studies, and experiments with chemically pure compounds should always be supplemented with studies using crude materials. Fourth, pomace contains meaningful amounts of HLCS inhibitors. It might be worthwhile considering purifying these compounds from pomace, which is typically considered as waste product in the production of wine and grape juice.

The following uncertainties remain. First, it is unknown whether HLCS inhibitors also affect gene repression through HLCS-dependent epigenetic mechanisms. We abstained from conducting such studies because effects of HLCS in gene repression are caused by HLCS/protein interactions that might not depend on the catalytic activity of HLCS [38-40]. Second, it is unknown which of the four domains in the HLCS domain interact with resveratrol and its metabolites [41]. Considering that the comparatively bulky glucose residue in piceid impaired inhibitor activity compared with resveratrol, one could assume

that the resveratrol binding site in HLCS is rather specific [25]. We also do not know whether effects of resveratrol compounds are stereospecific; trans isomers or piceid and resveratrol are more abundant than cis isomers in grape materials [25]. Third, he expression of HLCS is regulated by three promoters [42,43], but the responsiveness of regulatory elements in these promoters to HLCS inhibitors is unknown. These uncertainties are currently being addressed in our laboratories.

Taken together, resveratrol metabolites caused a substantial 50% fat loss in flies. Our studies suggest that loss of biotinylation events do not contribute to loss of body fat, and that the observed effects can be attributed to inhibition of the insulin receptor/Akt signaling pathway as proposed previously [9].

Acknowledgements

Supported in part by funds provided through the Hatch Act. Additional support was provided by NIH grants DK063945, DK077816, and P20GM104320 and the German Ministry of Education and Science (BMBF 01EA1317A). The authors wish to thank Jim Ballard from James Arthur Vineyards for providing samples.

Author contributions

All authors participated in the design, interpretation of the studies and analysis of the data and review of the manuscript; ELC, RA, DCT, and RZ conducted experiments; SO, PR, and FD supplied the PECKISH library and grape leaves, JZ wrote the manuscript.

Table 1. Inhibition of HLCS by bioactive compounds in grapes.

Compound[1]	Inhibitor activity[2]
Piceatannol	+++++
Resveratrol	+++++
Piceid	+++++
p-Coumaric acid	+++++
Quercetin	+++++
Cyanidin chlorid	+++++
Gallic acid	+++++
3-Hydroxybenzoic acid	+++++
Ellagic acid	++++
Chlorogenic acid	++++
4-Hydroxybenzoic acid	++++
Fumaric acid	+++
Citric acid	+++
Ascorbic acid	+++
Ferulic acid	+++
Caffeic acid	+++
Phytic acid	++
Hydroxyphenylethanol	+
Coenzym Q10	+

[1]Sorted by effect size.

[2]Symbols denote inhibitor activity (+++++, >90% inhibition of HLCS; ++++, >80% inhibition; +++, >60% inhibition; ++, >40% inhibition; +, <20% inhibition), judged by HLCS-dependent biotinylation of p67 in the gel-based HLCS assay and gel densitometry. Compounds were tested at concentrations of 0.05 to 5.7 mM.

Table 2. Concentrations of polyphenols in grape leaves in two varieties.[1]

Compound	*Gruner Veltliner*	*Edelweiss*
	µmol/kg	
Piceatannol	n.d.[2]	0.66±0.25
Resveratrol	n.d.	0.64±0.68
Piceid	3.07±0.11	1.74±0.44
Chlorogenic acid	8.42±0.39	0.92±0.30

[1]Values are means ± standard deviations.

[2]n.d., not detectable.

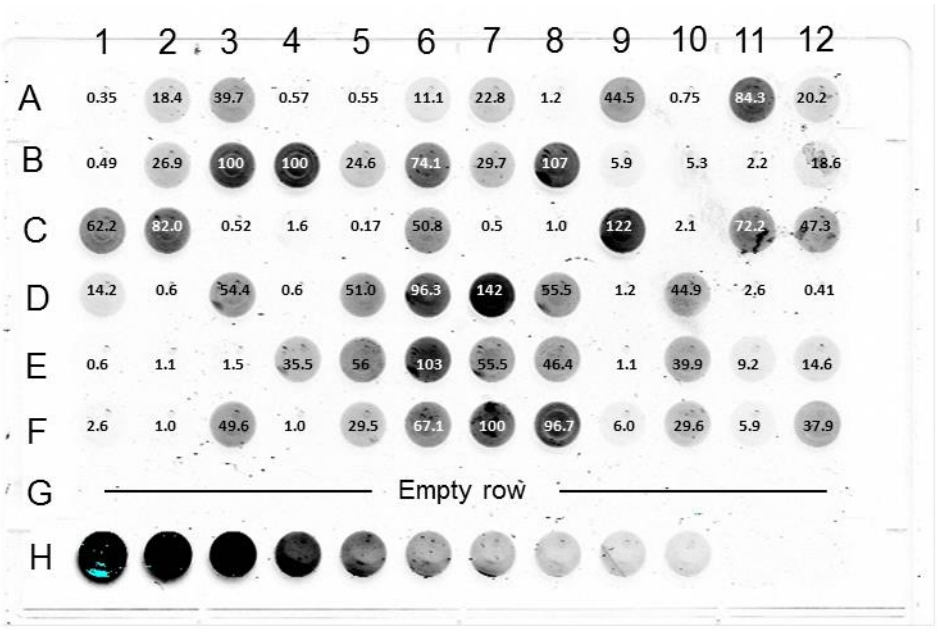

Fig. 1. Representative example of HLCS activity in samples treated with extracts from the PECKISH library of natural compounds. HLCS activity was assayed using a 96-well plate format, values in individual wells denote HLCS activity (% of controls). Identifiers: B3 and B4 = vehicle controls; C3 = grape leaf extract; A4 = *Cassia fistula*; C7 = *Syzygium cumini*; row H is the calibration curve containing defined amounts of HLCS.

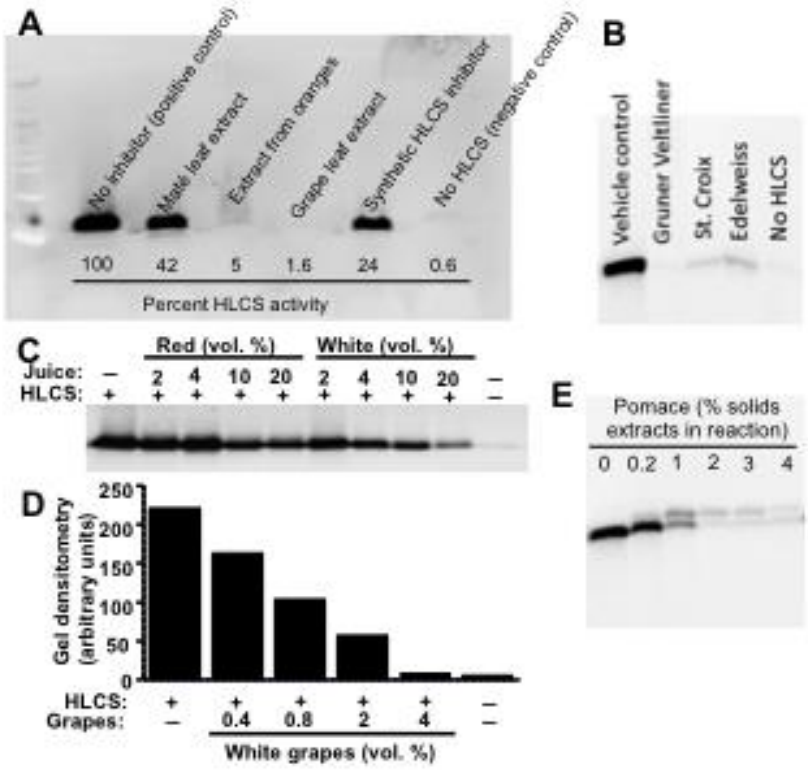

Fig. 2. Effects of grape products on HLCS activity. (A) Gel-based assay of HLCS activity in the absence and presence of grape leaf extract. A sample without HLCS was used as negative control. Extracts from maté leaves and oranges were not considered for subsequent studies, because of their inhibitor activity was caused by shifts in the assay pH as discussed in the text. (B) Comparison of leaf extracts from *Gruner Veltliner, St. Croix*, and *Edelweiss*. HLCS activity was measured in the presence of and aqueous extract of 500 µg grape leaves in a sample volume of 50 µL; controls were prepared using vehicle and by omitting HLCS. Lanes were electronically re-arranged to facilitate comparisons. (C) Effects of grape juices on HLCS activity. (D) Effects of crushed white grapes on HLCS activity, quantified by gel densitometry. (E) Effects of pomace extract (variety *Edelweiss*) on HLCS activity.

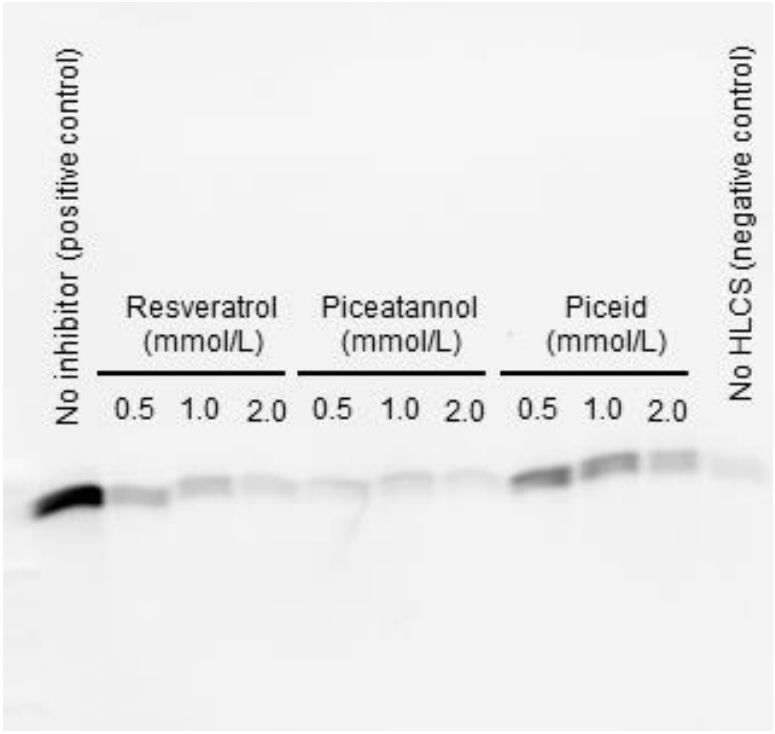

Fig. 3. Comparison of the effects of resveratrol, piceatannol, and piceid on the inhibition of HLCS.

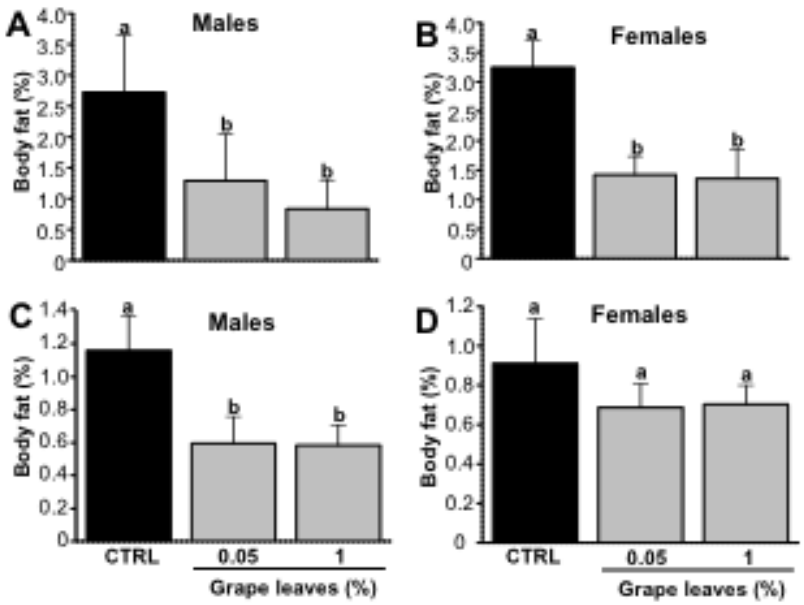

Fig. 4. Effect of grape leaf extract on body fat mass in male and female *Drosophila melanogaster brummer* mutants 15828 (panels A and B) and 15959 (panels C and D). Flies were fed a diet supplemented with 0.05 or 1% grape leaf solids (as extracts) for 21 days; controls were fed an extract-free diet. [a,b]Bars not sharing the same letter are significantly different ($P < 0.05$; n=4 tubes, each containing 40 flies).

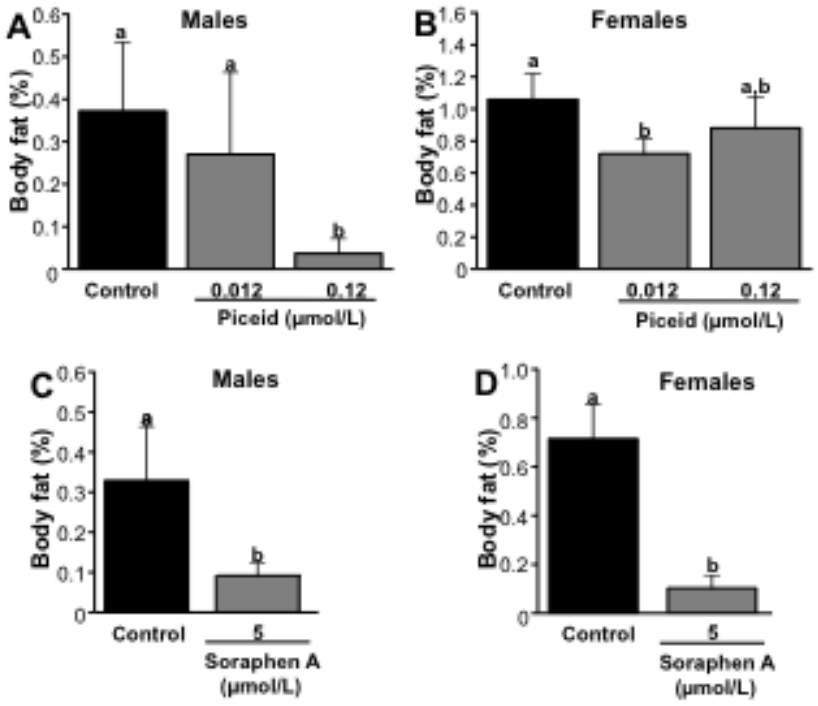

Fig. 5. Effect of piceid (panels A and B) and soraphen A (panels C and D) on body fat mass in male and female *Drosophila melanogaster brummer* mutant 15828. Flies were fed a diet supplemented with 0.012 µmol/L piceid, 0.12 µmol/L piceid, or 5 µmol/L soraphen A for 21 days; controls were fed piceid-free and soraphen A-free diets. [a,b]Bars not sharing the same letter are significantly different ($P < 0.05$; n=4 tubes, each containing 40 flies).

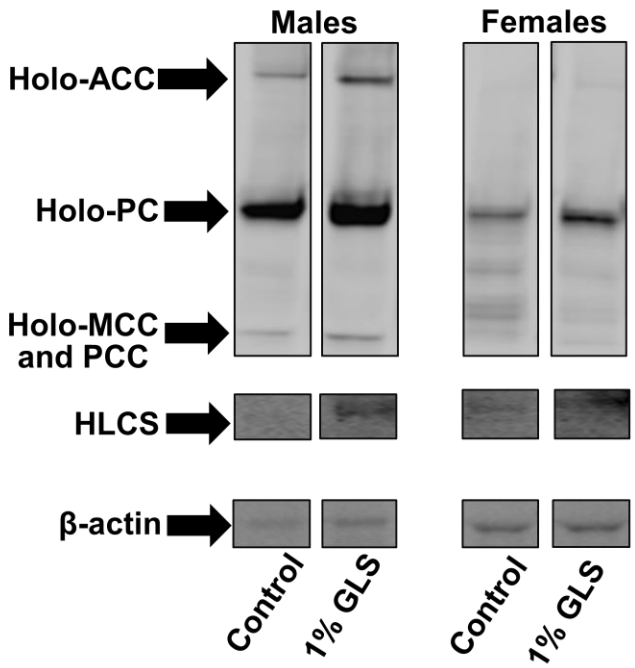

Fig. 6. Abundance of biotinylated holocaboxylases and HLCS in male and female *Drosophila melanogaster brummer* mutant 15828. Flies were fed a diet supplemented with 0.05 or 1% grape leaf solids (GLS, as extracts) for 21 days; controls were fed an extract-free diet. Biotinylated carboxylases, HLCS, and β-actin (control) were probed using streptavidin, anti-HLCS, and anti-β-actin, respectively. ACC, acetyl-CoA carboxylases; MCC, 3-methylcrotonyl-CoA carboxylase; PC, pyruvate carboxylase; PCC, propionyl-CoA carboxylase.

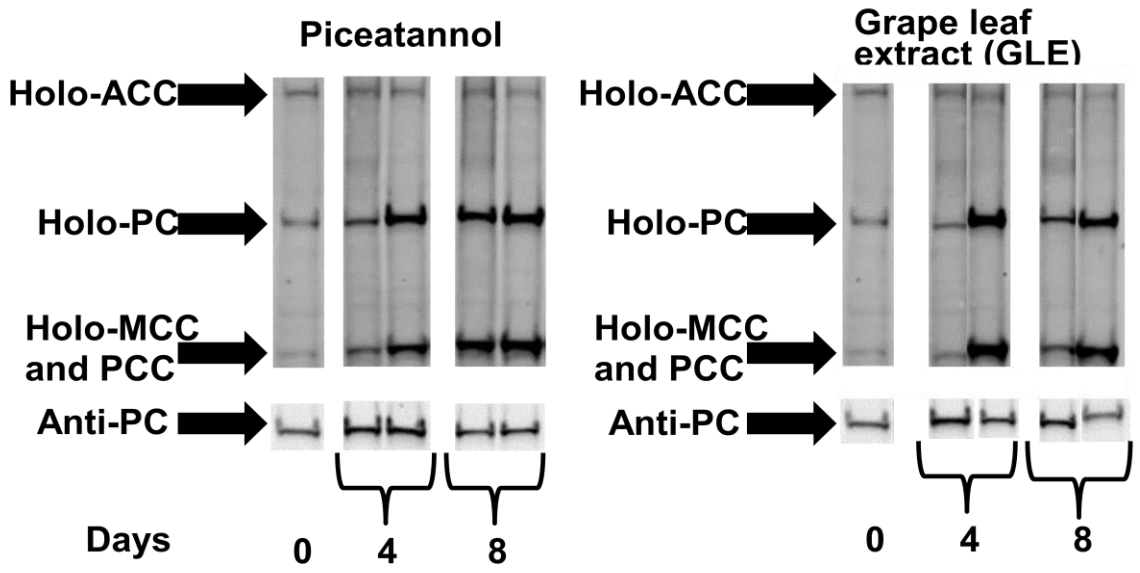

Figure 7. (Online Supplementary Fig. 1). Holocarboxylase profile of HEK293 cells treated with or without piceatannol or grape leaf extract. HEK293 cells were treated with either 50 μM piceatannol or 0.25% grape leaf solids for up to 8 days. Cells were collected for analysis of holocarboxylase abundance. Biotinylated carboxylases were probed with streptavidin. ACC, acetyl-CoA carboxylases; MCC, 3-methylcrotonyl-CoA carboxylase; PC, pyruvate carboxylase; PCC, propionyl-CoA carboxylase.

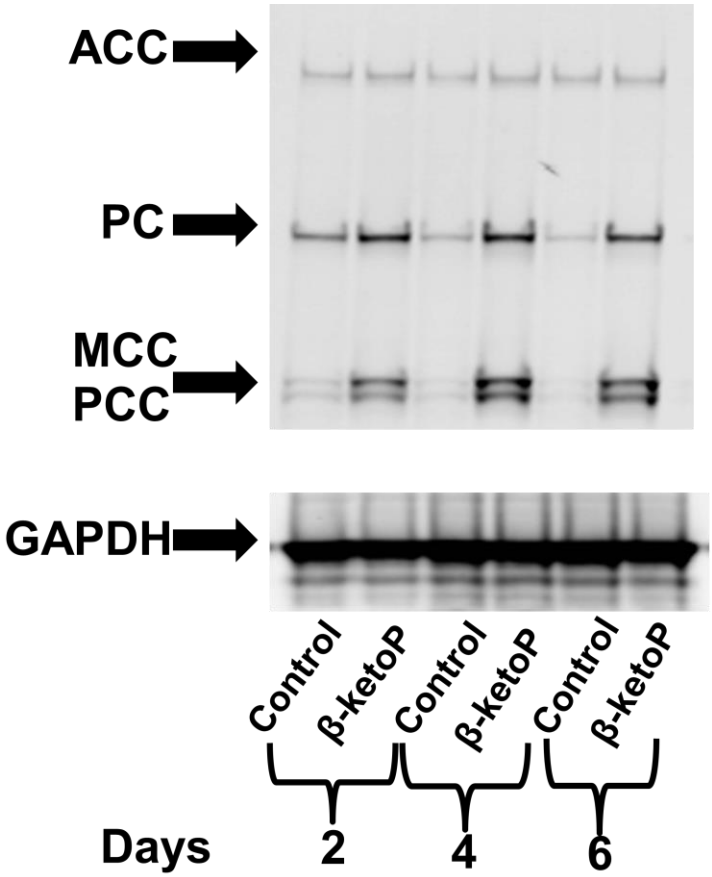

Figure 8. (Online Supplementary Fig. 2). Holocarboxylase profile of HEK293 cells treated with with or without β-ketophosphonate-5'-AMP. HEK293 cells were incubated with 250 μM β-ketophosphonate-5'-AMP for 6 days. Biotinylated carboxylases were probed with streptavidin. ACC, acetyl-CoA carboxylases; GAPDH, glyceraldehyde-3-phosphate dehydrogenase; MCC, 3-methylcrotonyl-CoA carboxylase; PC, pyruvate carboxylase; PCC, propionyl-CoA carboxylase.

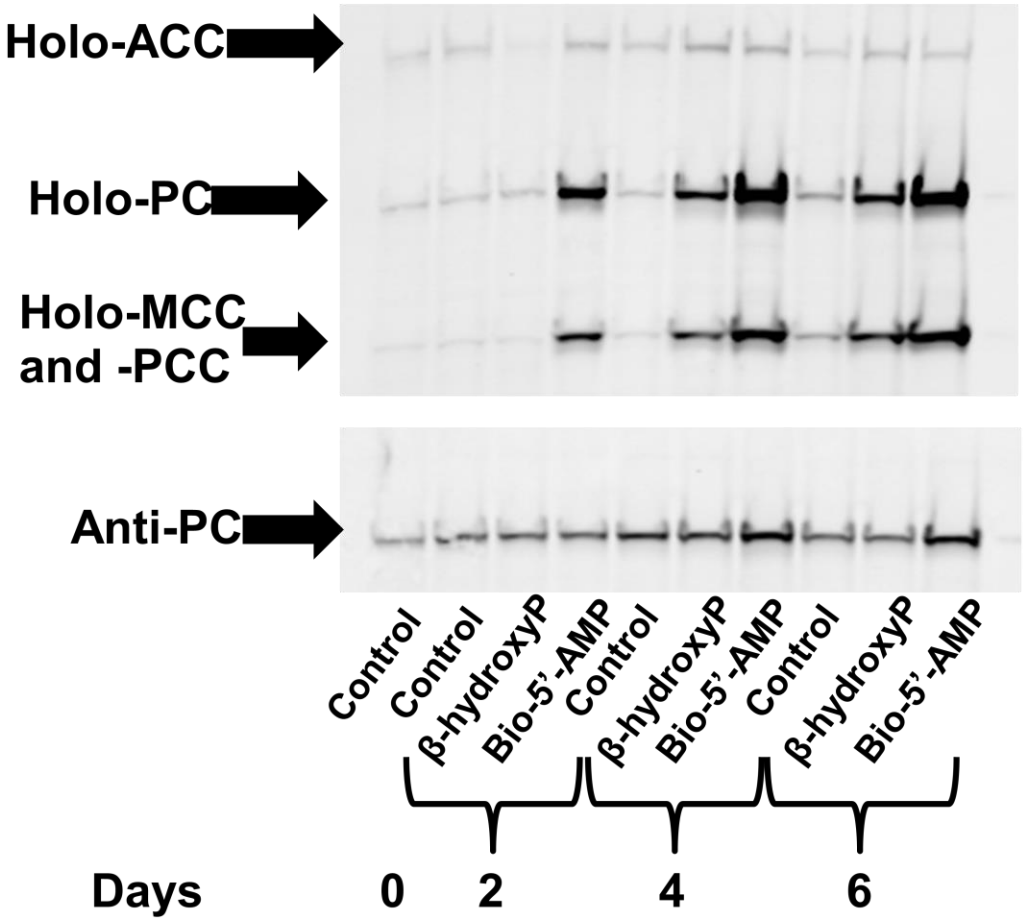

Figure 9. (Online Supplementary Fig. 3). Holocarboxylase profile of NIH3T3 cells treated with β-hydroxyphosphonate-5'-AMP, biotinol-5'-AMP or without inhibitor. NIH3T3 cells were incubated with 250 μM β-hydroxyphosphonate-5'-AMP for 6 days. Biotinylated carboxylases were probed with streptavidin. ACC, acetyl-CoA carboxylases; MCC, 3-methylcrotonyl-CoA carboxylase; PC, pyruvate carboxylase; PCC, propionyl-CoA carboxylase.

References

1. Zempleni J, Wijeratne SSK, Kuroishi T. Biotin. In: Erdman JW, Jr., Macdonald I, Zeisel SH eds, Present Knowledge in Nutrition. Washington, D.C.: International Life Sciences Institute; 2012:587-609
2. Li Y, Malkaram SA, Zhou J, Zempleni J. Lysine biotinylation and methionine oxidation in the heat shock protein HSP60 synergize in the elimination of reactive oxygen species in human cell cultures. J Nutr Biochem 2014;25:475-482
3. Xue J, Zhou J, Zempleni J. Holocarboxylase synthetase catalyzes biotinylation of heat shock protein 72, thereby inducing RANTES expression in HEK293 cells. Am J Physiol Cell Physiol 2013;305:C1240-C1245
4. Ha J, Lee JK, Kim KS, Witters LA, Kim KH. Cloning of human acetyl-CoA carboxylase-beta and its unique features. Proc Natl Acad Sci USA 1996;93:11466-11470
5. Choi CS, Savage DB, Abu-Elheiga L, et al. Continuous fat oxidation in acetyl-CoA carboxylase 2 knockout mice increases total energy expenditure, reduces fat mass, and improves insulin sensitivity. Proc Natl Acad Sci USA 2007;104:16480-16485
6. Olson DP, Pulinilkunnil T, Cline GW, Shulman GI, Lowell BB. Gene knockout of Acc2 has little effect on body weight, fat mass, or food intake. Proc Natl Acad Sci USA 2010;107:7598-7603
7. Hoehn KL, Turner N, Cooney GJ, James DE. Phenotypic Discrepancies in Acetyl-CoA Carboxylase 2-deficient Mice. Journal of Biological Chemistry 2012;287:15801
8. Abu-Elheiga L, Wu H, Gu Z, Bressler R, Wakil SJ. Acetyl-CoA carboxylase 2-/- mutant mice are protected against fatty liver under high-fat, high-carbohydrate dietary and de novo lipogenic conditions. Journal of Biological Chemistry 2012;287:12578-12588

9. Kwon JY, Seo SG, Heo YS, et al. Piceatannol, a natural polyphenolic stilbene, inhibits adipogenesis via modulation of mitotic clonal expansion and insulin receptor-dependent insulin signaling in the early phase of differentiation. Journal of Biological Chemistry 2012;287:11566-11578
10. Bao B, Pestinger V, I. HY, et al. Holocarboxylase synthetase is a chromatin protein and interacts directly with histone H3 to mediate biotinylation of K9 and K18. J Nutr Biochem 2011;22:470-475
11. Kobza K, Sarath G, Zempleni J. Prokaryotic BirA ligase biotinylates K4, K9, K18 and K23 in histone H3. BMB Reports 2008;41:310-315
12. Onur S, Stockmann H, Zenthoefer M, Piker L, Doring F. The plant extract collection Kiel in Schleswig-Holstein (PECKISH) is an open access screening library. J Food Res 2013;2:4
13. Williams A. Current protocols in food analytical chemistry: John Wiley & Sons, Inc.; 2002
14. Gronke S, Mildner A, Fellert S, et al. Brummer lipase is an evolutionary conserved fat storage regulator in Drosophila. Cell metabolism 2005;1:323-330
15. Shen Y, Volrath SL, Weatherly SC, Elich TD, Tong L. A mechanism for the potent inhibition of eukaryotic acetyl-coenzyme A carboxylase by soraphen A, a macrocyclic polyketide natural product. Mol Cell 2004;16:881-891
16. Hildebrandt A, Bickmeyer I, Kuhnlein RP. Reliable Drosophila body fat quantification by a coupled colorimetric assay. PLoS ONE 2011;6:e23796

17. Landenberger A, Kabil H, Harshman LG, Zempleni J. Biotin deficiency decreases life span and fertility but increases stress resistance in *Drosophila melanogaster*. J Nutr Biochem 2004;15:591-600

18. Abacus C. StatView. In. Berkeley, CA: Abacus Concepts Inc.; 1996

19. Ganapathy S, Chen Q, Singh KP, Shankar S, Srivastava RK. Resveratrol enhances antitumor activity of TRAIL in prostate cancer xenografts through activation of FOXO transcription factor. PLoS ONE 2010;5:e15627

20. Chen Q, Ganapathy S, Singh KP, Shankar S, Srivastava RK. Resveratrol induces growth arrest and apoptosis through activation of FOXO transcription factors in prostate cancer cells. PLoS ONE 2010;5:e15288

21. Youn J, Lee JS, Na HK, Kundu JK, Surh YJ. Resveratrol and piceatannol inhibit iNOS expression and NF-kappaB activation in dextran sulfate sodium-induced mouse colitis. Nutr Cancer 2009;61:847-854

22. Baile CA, Yang JY, Rayalam S, et al. Effect of resveratrol on fat mobilization. Ann NY Acad Sci 2011;1215:40-47

23. Rayalam S, Della-Fera MA, Baile CA. Synergism between resveratrol and other phytochemicals: implications for obesity and osteoporosis. Mol Nutr Food Res 2011;55:1177-1185

24. Meydani M, Hasan ST. Dietary polyphenols and obesity. Nutrients 2010;2:737-751

25. Romero-Perez AI, Ibern-Gomez M, Lamuela-Raventos RM, de La Torre-Boronat MC. Piceid, the major resveratrol derivative in grape juices. J Agric Food Chem 1999;47:1533-1536

26. Bavaresco L, Fregoni C, Cantu E, Trevisan M. Stilbene compounds: from the grapevine to wine. Drugs Exp Clin Res 1999;25:57-63

27. Bavaresco L, Fregoni M, Trevivan M, et al. The occurrence of the stilbene piceatannol in grapes. Vitis 2002;41:133-136

28. Agricultural MRC. Grapes profile. In: USDA and Iowa State University; 2010

29. Sittiwong W, Cordonier EL, Zempleni J, Dussault PH. beta-Keto and beta-hydroxyphosphonate analogs of biotin-5'-AMP are inhibitors of holocarboxylase synthetase. Bioorg Med Chem Lett 2014;24:5568-5571

30. Suzuki Y, Yang X, Aoki Y, Kure S, Matsubara Y. Mutations in the holocarboxylase synthetase gene *HLCS*. Human Mutat 2005;26:285-290

31. National CfBI. Entrez SNP. In: National Institutes for Health; 2008

32. Camporeale G, Eissenberg JC, Giordano E, Zempleni J. Lifespan and resistance to heat stress depend on histone biotinylation in *Drosophila melanogaster*. FASEB J 2006;20:A610

33. Chew YC, West JT, Kratzer SJ, et al. Biotinylation of histones represses transposable elements in human and mouse cells and cell lines, and in *Drosophila melanogaster*. J Nutr 2008;138:2316-2322

34. Gralla M, Camporeale G, Zempleni J. Holocarboxylase synthetase regulates expression of biotin transporters by chromatin remodeling events at the SMVT locus. J Nutr Biochem 2008;19:400-408

35. Centers fDC. Overweight and obesity. In. 8/1/2011 ed; 2011

36. Centers fDC. Diabetes public health resource. In. 9/21/2011 ed; 2011

37. Centers fDC. Heart Disease. In. 9/22/2011 ed; 2011

38. Li Y, Hassan YI, Moriyama H, Zempleni J. Holocarboxylase synthetase interacts physically with euchromatic histone-lysine N-methyltransferase, linking histone biotinylation with methylation events. J Nutr Biochem 2013;24:1446-1452

39. Xue J, Wijeratne S, Zempleni J. Holocarboxylase synthetase synergizes with methyl CpG binding protein 2 and DNA methyltransferase 1 in the transcriptional repression of long-terminal repeats. Epigenetics 2013;8:504-511

40. Liu D, Zempleni J. Holocarboxylase synthetase (HLCS) interacts physically with nuclear corepressor (N-CoR) and histone deacetylases (HDACs) to mediate gene repression. In: Zempleni J, Ross SA eds, Experimental Biology 2012. San Diego, CA: Federation of the American Society for Experimental Biology; 2012

41. Hassan YI, Moriyama H, Olsen LJ, Bi X, Zempleni J. N- and C-terminal domains in human holocarboxylase synthetase participate in substrate recognition. Mol Genet Metab 2009;96:183-188

42. Warnatz HJ, Querfurth R, Guerasimova A, et al. Functional analysis and identification of cis-regulatory elements of human chromosome 21 gene promoters. Nucleic Acids Res 2010;38:6112-6123

43. Xia M, Malkaram SA, Zempleni J. Three promoters regulate the transcriptional activity of the human holocarboxylase synthetase gene. J Nutr Biochem 2013;24:1963-1969

CHAPTER III. INHIBITION OF ACETYL-COA CARBOXYLASES ACTIVITY PREVENTS LIPID ACCUMULATION BUT NOT ADIPOGENESIS IN 3T3-L1 CELLS

Elizabeth L. Cordonier, Sarah Jarecke, Frances E. Hollinger, and Janos Zempleni

Department of Nutrition and Health Sciences, University of Nebraska-Lincoln, 316 Ruth Leverton Hall, Lincoln, NE 68583-0806, USA

**Corresponding author. Phone: (402) 472 3270; fax: (402) 472 1587; email: jzempleni2@unl.edu. Address: Department of Nutrition and Health Sciences, University of Nebraska-Lincoln, 316C Ruth Leverton Hall, Lincoln, NE 68583-0806, USA.

Abstract

Acetyl-CoA carboxylases (ACC) 1 and 2 catalyze the carboxylation of acetyl-CoA to malonyl-CoA and depend on biotin as a coenzyme. Malonyl-CoA produced by cytoplasmic ACC1 is a precursor in fatty acid (FA) synthesis. Malonyl-CoA produced by ACC2 in the outer mitochondrial membrane is an inhibitor of FA import into mitochondria for subsequent oxidation. We hypothesized that ACCs are checkpoints in adipocyte differentiation and tested this hypothesis using the ACC1 and ACC2 inhibitor soraphen A in murine 3T3-L1 preadipocytes. Treatment of 3T3-L1 cells with as little as 100 nM of the microbial ACC inhibitor soraphen A (SA) inhibited lipid droplet accumulation and was accompanied by a 29% and 11% decrease in the expression of PPARγ mRNA and FABP4 mRNA, respectively, as markers of adipocyte differentiation four days after treatment. Treatment of 3T3-L1 cells with 200 μM palmitate partially restored lipid accumulation and fully rescued PPARγ and FABP4 mRNA expression. This observation suggests that loss of ACC1-dependent FA synthesis might account for some of the effects of SA in lipid accumulation and adipocyte differentiation. We propose that loss of ACC2 also contributed to this phenomenon, based on our observation that treatment with 100nM SA caused a 300% higher rate of fatty acid oxidation compared with solvent controls. Glucose uptake is maintained in these cells despite decreased GLUT4 mRNA expression upon treatment with SA. SA did not alter lipid accumulation if treatment was initiated on day eight after induction of differentiation. We conclude that inhibition of ACC 1 and 2 alter lipid metabolism but not adipogenesis in 3T3-L1 cells.

Introduction

Acetyl-CoA carboxylase 1 and 2 (ACC 1 and 2) depend on biotin as a covalent bound coenzyme and catalyze the synthesis of malonyl-CoA through the carboxylation of acetyl-CoA. Malonyl-CoA synthesized from cytoplasmic ACC1 and mitochondrial membrane associated-ACC2 serves as the C2 donor in fatty acid synthesis and as a regulator of beta-oxidation of long chain fatty acids, respectively [1,2]. Malonyl-CoA produced from ACC2 is a potent inhibitor of carnitine palmitoyltransferase I (CPTI), the enzyme responsible for catalyzing the transfer of an acyl group from coenzyme A to carnitine[3]; the binding of carnitine to fatty acids is the rate-limiting step in mitochondrial fatty acid import for subsequent beta-oxidation[4].

Due to their key roles in fatty acid metabolism and intracellular lipid accumulation, ACCs have attracted considerable attention as potential targets for lipid lowering treatments. For example, whole body mutant ACC2-/- mice fed a high fat diet or high fat/high-carbohydrate diet for 4 months had lower body weights than their wild type cohorts. Additionally, increased glucose uptake and insulin sensitivity was displayed by the mutant mice demonstrating their protection from diabetes and this was accompanied by a decrease in triglyceride content in the liver and skeletal muscle in ACC2-/- mutant mice [5-7]. However, these findings are highly controversial. Other studies found no differences in overall energy balance between skeletal muscle-specific and global ACC2 knockout (ACC2KO) mice [8,9]. Body weights and food intake were similar in ACC2KO and wild-type controls [8,9] and this was accompanied by a decrease in malonyl-CoA levels and increased fatty acid oxidation in skeletal muscle. The increase in fatty acid oxidation can be attributed to inhibition of ACC2, which leads to a de-repression of CPTI, thereby increasing beta-oxidation.

Mice lacking ACC1 are embryonically lethal [10] and two liver specific knockouts of ACC1 (LACC1-/-) generated by Kusunoki's and Wakil's groups [11,12] show conflicting results. There were no differences in fatty acid synthesis of malonyl-CoA levels in Kusonoki's LACC1-/- mice liver samples compared to WT mice while liver samples from Wakil's LACC1-/- produced the opposite effects [11,12].

The inconsistent results between ACC1 and 2 knockout mice suggest that inhibition of both enzymes may be required to alter energy balance. Soraphen A (SA), originally isolated from the myxobacterium *Sorangium cellulosum,* is a macrocylic polyketide that displays antifungal activity. Genetic and biochemical studies indicate that eukaryotic ACC are inhibited by SA at concentrations [13,14] as low as 1 nM [15]. Structural studies demonstrate that the compound acts by binding to the biotin carboxylase domain of the ACC enzymes preventing dimerization of eukaryotic ACCs [15]. Male C57Bl/6 mice fed a high fat diet supplemented with SA had reduced weight gain, adipose tissue and fasting plasma insulin levels as compared to mice fed high fat diets without SA supplementation and these levels were comparable to those of the control [16]. One possible mechanism for the observed reduction in fat mass displayed by mice fed a high fat diet supplemented with SA is a reduction in adipocyte differentiation.

Lodhi et al. reported that fat-specific knockout of fatty acid synthase (FASKOF) in mice lessened diet-induced obesity and increased brown fat-like cells in these mice. PPARγ protein expression was unaffected in adipose tissue of FASKOF mice but protein expression of the PPARγ target aP2 (also known as FABP4) was decreased. Gene expression of PPARγ targets including aP2, lipoprotein lipase, fatty acid translocase (CD36), and CCAAT/enhancer binding protein alpha (C/EBPα) were also decreased in FASKOF mouse adipose tissue. Fatty acid synthase knockdown in 3T3-L1 cells led to a decrease in aP2 and CD36 protein expression [17].

We propose that inhibition of ACC1 and 2 by Soraphen A will prevent production of malonyl-CoA which feeds into the fatty acid biosynthesis pathways and prevents the production of endogenous ligands for PPARγ activation and adipogenesis.

Materials and Methods

Cell lines and cell culture

Mouse preadipocyte 3T3-L1 cells were purchased from American Type Culture Collection (Cat no. CL-173). Cells were seeded at a density of 1.5 x 10^5 in 12 well plates or 5 x 10^5 in T25 flasks and maintained at 37°C in a 5% CO_2/95% air atmosphere. 3T3-L1 preadipocytes were maintained in DMEM containing 25 mM glucose and 10% bovine calf serum (BCS) until 2 days after becoming confluent (designated as day 0) when media was switched to DMEM , 25 mM glucose, 10% fetal bovine serum (FBS), and one of the following differentiation cocktails: cocktail 1 produced final concentrations of 1.75 μM insulin, 1 μM dexamethasone, and 500 μM 3-isobutyl-1-methylxanthine (IBMX), and cells were treated with the cocktail for 2 days; cultures were continued for another two days in media supplemented with 1.75 μM insulin, but no dexamethasone and no 3-isobutyl-1-methylxanthine. Cocktail 2 produced final concentrations of 1 μM rosiglitazone and 1.75 μM insulin and was given to cells for 4 days when media was switched to DMEM/high glucose and 10% FBS without rosiglitazone and insulin. Where indicated, SA was added to cells at a concentration of 100 nM or 1 μM. SA was a gift from Dr. Rolf Jansen of the Helmholtz-Centre for Infection research in Braunschwig, German. Cell viability was determined using trypan blue exclusion [18].

RNA isolation and quantitative real-time PCR (RT-qPCR)

Total RNA was isolated using illustra RNA spin Mini RNA isolation kit (GE healthcare) and the ImProm-II™ reverse transcription system (Promega) was used to synthesize cDNAs. Relative

mRNA expression was quantified by RT-qPCR and the ΔCt protocol as described previously [19] using the primers in **Table 1**. Assays were performed in triplicate and results were normalized to 18s ribosomal RNA.

Fatty acid oxidation assay

The rate of fatty acid oxidation was assessed by measuring the release of tritiated water from radiolabeled palmitate [20]. Briefly, [9,10-^{3}H(N)]-palmitic acid (NEN Perkin Elmer) was mixed with unlabeled sodium palmitate (TCI America, Portland, OR); 20 mM in 0.01 N NaOH to adjust the specific radioactivity to about 32 mCi/mmol. Palmitate was complexed to ultra fatty acid free bovine serum albumin (BSA, Roche, Basel, Switzerland) at a 3:1 molar ratio using stock solutions of 2 mM BSA and 20 mM Na-palmitate. Desired quantity of radiolabled palmitate was added to 20mM palmitate prior to conjugation to BSA.

Cell differentiation was induced as described above. At 6 days post-differentiation, media was changed to MEM containing 2% FBS for 12 hours. Cells were treated with either 100 nM SA beginning at day 0 or 1 μM SA 12 hours prior to addition of radiolabeled fatty acids or with solvent (control). Etomoxir (Tocris Biosciences, Minneapolis, MN) inhibits fatty acid oxidation [21] and was added to cell cultures one hour prior to addition of palmitate (positive control). After 12 hours, media was replaced with serum free media and cells were incubated with radiolabeled palmitate at about 0.5 μCi/well; background radioactivity was assessed by incubating cells in fatty acid-free BSA. Incubations were continued for two hours. Media were collected and the release of tritiated water was assessed as described previously [20] with the following modifications. Trichloroacetic acid was added to media to produce a final concentration of 10 % trichloracetic acid, and samples were allowed to precipitate for 30 minutes at 4°C. Samples were centrifuged at 16000 *g* for 10 minutes at 4°C and 250 μL of supernatant

was transferred to new tubes containing 42 μL of 6 N NaOH. Samples were applied to a DOWEX™ 1x2,200-400 mesh, ion-exchange resin (1 mL packed volume), which retains the 3H-labeled water whereas [3H] palmitate elutes near the solvent front. Columns were washed with 300 μL of ultrapure water and radioactive water was eluted with 2 mL ultrapure water for analysis in a liquid scintillation counter. Results were normalized to total protein concentration.

Glucose uptake assays

The rate of glucose uptake was assessed by measuring cellular uptake of the radiolabled glucose analog 2-deoxy-*D*-glucose [22]. Cell differentiation was induced as described above. At 6 days post-differentiation, media was changed to MEM containing 10% FBS and 5.5mM D-glucose for 24 hours. Cells were treated with either 100 nM SA beginning at day 0, 1 μM SA 12 hours prior to addition of radiolabeled glucose, or with no SA. On day 7, media was replaced with 1 mL of HBSS with treatments and with or without 100 nM insulin, for 10 minutes followed by addition of 20 μL of HBSS containing 4 nmol 2-[1,2-3H(N)]deoxy-d-glucose [0.05 μCi/mL] for 90 min incubated at 37°C. Uptake was terminated by the addition of ice-cold KRBC supplemented with 25 mM D-glucose to remove background radioactivity. Cells were lysed using 300 μL 0.1% SDS-PBS and total cellular lysate was subjected to liquid scintillation counting to determine cellular uptake. Results were normalized to total protein concentration.

Protein expression

Cells were lysed directly in the culture dish using 0.5 mL RIPA buffer containing protease inhibitor cocktail. Cells were scraped off and lysate was transferred to a 1.5 mL tube where they were let stand for 5 minutes at 4°C after which lysate was spun down at 14000g for 15 minutes at 4°C and supernatant was transferred to another tube. Total protein concentration was measured by BCA assay and 4μg of protein was mixed with NuPage loading dye (Invitrogen) and heated

to 95°C for 10 minutes. Proteins were run on 3-8% Tris-acetate gels and transferred to polyvinylidene blots. The expression of biotinylated ACC1 and 2 was assessed using streptavidin as a probe [23].

Oil Red O (ORO) staining and lipid quantitation

Cells were fixed with 4% paraformaldehyde and lipids were stained using ORO[24]. Hematoxylin, which binds to the nucleus was used as a counter stain. Microscopy images were obtained using a Nikon Ti-S Inverted Fluorescence Microscope. The relative accumulation of lipids was quantified by extracting ORO using 100% isopropanol and measuring the absorbance at 490 nm by a spectrophotometer.

Statistics

One-way ANOVA was used to determine whether differences among treatment groups were significantly different. Dunnett's multiple comparisons t-test was used to determine if differences between the control and individual treatment groups were statistically significant. All data presented are means ± standard deviation. Statistical analysis was performed using Graph Pad Prism 6.0.

Results

Inhibition of ACCs by SA impairs adipogenic gene expression and lipid accumulation

We determined the effects of a SA dose response on lipid droplet accumulation in 3T3-L1 cells. 3T3-L1 cells were treated with either 100 nM, and 1 μM SA for 8 days and cells were fixed and stained with ORO. Concentrations as little as 100 nM SA resulted in a complete elimination of lipid droplets (**Fig 1. A**). Treatment did not affect cell viability (units = % viability): 88.6 ± 9.6 % for solvent control, 88.6 ± 9.7 % for 100 nM SA, and 90.2 ± 4.8 % for 1000 SA (P>0.05,

n=3). Reductions in lipid accumulation were observed with SA concentrations of ~50 nM (data not shown). Subsequent experiments were performed with 100 nM and 1 μM of SA. To understand the effects of ACC inhibition by SA on adipocyte differentiation, we looked at PPARγ mRNA expression; PPARγ is the master regulator of adipogenesis. Cells treated with 100 nM or 1 μM SA showed a dose-dependent decrease in PPARγ mRNA expression at both days 4 and 8 (**Fig 1. B**). Fatty acid binding protein 4 (FABP4 also known as aP2) transports fatty acids and lipophilic substances between the cytoplasm and nucleus and is a downstream target of PPARγ. Its gene expression was downregulated in a dose-dependent manner similar to PPARγ at days 4 and 8, although this was not significant (**Fig 1. C**).

Palmitate partially restores lipid accumulation and PPARγ expression in SA treated cells.

Palmitate has previously been shown to activate PPARγ in an vitro-ligand assay [25] and stimulate triacylglycerol accumulation and adipocyte differentiation in 3T3-L1 cells [26]. SA treatment caused a ~75% decrease in lipid accumulation compared with solvent controls, which was only partially restored by exogenous palmitate (**Fig.2A**). Importantly, exogenous palmitate restored the expression of the differentiation markers, PPARγ mRNA and FABP4 mRNA to control levels in SA-treated cells (**Fig. 2B, C**). Palmitate did not affect the viability of the cells. (data not shown).

SA treatment results in an increase in fatty acid oxidation

ACC1 is highly abundant in adipose tissue and plays a prominent role in de novo lipogenesis. ACC2 expression is comparatively lower in adipose tissue and would not be expected to be affected by SA treatment. To measure fatty acid oxidation, cells were treated with [9,10-^{3}H]-

palmitic acid after pretreatment with DMSO, 100 nM SA starting from day 0, or 1 μM SA for 12 hours. When [9,10-^{3}H]-palmitic acid undergoes dehydrogenation at the acyl-CoA dehydrogenase step, ^{3}H-lableled H_2O is released into the media and can be quantified. Cells treated with either 100 nM SA for 7 days or 1 μM SA for 12 hours had a ~3 fold and ~2 fold increase in fatty acid oxidation, respectively. Administration of BSA resulted in no change in fatty acid oxidation (FAO) between treatment groups. Etomoxir served as a negative control, inhibiting fatty acid oxidation by ~40% compared with controls (**Fig. 3**). There was no change in ACC protein expression between the control and treatment groups (data not shown).

Glucose uptake is maintained in SA treated cells

Impaired triacylglycerol storage can lead to insulin resistance [27]. Lipid accumulation is attenuated in our SA-treated cells and we wanted to observe the effects of SA on the expression of glucose transporter 4 (GLUT4) and glucose uptake. Treatment with 100nM SA was effective in reducing the amount of GLUT4 mRNA while the addition of palmitate rescued its expression (**Fig. 4A**). To determine if glucose uptake was affected upon treatment with SA treatment, cellular accumulation of glucose was measured using 2-[1,2-^{3}H(N)]deoxy-*D*-glucose. Despite changes in GLUT4 mRNA expression, glucose uptake was unchanged even upon stimulation with insulin, indicating that insulin sensitivity is maintained in these cells.

Continuous administration of SA is required to maintain an uncommitted phenotype

To determine if SA could completely block differentiation, a series of time course experiments were performed to establish a time frame during which cells would remain undifferentiated even upon removal of SA. Cells were treated with SA for 8,10, or 12 days and collected at day 16.

PPARγ and FABP4 mRNA expression was not significantly different between treatment groups when measured at day 16 (**Fig.5 A,B**). Interestingly, PPARγ and FABP4 mRNA expression, although not significant, showed a trend to increase in SA treated cells, possibly as a way to overcome the lack of activaton. Consistent with the lack of changes in adipogenic gene expression between treatment groups, lipid began accumulating upon removal of SA (data not shown). SA administration in terminally differentiated adipocytes does not eliminate lipid droplet formation.

Introduction of a dominant negative PPARγ into mature 3T3-L1 cells results in de-differentiataion of adipocytes with decreased expression of adipocyte markers and lipid accumulation [28]. We wanted to determine if SA could revert the phenotype of terminally differentiated 3T3-L1 cells by downregulating the expression of PPARγ and lipid accumulation. cells were differentiated for 8 days and subsequently treated with either 100 nM or 1 μM SA for 4 days. There was no change in the size or the amount of lipid droplets after 4 days of SA administration at either concentration when administration started at day 8 (**Fig. 5B**). These results indicate that continuous administration of SA beginning in early stages of differentiation is required to inhibit lipid accumulation in 3T3-L1 cells.

Differentiation by rosiglitazone and insulin maintains adipogenic gene expression upon treatment with SA

Rosiglitazone, a member of the thiazolidinediones, a class of drugs that is prescribed as Type 2 diabetes medication, is an agonist of PPARγ that binds to the receptor with a K_d of 40 nM [29]. Cells were differentiated with rosiglitazone and insulin and treated with either 100 nM SA with or without 200 μM palmitate. Surprisingly, gene expression analysis at day 8, showed an increase in PPARγ and FABP4 expression when treated with both SA 100 nM or SA 100 nM

and 200 μM palmitate (**Fig. 6A,B**) compared with controls. Treatment with 200 μM palmitate was particularly effective in elevating PPARγ and FABP4 mRNA expression. There were no significant differences in GLUT4 mRNA expression between treatment groups (**Fig. 6C**). Despite these changes in gene expression, the control cells had the most lipid accumulation(**Fig. 6D**).

Discussion

Soraphen A is a naturally occurring compound derived from the soil dwelling myxobacterium *Sorangium cellulosum*. This polyketide is likely essential for its survival, protecting bacteria from pathogenic fungi [30]. The goal of this study was to determine if inhibition of ACCs by SA is capable of blocking adipocyte differentiation. The rationale for this study is based on the fact that malonyl-CoA produced from ACCs feeds into the fatty acid synthesis pathway that produces endogenous ligands for PPARγ, thus promoting adipogenesis. Previously, mice fed a high fat diet supplemented with SA, were found to have reduced adiposity and weight gain [16]. The study did not provide a reason for the observed decrease in body fat but it may be due to the inhibition of adipogenesis. A fat-specific FAS knockout mouse model was shown to lead to an increase in brown fat-like adipocytes in subcuanteous adipose tissue and increased energy expenditure [17]. This is the first report to observe that SA decreases adipogenesic gene expression and by triacylglycerol accumulatio in 3T3-L1 cells. Our findings that FABP4 is decreased in 3T3-L1 cells is consistent with the observation that in primary mouse embryonic fibroblasts, protein and gene expression of aP2 (FABP4) was decreased when there was FAS knockdown in these cells. Additionally, 3T3-L1 cells with FAS knockdown, [17] also showed a decrease in aP2 and CD36 protein expression. However, we also saw a decrease in gene

expression of PPARγ while Lodhi et al. reported no change in PPARγ protein expression. They attribute these changes to a lack of PPARγ activation. Our finding that PPARγ gene expression is decreased in SA-treated cells does agree with a previous report that found that an inhibitor of the CT domain in ACCs, choloracetylated biotin derivative (CABI), blocked adipogenesis as observed by inhibition of PPARγ protein expression and a decrease in lipid accumulation [31]. However, CABI is less potent than SA at inhibiting lipid accumulation and adipogenic protein expression. Concentrations of 8 μM of CABI were required to see a reduction in PPARγ protein expression and lipid accumulation whereas 100 nM of SA was sufficient to block adipogenic gene expression and lipid accumulation. (**Fig1A,C-D**).

Lipogenesis is favored upon insulin activation of ACC with the majority of de novo lipogenesis feeding into triglyceride accumulation [32]. Because lipid accumulation was completely eliminated in SA treated cells palmitate supplementation was administered to see if it could restore adipogenesis. Palmitate has previously been shown to stimulate triacylglycerol accumulation and adipocyte differentiation in 3T3-L1 cells [26] and activates PPARγ in an vitro-ligand assay [25]. Palmitate was able to restore adipogenic gene expression however, it only resulted in a slight increase in lipid accumulation (**Fig2A,C-D**). While we saw this restoration of PPARy and FABP4 expression upon treatment with palmitate, this may just be the result of lipid droplet formation from palmitate accumulation and not necessarily indicate an increase in lipogenesis, especially since this increase in lipid accumulation is not equal to that of control cells. Interestingly, palmitoyl-CoA acts similarly to SA by binding to the BC domain of ACCs promoting their dissociation and inhbition of ACCs and consequently increasing FAO [33].

The role of ACC1 in de novo lipogenesis is well established [2] and ACC1 is highly expressed in adipose tissue [34]. ACC2 is expressed abundantly in skeletal muscle while mouse adipose

tissue has low levels of ACC2 [34], the ACC isoform responsible for production of malonyl-CoA that inhibits CPTI, the enzyme responsible for catalyzing the rate limiting step in fatty acid oxidation of long chain fatty acids [4]. Increases in fatty acid oxidation upon treatment with SA have previously been observed in liver HepG2 cells, and prostate cancer cell lines in LNCaP and PC-3M cells [35] [36]. Interestingly, we found a ~3- and ~2-fold increase in fatty acid oxidation with both chronic and acute treatment of SA, respectively (**Fig.3**) and this increase is comparable to those achieved in other cell lines, ~3-fold in HepG2 cells and ~2-fold in LNCaP cells [35,36]. These results suggest that fatty acid oxidation is at least partially responsible for the lack of triacylglycerol accumulation in SA treated cells.

Impairment of triacylglycerol storage and inhibition of *de novo* lipogenesis impairs insulin sensitivity [27] and promoting glucose uptake into adipose tissue prevents diabetes in mice with transgenic enhancement of the insulin-sensitive glucose transporter, GLUT4(Shepherd, J. biol. Chem, 1993). Because we saw a decrease in other adipogenic target genes and lipid accumulation, we investigated whether GLUT4, another transcriptional target of PPARγ and glucose uptake is affected by SA administration. Treatment with SA decreased GLUT4 mRNA expression and was restored to levels of the control with palmitate supplementation. However, we found that insulin-mediated glucose uptake was unaffected in 3T3-L1 cells treated with SA upon insulin (**Figure 4A,B**). Upon stimulation by insulin, GLUT4 is translocated to the plasma membrane independently of transcription and translation[37] and this may explain why glucose uptake is unaffected by SA treatment even though there is a change in GLUT4 mRNA expression. This is particularly important to note as adipose tissue-GLUT4 depletion leads to insulin resistance in liver and muscle tissue [38] even though adipose tissue is not the primary tissue responsible for glucose disposal [39]. Our glucose uptake results are in agreement with

those results obtained from animal studies. Mice fed high fat diets supplemented with SA maintained insulin sensitivity as observed by insulin-stimulated disposal rates and glucose infusion rates similar to mice fed a chow diet [16].

Inhibition of adipogenic genes and lipid accumulation by SA only occurred if SA was continuously added to the media at the beginning of differentiation. Surprisingly, though at day 16 of SA administration, PPARγ and FABP4 gene expression were elevated compared to control cells and cells that had had SA removed at either day 8, 10 or 12. This may have been the cell's attempt to overcome SA treatment and promote triacylglycerol storage. Even when SA was administered for more than 16 days, upon its removal, the cells would resume differentiation. This has been reported previously with the dual ACC inhibitor, CABI [31]. Adipogenesis is a highly regulated process and involves a number of transcription factors and signaling pathways [40]. We suspect that even though PPARγ is downregulated, there may be other factors that are unaffected by SA inhibition. The CCAAT-enhancer-binding protein beta (C/EBPβ) is found to be crucial for adipogenesis in immortalized preadipocyte line but may not be necessary for mouse embryonic fibroblasts (MEFs) [41]. We found that C/EBPβ mRNA expression is unaffected by SA treatment (**Supplemental Fig. 1**) and this may explain in part why 3T3-L1 cells proceed through adipogenesis upon removal of SA.

If SA was administered in later stages of differentiation, there was no change in the size or amount of lipid droplets and the adipogenic genes remain unchanged. Work by Camp et al. demonstrated that a novel potent antagonist, PD068235 was unable to cause dedifferentiation of mature adipocytes indicating that PPARγ activation is minimal in differentiated adipocytes [42]. We tested the effect of differentiating cells with rosiglitazone, a PPARγ agonist, and insulin and observed the effects on adipogenesis while simultaneously administering SA. Surprisingly, we

found that PPARγ and FABP4 gene expression were increased despite treatment with SA. Administering SA in combination with palmitate resulted in even more dramatic increase in PPARγ and FABP4. This contrasts with the results we obtained when administering SA in 3T3-L1 cells that are differentiated with the classic differentiation cocktail of insulin, IBMX, and dexamethasone where SA treatment decreased adipogenic markers. These differences in adipogenic gene expression in cells differentiated by the two differentiation methods indicate that what we have observed may not necessarily be inhibition of adipocyte differentiation but rather an altered adipocyte phenotype that prevents lipid accumulation.

We report here that inhibition of ACCs by SA decreases adipogenic gene expression and lipid accumulation. Fatty acid oxidation is at least partially responsible for the lack of lipid droplet accumulation. Treatment with SA maintains insulin sensitivity in these cells despite a reduction in GLUT4 mRNA translocation. Upon removal of SA, 3T3-L1 cells proceed through adipogenesis. We propose that ACC inhibition alters lipid metabolism but not adipogenesis in 3T3-L1 cells.

Table 1. PCR primers

Gene	Primers
Mouse 18S ribosomal RNA	FWD 5'-CTGAGAAACGGCTACCACATC-3' REV 5'-GCCTCGAAAGAGTCCTGTATTG-3'
Mouse peroxisome proliferator-activated receptor gamma transcript variant 2(PPARγ)	FWD 5'-AGATTCTCCTGTTGACCCAGAGCA-3' REV 5'-ATTCCGAAGTTGGTGGGCCAGAAT-3'
Mouse fatty acid binding protein 4 (FABP4)	FWD 5'-ATGAAATCACCGCAGACGACAGGA-3' REV 5'-TGTGGTCGACTTTCCATCCCACTT-3'
Mouse glucose transporter 4 (GLUT4)	FWD 5'-GGAGGGAGCCTTTGGTATTT-3' REV 5'-CAGCACAGGACACTCATCTT-3'
Mouse CCAAT-enhancer binding protein beta (C/EBPβ)	FWD 5'-CTTGATGCAATCCGGATCAAAC-3' REV 5'-CCCGCAGGAACATCTTTAAGT-3'
Mouse acetyl-CoA carboxylase 1 (ACC1)	FWD 5'-TAACAGAATCGACACTGGCTGGCT-3' REV 5'-ATGCTGTTCCTCAGGCTCACATCT-3'
Mouse acetyl-coA carboxylase 2 (ACC2)	FWD 5'-ACCCACTGTCTTCCAATGACACCT-3' REV 5'-TCAGCTGTCTCTTGATGTGTGCCT-3'

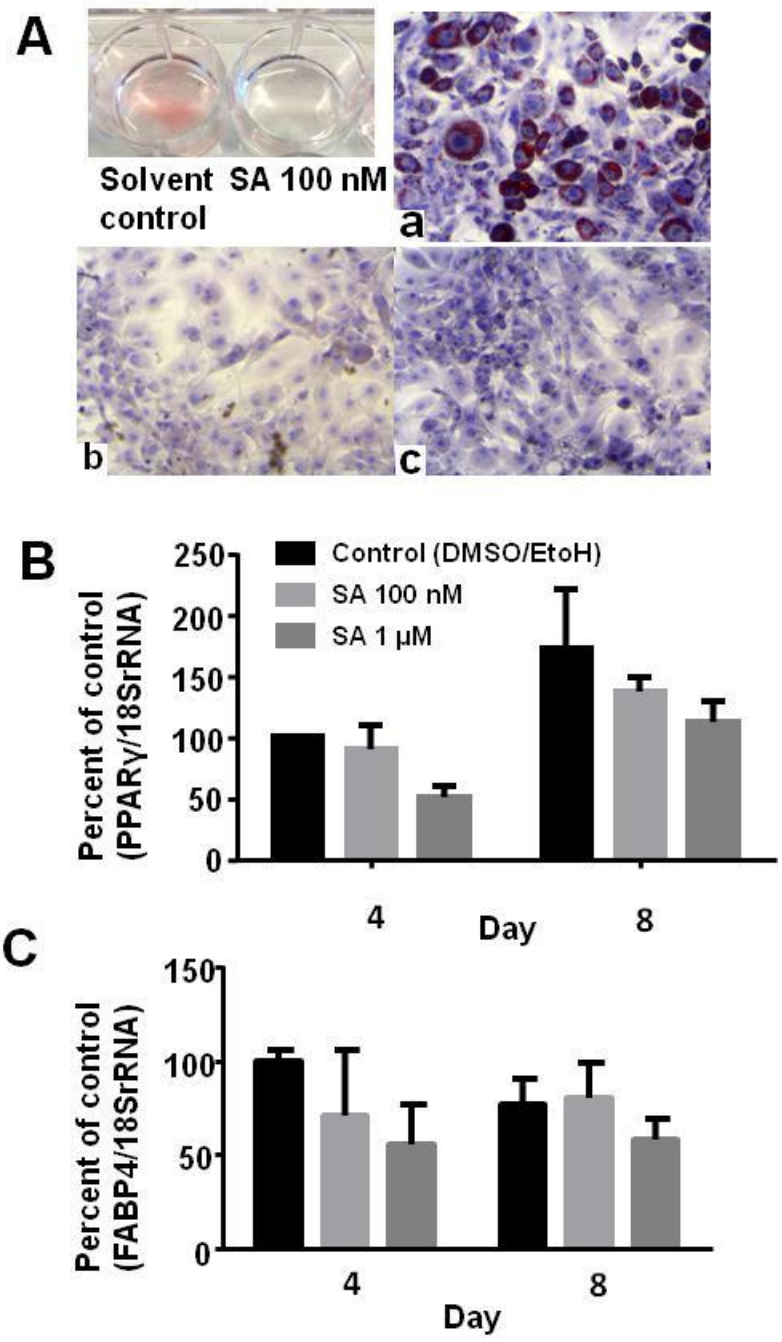

Figure 1. Soraphen A decreases lipid accumulation and adipogenic gene expression. A) 3T3-L1 cells were treated with a DMSO vehicle control (a) or either 100 nM (b) or 1 µM (c) SA for 8 days and cells were fixed at Day 8 and stained with Oil Red O. Gene expression of B) PPARγ and C) FABP4 was measured at day 4 and 8. mRNA expression was normalized to 18srRNA and

calculated as % of control (2-way ANOVA *$p<0.05$). Results are representative of 3 different experiments.

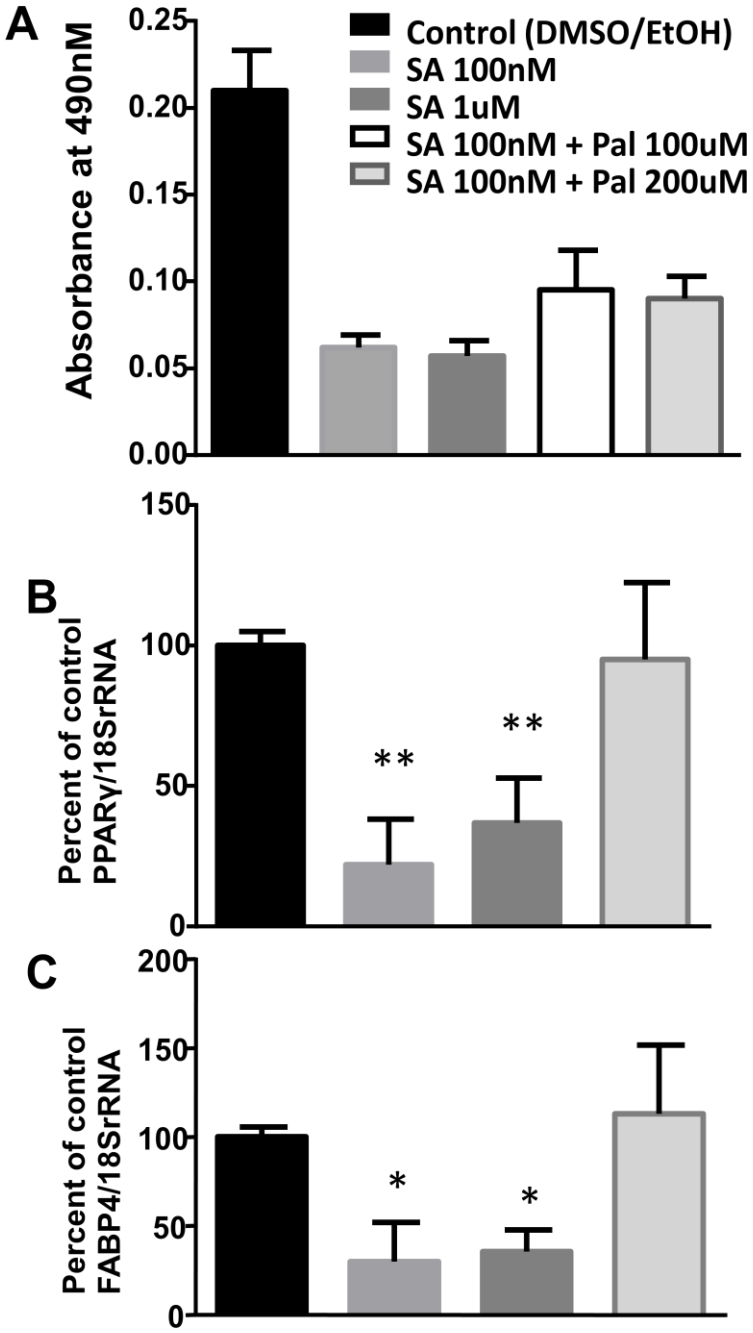

Figure 2. Palmitate rescues expression of PPARγ and FABP4 and partially restores lipid droplet accumulation. A) 3T3-L1 cells were treated with SA for 8 days (a) or SA and 100μM or 200μM

palmitate. Cells were fixed at Day 8 and stained with Oil Red O and absorbance at 490nM was measured. Gene expression of B) PPARγ and C) FABP4 upon treatment with or without SA and/or palmitate treatment. mRNA expression was normalized to 18srRNA and calculated as % of control (One way ANOVA**$p<0.01$). D) Cell viability. Results are representative of 3 different experiments. **$p<0.01$;*$p<0.05$, significantly different from control.

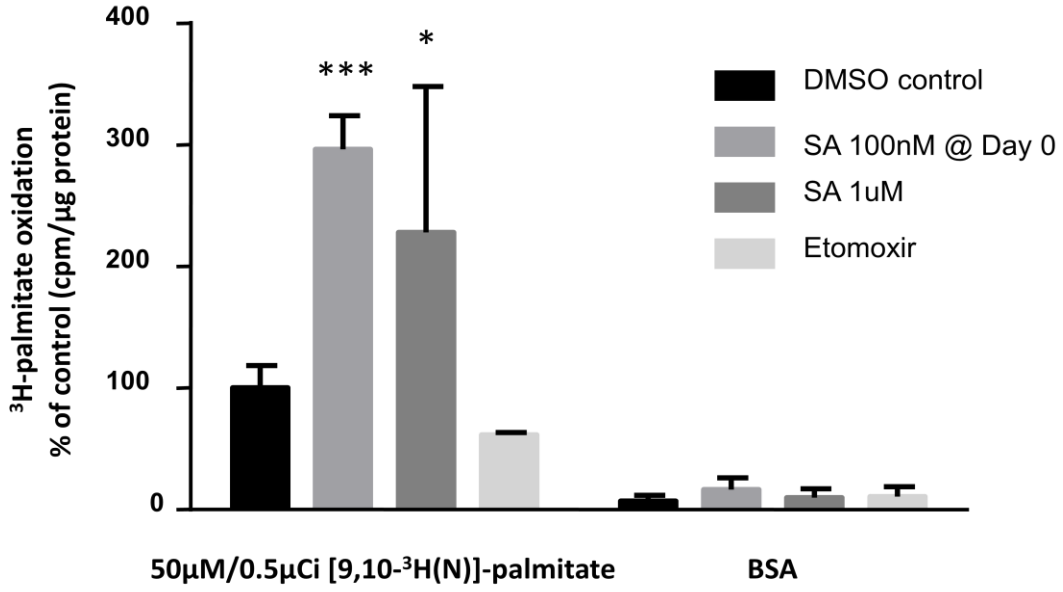

Figure 3. Fatty acid oxidation is increased in SA treated cells. A) 3T3-L1 cells were differentiated for 7 days and treated with or without 100nM SA beginning at Day 0 or SA 1µM for 12 hours prior to addition of either BSA or 50µM/0.5µCi [9,10-^{3}H]-palmitate for 2 hours. Samples were processed as described and ^{3}H-labeled H_2O was quantified by liquid scintillation counting. Results were calculated as counts per minute/ug protein and expressed as % of control. Results are representative of 5 different experiments. ***p<0.001;**p<0.01;*p<0.05, significantly different from control.

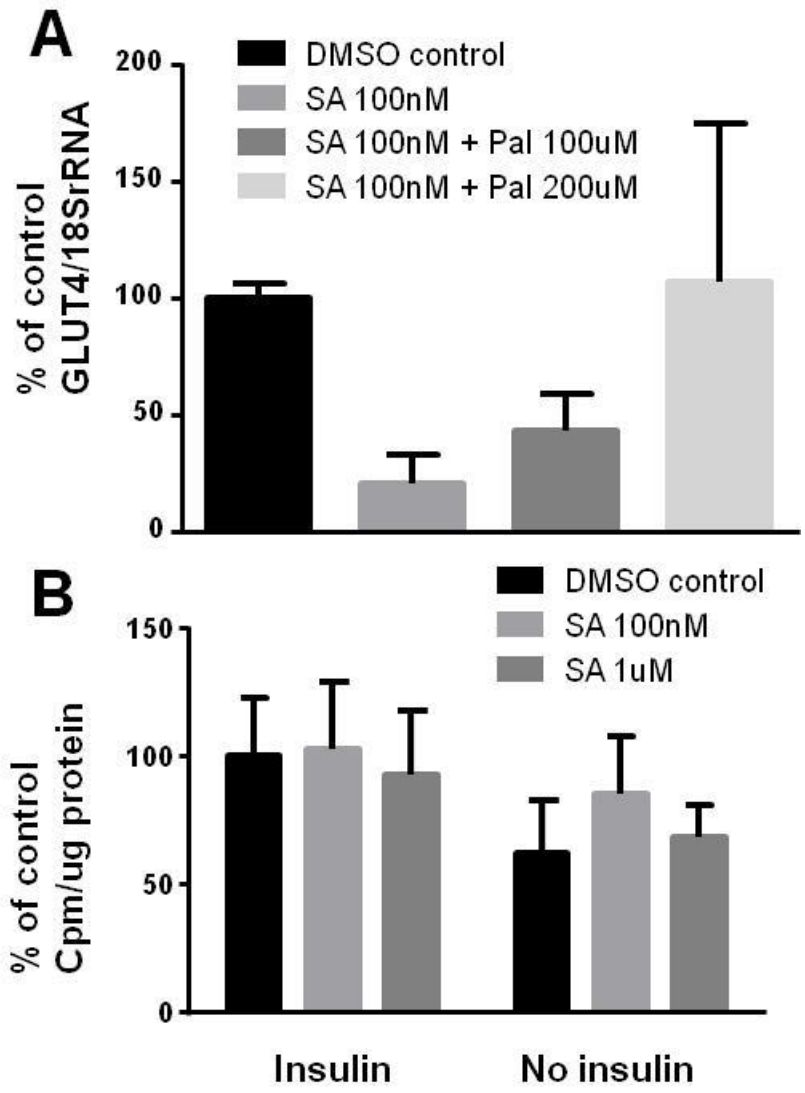

Figure 4. Insulin sensitivity is maintained in SA treated cells. A) GLUT4 mRNA expression upon treatment with or without SA and/or palmitate treatment. mRNA expression was normalized to 18srRNA and calculated as % of control. B) Glucose uptake assays. 3T3-L1 cells were differentiated for 7 days and treated with or without 100nM SA beginning at Day 0 or SA 1μM for 12 hours prior to addition of 2-[1,2-3H(N)]deoxy-d-glucose [0.05μCi/mL] for 90 minutes. Samples were processed as described and quantified with a liquid scintillation counter.

Results were calculated as counts per minute/μg protein and expressed as % of control. Results are representative of 3 different experiments.

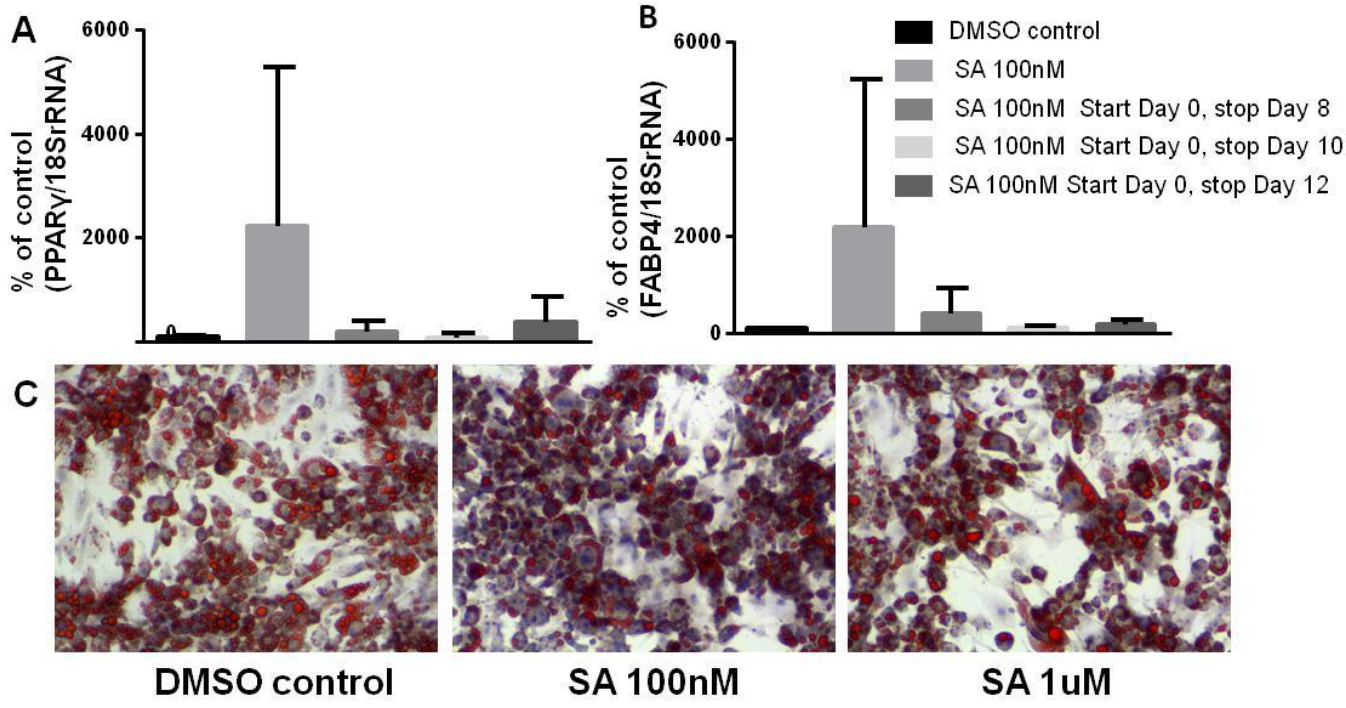

Figure 5. Time course additions of SA. Cells were treated with SA for 8, 10, 12, 0r 16 days followed by sample collection after Day 16. Gene expression of A) PPARγ or B) FABP4 from cells treated for SA for various times. C) 3T3-L1 cells were treated with either 100 nM or 1 μM SA beginning at 8 days post-differentiation and fixed at Days 12. Cells were stained with ORO and viewed at 4x using a Nikon Ti-S Inverted Fluorescence Microscope.

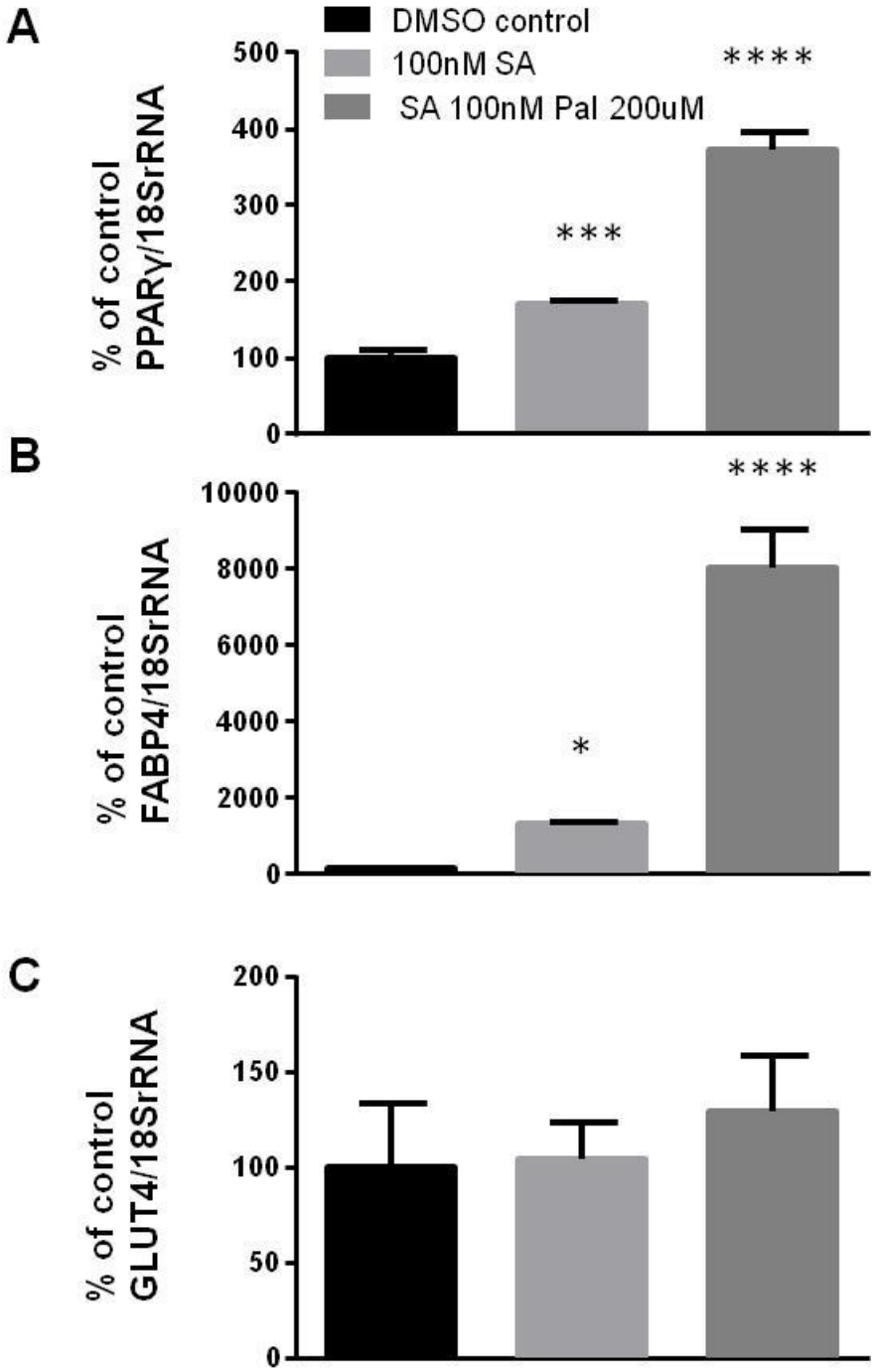

Figure 6. Rosiglitazone rescues adipogenic gene expression despite treatment with SA. Cells were differentiated with a rosiglitazone/insulin cocktail and treated with either 100 nM SA with or without 200 μM palmitate. Gene expression of A)PPARγ B)FABP4 C)GLUT4 was quantified using RT-qPCR. mRNA expression was normalized to 18srRNA and calculated as % of control

(One-way ANOVA $p<0.0001$ for PPARγ and FABP4; GLUT4 n.s.).Results are representative of 3 different experiments.****$p<0.0001$;***$p<0.001$; **$p<0.01$;*$p<0.05$, significantly different from control.

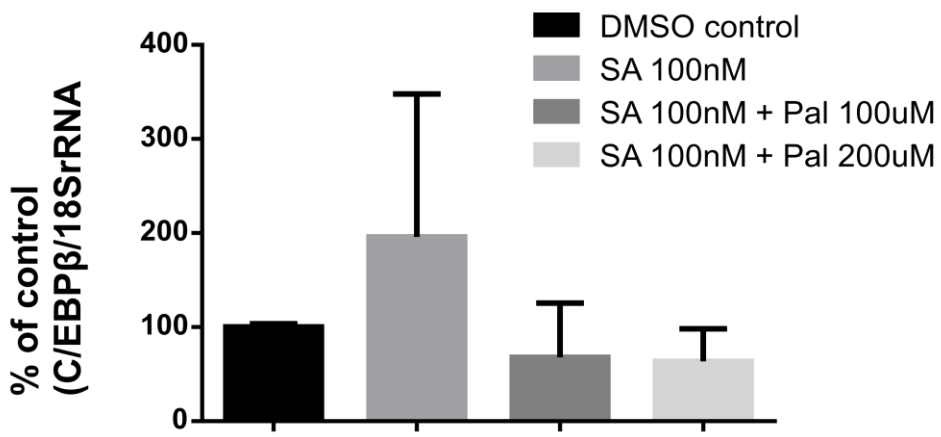

Supplemental Figure 1. Gene expression of C/EBPβ upon treatment with or without SA and/or palmitate treatment. mRNA expression was normalized to 18SrRNA and calculated as % of control. Results are representative of 3 different experiments.

References

1. Wakil S, Gibson DM. Studies on the mechanism of fatty acid synthesis. VIII. the participation of protein-bound biotin in the biosynthesis of fatty acids. Biochim Biophys Acta 1960;41:122-129
2. Wakil SJ, Stoops JK, Joshi VC. Fatty acid synthesis and its regulation. Annu Rev Biochem 1983;52:537-579
3. McGarry JD, Leatherman GF, Foster DW. Carnitine palmitoyltransferase I. The site of inhibition of hepatic fatty acid oxidation by malonyl-CoA. J Biol Chem 1978;253:4128-4136
4. McGarry JD, Brown NF. The mitochondrial carnitine palmitoyltransferase system. From concept to molecular analysis. Eur J Biochem 1997;244:1-14
5. Abu-Elheiga L, Matzuk MM, Abo-Hashema KA, Wakil SJ. Continuous fatty acid oxidation and reduced fat storage in mice lacking acetyl-CoA carboxylase 2. Science 2001;291:2613-2616
6. Oh SY, Park SK, Kim JW, et al. Acetyl-CoA carboxylase beta gene is regulated by sterol regulatory element-binding protein-1 in liver. J Biol Chem 2003;278:28410-28417
7. Choi CS, Savage DB, Abu-Elheiga L, et al. Continuous fat oxidation in acetyl-CoA carboxylase 2 knockout mice increases total energy expenditure, reduces fat mass, and improves insulin sensitivity. Proc Natl Acad Sci USA 2007;104:16480-16485
8. Hoehn KL, Turner N, Swarbrick MM, et al. Acute or chronic upregulation of mitochondrial fatty acid oxidation has no net effect on whole-body energy expenditure or adiposity. Cell Metab 2010;11:70-76

9. Olson DP, Pulinilkunnil T, Cline GW, Shulman GI, Lowell BB. Gene knockout of Acc2 has little effect on body weight, fat mass, or food intake. Proc Natl Acad Sci USA 2010;107:7598-7603

10. Abu-Elheiga L, Matzuk MM, Kordari P, et al. Mutant mice lacking acetyl-CoA carboxylase 1 are embryonically lethal. Proc Natl Acad Sci USA 2005;102:12011-12016

11. Harada N, Oda Z, Hara Y, et al. Hepatic de novo lipogenesis is present in liver-specific ACC1-deficient mice. Mol Cell Biol 2007;27:1881-1888

12. Mao J, DeMayo FJ, Li H, et al. Liver-specific deletion of acetyl-CoA carboxylase 1 reduces hepatic triglyceride accumulation without affecting glucose homeostasis. Proc Natl Acad Sci U S A 2006;103:8552-8557

13. Gerth K, Bedorf N, Irschik H, Hofle G, Reichenbach H. The soraphens: a family of novel antifungal compounds from Sorangium cellulosum (Myxobacteria). I. Soraphen A1 alpha: fermentation, isolation, biological properties. J Antibiot (Tokyo) 1994;47:23-31

14. Vahlensieck HF, Pridzun L, Reichenbach H, Hinnen A. Identification of the yeast ACC1 gene product (acetyl-CoA carboxylase) as the target of the polyketide fungicide soraphen A. Curr Genet 1994;25:95-100

15. Shen Y, Volrath SL, Weatherly SC, Elich TD, Tong L. A mechanism for the potent inhibition of eukaryotic acetyl-coenzyme A carboxylase by soraphen A, a macrocyclic polyketide natural product. Mol Cell 2004;16:881-891

16. Schreurs M, van Dijk TH, Gerding A, et al. Soraphen, an inhibitor of the acetyl-CoA carboxylase system, improves peripheral insulin sensitivity in mice fed a high-fat diet. Diabetes Obes Metab 2009;11:987-991

17. Lodhi IJ, Yin L, Jensen-Urstad AP, et al. Inhibiting adipose tissue lipogenesis reprograms thermogenesis and PPARgamma activation to decrease diet-induced obesity. Cell Metab 2012;16:189-201

18. Zempleni J, Mock DM. Uptake and metabolism of biotin by human peripheral blood mononuclear cells. Am J Physiol Cell Physiol 1998;275:C382-C388

19. Kaur Mall G, Chew YC, Zempleni J. Biotin requirements are lower in human Jurkat lymphoid cells but homeostatic mechanisms are similar to those of HepG2 liver cells. J Nutr 2010;140:1086-1092

20. Manning NJ, Olpin SE, Pollitt RJ, Webley J. A comparison of [9,10-3H]palmitic and [9,10-^{3}H]myristic acids for the detection of defects of fatty acid oxidation in intact cultured fibroblasts. J Inherit Metab Dis 1990;13:58-68

21. Horn CC, Ji H, Friedman MI. Etomoxir, a fatty acid oxidation inhibitor, increases food intake and reduces hepatic energy status in rats. Physiol Behav 2004;81:157-162

22. Brown JM, Boysen MS, Chung S, et al. Conjugated linoleic acid induces human adipocyte delipidation: autocrine/paracrine regulation of MEK/ERK signaling by adipocytokines. J Biol Chem 2004;279:26735-26747

23. Rios-Avila L, Prince SA, Wijeratne SSK, Zempleni J. A 96-well plate assay for high-throughput analysis of holocarboxylase synthetase activity. Clin Chim Acta 2011;412:735-739

24. Kwon JY, Seo SG, Heo YS, et al. Piceatannol, a natural polyphenolic stilbene, inhibits adipogenesis via modulation of mitotic clonal expansion and insulin receptor-dependent insulin signaling in the early phase of differentiation. J Biol Chem 2012;287:11566-11578

25. Kliewer SA, Sundseth SS, Jones SA, et al. Fatty acids and eicosanoids regulate gene expression through direct interactions with peroxisome proliferator-activated receptors alpha and gamma. Proc Natl Acad Sci U S A 1997;94:4318-4323

26. Madsen NB, Shechosky S, Fletterick RJ. Site-site interactions in glycogen phosphorylase *b* probed by ligands specific for each site. Biochem 1983;22:4460-4465

27. Czech MP, Tencerova M, Pedersen DJ, Aouadi M. Insulin signalling mechanisms for triacylglycerol storage. Diabetologia 2013;56:949-964

28. Zhang J, Fu M, Cui T, et al. Selective disruption of PPARgamma 2 impairs the development of adipose tissue and insulin sensitivity. Proc Natl Acad Sci U S A 2004;101:10703-10708

29. Lehmann JM, Moore LB, Smith-Oliver TA, et al. An antidiabetic thiazolidinedione is a high affinity ligand for peroxisome proliferator-activated receptor gamma (PPAR gamma). J Biol Chem 1995;270:12953-12956

30. Ligon J, Hill S, Beck J, et al. Characterization of the biosynthetic gene cluster for the antifungal polyketide soraphen A from *Sorangium cellulosum* So ce26. Gene 2002;285:257-267

31. Levert KL, Waldrop GL, Stephens JM. A biotin analog inhibits acetyl-CoA carboxylase activity and adipogenesis. J Biol Chem 2002;277:16347-16350

32. Mackall JC, Student AK, Polakis SE, Lane MD. Induction of lipogenesis during differentiation in a "preadipocyte" cell line. J Biol Chem 1976;251:6462-6464

33. Tong L. Acetyl-coenzyme A carboxylase: crucial metabolic enzyme and attractive target for drug discovery. Cell Mol Life Sci 2005;62:1784-1803

34. Castle JC, Hara Y, Raymond CK, et al. ACC2 is expressed at high levels in human white adipose and has an isoform with a novel N-terminus [corrected]. PLoS ONE 2009;4:e4369

35. Jump DB, Torres-Gonzalez M, Olson LK. Soraphen A, an inhibitor of acetyl CoA carboxylase activity, interferes with fatty acid elongation. Biochem Pharmacol 2011;81:649-660

36. Beckers A, Organe S, Timmermans L, et al. Chemical inhibition of acetyl-CoA carboxylase induces growth arrest and cytotoxicity selectively in cancer cells. Cancer Res 2007;67:8180-8187

37. Herman MA, Kahn BB. Glucose transport and sensing in the maintenance of glucose homeostasis and metabolic harmony. J Clin Invest 2006;116:1767-1775

38. Abel ED, Peroni O, Kim JK, et al. Adipose-selective targeting of the GLUT4 gene impairs insulin action in muscle and liver. Nature 2001;409:729-733

39. Bluher M, Michael MD, Peroni OD, et al. Adipose tissue selective insulin receptor knockout protects against obesity and obesity-related glucose intolerance. Developmental cell 2002;3:25-38

40. Rosen ED, MacDougald OA. Adipocyte differentiation from the inside out. Nat Rev Mol Cell Biol 2006;7:885-896

41. Tang QQ, Otto TC, Lane MD. CCAAT/enhancer-binding protein beta is required for mitotic clonal expansion during adipogenesis. Proc Natl Acad Sci U S A 2003;100:850-855

42. Camp HS, Chaudhry A, Leff T. A novel potent antagonist of peroxisome proliferator-activated receptor gamma blocks adipocyte differentiation but does not revert the phenotype of terminally differentiated adipocytes. Endocrinology 2001;142:3207-3213

Outlook

We have demonstrated that inhibitors designed against HLCS work *in vitro*. However, in a cell culture system we were unable to observe a decrease in biotinylated carboxylases and saw an increase in carboxylase biotinylation. These results indicate the need for further studies with respect to the development of HLCS inhibitors. However, this could prove challenging given the difficulty in developing inhibitors that selectively target the mammalian HLCS over the bacterial homologs and vice versa. To date, only one class of inhibitors specific to Staphylococcus aureus biotin protein ligase has been developed [1]. The value of HLCS inhibitors is that they provide a means by which to study the impact of HLCS on gene regulation and enzyme activity within a cellular context. Given that there is no living *HLCS* null individual and that mutations in HLCS can present with severe symptoms and possibility of fatality, using these inhibitors in animals or humans to study HLCS within a mammalian system would most likely be dangerous [2-4]. To validate previous *in vitro* observations and perform animal studies that are currently not feasible, development of a conditional HLCS knockout (KO) mouse model will allow us to investigate HLCS interactions *in vivo*. We are in the process of creating a conditional HLCS KO mouse in which expression can be controlled both spatially and temporally. These mice will allow us to knock out HLCS gene in specific tissues at defined developmental stages and investigate the impacts of HLCS on gene regulation, and genome stability, and HLCS-dependent enzyme activity under controlled conditions.

The ACCs continue to be an active area of research as drug targets in the treatment of metabolic disorders [5]. Animal studies have demonstrated that treatment with Soraphen A prevents mice from diet induced obesity and weight gain[6]. Here we report that Soraphen A, an inhibitor of eukaryotic ACC activity prevents adipogenic gene expression and lipid accumulation in 3T3-L1

cells. However, it is unknown whether or not these results carry over to humans. It would be important to first establish if lipogenesis is blocked upon treatment with Soraphen A or other ACC inhibitors in human adipogenic stem cells. There are other considerations to take into account as well. Adipose tissue is not the primary site of *de novo* lipogenesis upon high fat feeding in humans [7]. Fat-specific fatty acid synthase knockout mice demonstrate decreased adipogenesis and increased thermogenesis [8]. It is unknown if a similar outcome would be observed upon inhibition of lipogenic genes in human adipose tissue. Additionally, it is unknown how ACC inhibitors would act in humans. The ACCs are present in multiple tissues and serve different roles depending on the tissue. Administering these inhibitors *in vivo* could have detrimental effects if the distribution of ACC inhibitors is nonspecific. These questions demonstrate the need for more research into the effects of ACC inhibitors in human adipogenic stem cells and *in vivo* human studies.

References

1. Soares da Costa TP, Tieu W, Yap MY, et al. Selective inhibition of biotin protein ligase from Staphylococcus aureus. J Biol Chem 2012;287:17823-17832
2. Suzuki Y, Yang X, Aoki Y, Kure S, Matsubara Y. Mutations in the holocarboxylase synthetase gene *HLCS*. Human Mutat 2005;26:285-290
3. Dupuis L, Campeau E, Leclerc D, Gravel RA. Mechanism of biotin responsiveness in biotin-responsive multiple carboxylase deficiency. Mol Genet Metabol 1999;66:80-90
4. Wilson CJ, Myer M, Darlow BA, et al. Severe holocarboxylase synthetase deficiency with incomplete biotin responsiveness resulting in antenatal insult in samoan neonates. Journal of Pediatrics 2005;147:115-118
5. Bourbeau MP, Bartberger MD. Recent advances in the development of acetyl-CoA carboxylase (ACC) inhibitors for the treatment of metabolic disease. J Med Chem 2015;58:525-536
6. Schreurs M, van Dijk TH, Gerding A, et al. Soraphen, an inhibitor of the acetyl-CoA carboxylase system, improves peripheral insulin sensitivity in mice fed a high-fat diet. Diabetes Obes Metab 2009;11:987-991
7. Letexier D, Pinteur C, Large V, Frering V, Beylot M. Comparison of the expression and activity of the lipogenic pathway in human and rat adipose tissue. J Lipid Res 2003;44:2127-2134
8. Lodhi IJ, Wei X, Semenkovich CF. Lipoexpediency: de novo lipogenesis as a metabolic signal transmitter. Trends Endocrinol Metab 2011;22:1-8

Appendix

-Raw data for each chapter

Chapter I.

Inhibition of HLCS by biotin β-ketophosphonate

Table 1. Dose response curve of biotin β-ketophosphonate

β-ketoP	Gel densitometry			
0μM	172.49	111.94	56.37	110.45
50μM	61.80	40.00	40.38	78.77
100μM	53.63	29.38	36.89	67.29
250μM	33.59	18.35	27.86	57.44
500μM	13.76	11.53	15.20	32.51

Table 2. Competitive inhibition assays w/ biotin β-ketophosphonate

No β-ketoP Biotin conc.	Gel densitometry			
0μM	19.32	14.94	5.20	22.11
10μM	589.01	469.77	482.27	497.00
20μM	608.30	523.34	475.31	436.87
40μM	436.74	387.80	516.05	480.83
80μM	480.39	463.88	519.09	530.11
160μM	629.16	438.98	516.77	573.15
320μM	524.91	529.18	513.16	489.21

W/ β-ketoP Biotin Conc.	Gel densitometry			
0μM	7.67	4.68	9.02	1.64
10μM	85.50	94.56	80.18	12.83
20μM	180.18	114.23	172.13	30.59
40μM	191.93	200.85	254.83	101.83

80µM	369.72	232.02	380.98	365.46
160µM	451.58	378.07	453.76	611.73
320µM	485.12	527.53	516.35	498.39

Inhibition of HLCS by biotin β-hydroxyphosphonate

Table 3. Dose response curve of biotin β-hydroxyphosphonate

βhydroxyP	Gel densitometry			
0µM	143.29	87.64	207.85	297.98
50µM	148.12	64.16	164.16	237.01
100µM	97.43	56.22	111.82	222.16
250µM	66.73	38.28	70.72	144.53
500µM	55.73	37.58	47.96	73.08

Table 4. Competitive inhibition assays w/ biotin β-hydroxyphosphonate

No β-hydroxyP Biotin conc.	Gel densitometry			
0µM	13.12	16.56	28.29	12.87
10µM	384.34	319.61	576.00	407.24
20µM	380.12	357.86	444.50	448.87
40µM	380.70	338.24	530.13	445.51
80µM	399.70	317.41	498.36	437.09
160µM	381.88	303.64	486.62	478.20
240µM	436.39	323.15	661.25	524.07
320µM	536.18	333.53	719.23	659.66

w/β-hydroxyP Biotin conc.	Gel densitometry			
0µM	4.90	8.08	12.00	3.28
10µM	40.78	72.35	50.03	38.71
20µM	56.49	123.84	81.37	79.02
40µM	111.99	152.42	156.73	97.89
80µM	210.64	198.26	218.12	159.64
160µM	260.63	277.19	279.76	243.84
240µM	346.21	313.64	295.54	285.58

320µM	491.75	335.69	291.37	287.25

Inhibition of HLCS by biotinol-5'-AMP

Table 5. Dose response curve of biotinol-5'-AMP

Bio-5'-AMP	Gel densitometry		
0µM	125.91	290.11	112.77
50µM	11.37	44.42	14.47
100µM	6.11	18.66	3.38
250µM	5.34	8.97	2.56
500µM	2.66	5.51	2.20

Table 6. Competitive inhibition assays w/ biotinol-5'-AMP

Chapter II.

Table 7. Effect of grape leaf extract on body fat mass in male and female *Drosophila melanogaster brummer* mutants 15828.

Control and experimental Groups of *Brummer* flies	Results in mg of lipid/ grams of fly weight			
	1	2	3	4
Control-Male	31.87	31.27	32.4	13.35
Grape leaf extract 0.5% Male	19.00	3.01	18.63	10.90
Grape leaf extract 10% Male	10.28	12.36	9.21	1.55
Control-Female	29.91	31.33	39.21	29.26
Grape leaf extract 0.5% Female	18.46	14.46	11.44	12.58
Grape leaf extract 10% Female	10.1	8.65	17.71	17.93

Table 8. Effect of grape leaf extract on body fat mass in male and female *Drosophila melanogaster brummer* mutants 15959.

Control and experimental Groups of *Brummer* flies	Results in mg of lipid/ grams of fly weight			
	1	2	3	4
Control-Male	9.43	10.38	14.38	12.43
Grape leaf extract 0.5%-Male	6.54	7.98	4.65	4.70
Grape leaf extract 10%-Male	4.08	6.68	6.76	5.85
Control-Female	6.89	10.96	11.15	7.41
Grape leaf extract 0.5%-Female	6.94	8.31	6.82	5.35
Grape leaf extract 10%-Female	5.83	8.16	6.80	7.33

Table 9. Effect of piceid on body fat mass in male and female *Drosophila melanogaster brummer* mutants 15828.

Control and experimental Groups of *Brummer* flies	Results in mg of lipid/ grams of fly weight			
	1	2	3	4
Control-Male	5.91	2.19	3.95	2.81
Piceid 0.012 µM-Male	1.92	1.28	4.90	
Piceid 0.12 µM-Male	0.68	0.44	0	
Control-Female	9.38	9.13	12.26	11.60
Piceid 0.012 µM-Female	7.04	6.40	8.21	
Piceid 0.12 µM-Female	11.03	7.46	7.87	

Table 10. (Chapter III) Effect of soraphen A on body fat mass in male and female *Drosophila melanogaster brummer* mutants 15828.

Control and experimental Groups of *Brummer* flies	Results in mg of lipid/ grams of fly weight			
	1	2	3	4
Control-Male	2.27	3.43	2.28	5.14
Soraphen A 5 µM-Male	0.84	0.49	1.27	1.04
Control-Female	7.36	5.59	8.97	6.69
Soraphen A 5 µM-Female	0.22	1.39	1.10	1.37

Chapter III

Table 11. Adipogenic gene expression

FABP4 mRNA expression	RT-PCR Ct values normalized by M18SrRNA			
Treatment	Repeat	1	2	3
Day 0 Control		1.00	1.00	1.00
Day 4 Control		113.79	76.66	311.41
Day 4 Soraphen A 100nM		125.41	43.82	138.15
Day 4 Soraphen A 1µM		89.78	38.24	113.87
Day 8 Control		93.11	46.75	272.13
Day 8 Soraphen A 100nM		70.04	75.46	251.33
Day 8 Soraphen A 1µM		56.44	42.24	217.88

PPARγ mRNA expression	RT-PCR Ct values normalized by M18SrRNA			
Treatment	Repeat	1	2	3
Day 0 Control		1.01	1.00	1.01
Day 4 Control		151.94	118.34	135.14
Day 4 Soraphen A 100nM		146.05	80.90	113.47

Day 4 Soraphen A 1µM	92.05	50.45	71.25
Day 8 Control	343.66	154.71	249.18
Day 8 Soraphen A 100nM	190.04	172.48	181.26
Day 8 Soraphen A 1µM	168.23	114.83	141.53

Table 12. Cell viability of cells treated with or without SA.

Treatment	#Live cells	#Dead cells
Control	1920000	48000
	1900000	216000
	1,488,000	408000
SA 100nM	1180000	72000
	1180000	72000
	576,000	168000
SA 1uM	1030000	48000
	912,000	144,000
	936,000	120000

Table 13. Adipogenic gene expression is rescued upon treatment with palmitate.

PPARy	RT-PCR Ct values normalized to 18SrRNA control		
Treatment	Repeat 1	2	3
Day 0 Ctrl	1.00	1.00	1.00
Day 8 Ctrl	448.31	241.95	989.34
Day 8 Sa 100nM SA	31.18	94.60	195.98
Day 8 +100nM SA +100uM Pal	123.98	133.77	273.45
Day 8 +100nM SA +200uM Pal	462.53	284.21	639.54

FABP4	RT-PCR Ct values normalized to 18SrRNA control		
Treatment	Repeat 1	2	3
Day 0 Ctrl	1.00	1.00	1.00

Day 8 Ctrl	576.09	334.33	816.83
Day 8 Sa 100nM SA	54.59	54.59	212.97
Day 8 +100nM SA +100uM Pal	148.23	164.68	260.49
Day 8 +100nM SA +200uM Pal	906.22	323.29	691.47

Table 14. Cell viability of 3T3-L1 treated with or without SA or SA and palmitate

Treatment	#Live	# Dead
Ctrl No SA	1296000	96000
	936000	216000
	2040000	336000
Ctrl +SA 100nM	1488000	72000
	600000	144000
	1440000	264000
SA100nM and Pal100uM	1464000	96000
	1464000	144000
	2112000	216000
SA100nM and Pal200uM	1248000	192000
	1104000	72000
	2160000	192000

Table 15. Oil Red O quantitation

Treatment	Absorbance at 490nM				
Control DMSO	0.240	0.187	0.199	0.199	0.206
SA 100nM	0.053	0.071	0.060	0.063	0.062
SA 1uM	0.066	0.047	0.051	0.064	0.057
SA 100nM Pal 200uM	0.104	0.097	0.075	0.083	0.090
SA 100nM Pal 100uM	0.074	0.084	0.095	0.127	0.095

Table 16. Fatty acid oxidation upon treatment with SA.

	Counts per minute normalized to total protein concentration					
Treatment	Repeat	1		2		3	
Control No SA + 50uM Pal		14.14	13.67	10.01	9.69	17.18	16.65

SA 100nM @ Day 0 + 50uM Pal	32.70	31.70	28.61	27.79	52.78	51.05
SA 1uM + 50uM Pal	45.22	43.80	45.04	43.65	38.92	37.71
Etomoxir + 50uM Pal	8.93	8.64	6.09	5.90	9.89	9.56
Control No SA + BSA	0.60	0.59	0.63	0.62	0.17	0.17
SA 100nM @ Day 0 + BSA	1.44	1.40	1.35	1.32	1.11	1.09
SA 1uM @ Day 0 + BSA	1.27	1.22	0.54	0.52	0.26	0.25
Etomoxir + BSA	0.36	0.34	1.62	1.57	0.15	0.14

	4		5	
Control No SA + 50uM Pal	5.33	5.16	6.69	6.50
SA 100nM @ Day 0 + 50uM Pal	18.72	18.18	19.25	18.68
SA 1uM + 50uM Pal	9.22	8.94	7.97	7.71
Etomoxir + 50uM Pal	3.93	3.81	3.59	3.48
Control No SA + BSA				
SA 100nM @ Day 0 + BSA				
SA 1uM @ Day 0 + BSA				
Etomoxir + BSA				

Table 17. GLUT4 expression is rescued upon treatment with palmitate.

GLUT4	RT-PCR Ct values normalized to 18SrRNA control		
Treatment	Repeat 1	2	3
Day 0 Ctrl	1.05	1.05	1.05
Day 8 Ctrl	355.53	31.45	555.94
Day 8 Sa 100nM SA	90.37	1.86	164.85
Day 8 +100nM SA +100uM Pal	102.67	19.07	220.55
Day 8 +100nM SA +200uM Pal	646.03	15.86	494.99

Table 18. Glucose uptake assays

	Counts per minute normalized to total protein concentration					
Treatment	Repeat 1		2		3	
Control No SA + Insulin	2.63	2.53	1.93	1.86	1.62	1.55
SA 100nM + Insulin	2.78	2.67	1.59	1.53	1.97	1.91
SA 1uM + Insulin	2.56	2.46	1.73	1.65	1.45	1.39
Control No SA	1.82	1.74	1.13	1.10	0.87	0.84
SA 100nM	2.25	2.19	1.78	1.72	1.23	1.18

Sa 1uM		1.74	1.68	1.28	1.23	1.22	1.18

Table 19. Adipogenic gene expression in 3T3-L1 cells upon treatment with SA in late stages of differentiation.

PPARγ	RT-PCR Ct values normalized to 18SrRNA control		
Treatment	Repeat	1	2
Day 0 -undifferentiated cells		1.01	1.01
Ctrl DMSO 0.3uL Coll. Day 16		3.45	19.66
Ctrl SA 100nM (0.3ul) Coll. Day 16		151.27	16.71
SA 100nM (0.3ul) Start Day 0, stop Day 8, Coll. Day 16		11.51	4.15
SA 100nM (0.3uL) Start Day 0, stop Day 10, Coll. Day 16		4.73	3.68
SA 100nM (0.3uL) Start Day 0, stop Day 12, Coll. Day 16		24.70	3.08

FABP4	RT-PCR Ct values normalized to 18SrRNA control		
Treatment	Repeat	1	2
Day 0 -undifferentiated cells		1.01	1.01
Ctrl DMSO 0.3uL Coll. Day 16		6.25	9.69
Ctrl SA 100nM (0.3ul) Coll. Day 16		270.23	135.35
SA 100nM (0.3ul) Start Day 0, stop Day 8, Coll. Day 16		47.80	24.71
SA 100nM (0.3uL) Start Day 0, stop Day 10, Coll. Day 16		8.04	9.76
SA 100nM (0.3uL) Start Day 0, stop Day 12, Coll. Day 16		14.77	14.28

Table 20. C/EBPβ gene expression upon treatment with SA or SA and palmitate

c/EBPβ	RT-PCR Ct values normalized to 18SrRNA control		
Treatment	Repeat 1	2	3
Day 0 Ctrl	1.03	1.00	1.03
Day 8 Ctrl	2.94	0.61	0.67
Day 8 Sa 100nM SA	3.10	2.28	0.74

Day 8 +100nM SA +100uM Pal		1.25	0.82	0.18
Day 8 +100nM SA +200uM Pal		0.72	0.45	0.61